Response to Reviewer Comments

Manuel Baumgartner[1,2], Ralf Weigel[2], Allan H. Harvey[3], Felix Plöger[4,5], Ulrich Achatz[6], and Peter Spichtinger[2]

[1]*Zentrum für Datenverarbeitung, Johannes Gutenberg University Mainz, Germany*
[2]*Institute for Atmospheric Physics, Johannes Gutenberg University Mainz, Germany*
[3]*Applied Chemicals and Materials Division, National Institute of Standards and Technology, Boulder, CO, USA*
[4]*Forschungszentrum Jülich GmbH, Institute of Energy and Climate Research (IEK-7), Jülich, Germany*
[5]*Institute for Atmospheric and Environmental Research, University of Wuppertal, Wuppertal, Germany*
[6]*Institut für Atmosphäre und Umwelt, Goethe-Universität Frankfurt, Frankfurt am Main, Germany*

August 26, 2020

Contents

1 General Response

We thank both reviewers for the effort they spent in preparing their reviews, their helpful comments and suggestions which led to a significantly improved manuscript.

This document contains our responses to the reviewer comments together with the output of "latexdiff" to highlight the changes made to the manuscript (blue text is added, red text is removed). After some general responses to points raised by the reviewers, we list all individual comments (pasted to this document in blue) together with our responses (in black).

1. We agree with Pascal Marquet, that not all values of c_p from literature, as presented in our Table 1, are recent values, in particular the value $c_p = 994\,\mathrm{J\,kg^{-1}\,K^{-1}}$ from Wegener and Wegener (1935) is comparatively old and may appear outdated. However, the main goal of this table is to provide the reader a (naturally non-complete) synopsis of values that he or she may encounter in the literature. In our literature search, we focused on textbooks in atmospheric science, which are expected to be frequently used by researchers in this field in looking up values for (physical) constants. Thus, the minimum and maximum value within this table serve to encompass the range of suggested literature values, including older sources. We also agree that in particular the old values appear greatly exaggerated, however also more recent textbooks contain values that deviate significantly from the recommended value $1005\,\mathrm{J\,kg^{-1}\,K^{-1}}$ by the WMO (1966), where the lower bound $c_p = 1000\,\mathrm{J\,kg^{-1}\,K^{-1}}$ stems from Roedel and Wagner (2011) and the upper bound $c_p = 1010\,\mathrm{J\,kg^{-1}\,K^{-1}}$ from Chang et al. (2006), Tiwary and Williams (2019), and Brusseau et al. (2019). Arguably, these values are also rather extreme, but they are found in recently published literature sources, hence these values should be included in our synopsis.

   We adapted Figure 2b and included the absolute difference $\theta_{1000} - \theta_{1010}$ in addition to the difference $\theta_{994} - \theta_{1011}$, where the latter corresponds to the original curve shown in the initially submitted manuscript and is now designated as "historical".

   We reformulated the text to emphasize, that, on the one hand, the difference plots in Figure 2b only serve to indicate the possible range of values of the potential temperatures, depending on which value for c_p is chosen or found in literature. On the other hand, these plots also illustrate the sensitivity of θ_{c_p} on comparatively small changes in c_p. We also emphasize, that the extreme values $\theta_{994}, \theta_{1000}, \theta_{1010}, \theta_{1011}$ are only

included for illustration purposes, while all comparisons in the sequel are made to θ_{1005}, based on the recommended value $c_p = 1005\,\mathrm{J\,kg^{-1}\,K^{-1}}$ by the WMO (1966).

2. The main concept of the (dry air) potential temperature is the imaginary (dry air) adiabatic descent of an air parcel at absolute temperature T and pressure p down to pressure level p_0, where the air parcel would attain the potential temperature as its absolute temperature. The reviewer is correct that the absolute temperature of an air parcel is limited to "atmospheric values", e.g. not larger than about 350 K. However, its potential temperature can attain significantly larger values as is already illustrated by the curves in Figure 2a, where values of up to $\sim 2000\,\mathrm{K}$ are visible for air parcels in the stratosphere. Although the curves in Figure 2a are based on the (historical) extreme values, the curve for θ_{1005} (corresponding to the recommended value) is in between the curves shown, hence also θ_{1005} attains values of up to $\sim 2000\,\mathrm{K}$ in the stratosphere.

   Since our reference potential temperature θ_{ref} is determined as the upper bound of the integral

$$\int_{T}^{\theta_{\mathrm{ref}}} \frac{c_p^0(T')}{T'}\,\mathrm{d}T' \tag{1}$$

   within the equation

$$R_a \log\left(\frac{p_0}{p}\right) = \int_{T}^{\theta_{\mathrm{ref}}} \frac{c_p^0(T')}{T'}\,\mathrm{d}T'\,, \tag{2}$$

   values of the integrand $\frac{c_p^0(T')}{T'}$ are required for temperatures up to $\sim 2000\,\mathrm{K}$, because we also need to expect that θ_{ref} will attain comparably large values as θ_{1005}. As specified in Lemmon et al. (2000), the parameterization $c_p^0(T')$ is accurate and valid up to 2000 K. Therefore, the resulting potential temperatures $\theta_{\mathrm{ref}} \leq 2000\,\mathrm{K}$ are expected to be accurate. However, due to the division of the specific heat capacity $c_p^0(T')$ by the temperature T' in the integrand, the influence of $c_p^0(T')$ on the integrand $\frac{c_p^0(T')}{T'}$ is diminished for large values of T'. Moreover, the parameterization $c_p^0(T')$ should extend in a physically consistent way to temperatures above 2000 K. In summary, although the accuracy of the reference potential temperature for values above 2000 K is not guaranteed by Lemmon et al. (2000), we nevertheless expect these values to be close to the correct value.

3. Due to the major comment #7 by Pascal Marquet, we rewrote and restructured Section 7 completely (please also see our response to the respective major comment #7). As Section 7 within the original submission, also the new and restructured Section 7 is focused on the use of our new reference potential temperature θ_{ref}. Four typical uses of potential temperature are highlighted, where we show the (dis-)agreement between computations using either θ_{ref} or the conventional θ_{1005}.

   - Section 7.1 is motivated by the very helpful major comment #7 by Pascal Marquet on our initial submission and illustrates a typical pitfall in the use of our new reference potential temperature θ_{ref}: a simple substitution of the occurence of θ by θ_{ref} in a formula might lead to a wrong formula, if the derivation of this particular formula is based on the assumption of the constancy of c_p. Hence we showcase this pitfall at the example of the computation of the Brunt-Väisälä frequency and also indicate that we do not observe any significant deviations in the values of the Brunt-Väisälä frequency in using θ_{ref} (with the correct formula) over the conventional potential temperature θ_{1005}.
   - Section 7.2 illustrates the (dis-)agreement of the values of Ertel's potential vorticity in a special case, where one computation uses θ_{ref} and the other θ_{1005}.
   - Section 7.3 provides a general remark on the vertical sorting of (measurement) data with respect to intervals of potential temperature. Here, the difference $\theta_{\text{ref}} - \theta_{1005}$ might mainly affect data at high altitudes, e.g. at stratospheric altitudes and beyond.
   - Section 7.4 explores the effect of diabatic heating on the absolute and potential temperature of an air parcel. Only small differences are observed for the change of absolute temperature, either computed with the temperature dependent or the constant specific heat capacity. However, significant differences are observed in the corresponding rates for the change in the potential temperature. This difference could be significant for Lagrangian models based on isentropic coordinates, which are used for chemical transport models for the stratosphere.

   We emphasize in the new Section 7, that a general assessment of the impact of using θ_{ref} instead of θ_{1005} is not possible due to the wide range of possible applications of potential temperature in atmospheric science. Instead, our list is meant to show possible deviations in typical applications

and help the reader to make an informed decision whether it is worth to adopt the new potential temperature in the respective application.

2 Response to Pascal Marquet

2.1 General response

We thank Pascal Marquet for his thorough review, including numerous valuable suggestions and hints.

2.2 Response to General Major Comments / Recommendations

1. the authors present in section 3 a range of possible dry-air values of c_p that appear to be greatly exaggerated, ranging from 994 to 1011 J/K/kg. I show in this review that the uncertainty interval must be much smaller (1004.5 to 1007.5 J/K/kg), which must imply impacts on values of θ about 7 times smaller than those considered at high altitude in the document. The authors should modify sections 2 to 5 and Figures 2, 3 and 4, by reducing the uncertainty on c_p and by retaining only the more recent and realistic values.
   We agree that the values $994\,\mathrm{J\,kg^{-1}\,K^{-1}}$ and $1011\,\mathrm{J\,kg^{-1}\,K^{-1}}$ are rather extreme, but we included these for illustration purposes only. We reformulated certain parts of the text to emphasize this fact. Please also see our general response #1.

2. I show from copies of previously published papers, tables and figures that the observed values of $c_p(T)$ for T $<$ 320 K contradict values above 1007.5 J/K/kg, those under 1004.5 J/K/kg and the (ideal gas) formulations of Lemmon et al. (2000) and Dixon (2007) considered in section 4 by the authors. Observed values of $c_p(T)$ for T $<$ 320 K are rather consistent with the (real gas) NIST-REFPROP formulation considered in section 6 and with the IAPWS-TEOS10 formulation.
   We include our response to this item in the response to your general comment #5 below.

3. In this sense, the approach followed by the authors to calculate first values of θ_{ref} from the ideal-gas formulation of $c_p(T)$ by Lemmon et al (2000), and then those of θ_{real} for the real-gas NIST-REFPROP formulation, seems attractive, with however a comparison to irrelevant and too extreme constant values of 1011 and 994 J/K/kg in Figure 4 of the paper.

We include our response to this item in the response to your general comment #5 below.

4. Moreover the results of your section 6 seem strange to me, because the comparison of θ_{ref} deduced from the ideal-gas Lemmon's formulation (purple curve in your figure 3) with θ_{real} deduced from the real-gas NIST-REFPROP's formulation (yellow discs in your figure 3) gives very small differences on figures 8. Indeed, the differences $\theta_{\text{real}} - \theta\text{ref}$ of less than 0.05 K for $\theta > 700$ K above 20 km (less than 0.007%) seem unrealistic and not consistent with differences of 4.5 J/K/kg (or 4.5 %) for $c_p(T)$ at 200 K, 2.8J/K/kg (or 2.8%) at 250K and 1.3 J/K/kg (or 1.3 %) at 300 K (values deduced from the yellow discs and the purple curve in your figure 3).

   I guess that the relative differences $(\theta_{\text{real}} - \theta_{\text{ref}})/\theta_{\text{ref}}$ should be of the order of a few percent above 25 km and should increase with height, as indicated by a rough analysis of the differences between curves of your Figure 4b (to be checked by you, however, from direct computations and/or from a version with a linear scale of your figure 4b).

   Differences of several percent between ideal-gas and real-gas formulations of $c_p(T)$ should lead to larger differences in the gap between θ_{real} and θ_{ref}. This should result in a likely change in the conclusion in your section 6 and the use of formulations from IAPWS-TEOS10 (free) or INIST-REFPROP (to buy), rather than the analytical formula of Lemmon et al (2000, Eq.18, page 345) that is contradict by the values of $c_p(T)$ published in Table A2 (pages 366-367) of the same paper (see Fig.9 in section 3 bellow)
   We include our response to this item in the response to your general comment #5 below.

5. In fact, after reflection and analysis of this aspect (4), this is probably a false problem. Indeed, everything seems to be explained by the fact that the major differences for your θ come from values of c_p for highest T temperatures, say between 400 K and 2000 K. This aspect is not documented in your figure 3, where the values of c_p are only plotted up to 485 K.

   The fact that the values of your θ_{real} and θ_{ref} are very close must be explained by a low sensitivity of your θ to values of c_p for ambient temperatures (let's say those ranging from 200 K to 320 K and which define how the physical parameterizations should influence the weather parameters), with, on the other hand, a strong sensitivity of your θ to values of c_p for temperatures above 400 K (temperatures that are not

observed in the real atmosphere but that intervene numerically in the calculation of your θ when passing from high altitudes where the pressure is very low and returning adiabatically towards the ground level through very high artificial temperatures).

Therefore, if you are interested in the values of θ calculated by an adiabatic evolution from a very low pressure p to a (surface) pressure $p_0 = 1000$ hPa, you should better describe the accuracy of the values of $c_p(T)$ for $T > 400$ K.

Most of the issues (primarily expressed in your major comment #4) arise from the differences between real-gas and ideal-gas heat capacities shown in Figure 3. The key point is that the "real gas" (REFPROP) numbers shown on this graph are at 1013.25 hPa. The deviation between real gas and ideal gas is roughly proportional to the pressure, so at much lower pressures (for example, in the stratosphere) the real-gas effects are much smaller. Real-gas effects are also smaller at high temperatures (as can already be seen in Figure 3), so that, by the time a calculation reaches a pressure near sea level where nonideality could be significant, the (potential) temperature is high enough to make the behavior close to an ideal gas. This is why the real-gas effect on these calculations is small, as explained in the last paragraph of Section 6.

With regard to various formulations including those in REFPROP and TEOS-10, the paper of Lemmon et al. (2000) contains *two* real-gas air models (both of which use the same ideal-gas heat capacity that we use here). The most rigorous model treats air as a mixture of nitrogen, oxygen, and argon, using the reference EOS for each pure fluid. That model (implemented in REFPROP) is the real-gas model used here. Lemmon et al. (2000) also presents a simpler model where air is treated as a pseudo-pure fluid, and that model was used in the TEOS-10 package developed primarily for oceanographers. Since we use the more rigorous real-air model for our calculations in Section 6, we prefer not to introduce confusion by discussing alternative models such as the pseudo-pure fluid approach (especially since we find that real-gas effects are negligible in this context).

On his general comment #5, the reviewer is correct that the high-temperature behavior of c_p^0 is important. We already state the range of validity of the c_p^0 formulation (up to 2000 K) below Equation (19), but because of the importance we add the additional sentence: **Because the underlying calculations are based on rigorous statistical mechanics and accurate spectroscopic data, c_p^0 should be accurate**

to within 0.01 % **throughout this range, as discussed by Span et al. (2000).**

In addition, we correct an error in the caption of Figure 3 that may have caused confusion, changing c_p to c_p^0 for the indicated parameterizations.

Concerning the influence of large values of θ on our computations, please also see our general response #1.

6. Another aspect should be addressed in this article. One of the goals of our community is to provide efficient and applicable numerical methods for climate and numerical weather prediction models. In this sense, it would be useful to quantify the iterative processes designed and tested in this article: what is the extra cost (in CPU) for the calculation of $\theta_{\rm ref}$ and $\theta_{\rm real}$ compared to the direct calculation θ_{c_p} for a constant c_p? (make this evaluation for example for a set of vertical columns of standard atmosphere)
We appreciate this suggestion and added a short subsection on "Implementation aspects", being now Section 5.3. The additional computational overhead of computing $\theta_{\rm ref}$ highly depends on the number of iterations made with Newton's method. Restricting the attention to our suggested approximation $\theta^{(2)}$, seven additional computations, i.e. evaluations of mathematical expressions and function evaluations, need to be done. In this respect, a single computation of $\theta^{(2)}$ introduces an overhead of about seven, but the algorithmic complexity is constant, i.e. for all input values the required computational effort does not change.

7. For me, the most problematic aspect concerns the application you chose in section 7, by assuming that the squared Brunt-Väisälä frequency could be
$$N^2 = \frac{g}{\theta}\frac{\partial \theta}{\partial z},$$
where θ would be calculated by the particle method (by an adiabatic evolution from a very low pressure p to a surface pressure $p_0 = 1000$ hPa).

Differently, we recalled in Marquet and Geleyn (2013, MG13) that N^2 should be calculated from the local gradients of basic meteorological parameters (temperature and pressure if dry air is considered), and not from the variable θ that you study in your article (by an adiabatic evolution from a very low pressure p to a surface pressure $p_0 = 1000$ hPa).

In fact N^2 corresponds to adiabatic fluctuations of the density, before anything else. Accordingly, equations (B2) and (1) of MG13 applied to

dry air give the corresponding expression of N^2 as a function of local vertical gradients of density (ρ) and specific entropy (s):

$$N^2 = \frac{g}{\rho}\left.\frac{\partial \rho}{\partial z}\right|_s - \frac{g}{\rho}\frac{\partial \rho}{\partial z} = \left(-\frac{g}{\rho}\left.\frac{\partial \rho}{\partial s}\right|_p\right)\frac{\partial s}{\partial z},$$

where the first vertical derivative (of density with respect to z) is computed at constant entropy and the second vertical derivative (of density with respect to s) is computed at constant pressure. The local state equation $p = \rho RT$ and $\rho = p/(RT)$ with constant R and p implies

$$\left.\frac{\partial \rho}{\partial s}\right|_p = -\frac{\rho}{T}\left.\frac{\partial T}{\partial s}\right|_p .$$

The dry-air Gibbs equation writes $Tds = dh - dp/\rho$, with $dh = c_p(T)dT$ and with possibly $c_p(T)$ depending on absolute temperature. For constant pressure, this Gibbs equation reduces to $Tds|_p = c_p(T)\, dT|_p$, leading to $dT/ds|_p = T/c_p(T)$, and thus to $d\rho/ds|_p = -\rho/c_p(T)$. The squared dry-air Brunt-Väisälä frequency is therefore equal to

$$N^2 = \frac{g}{c_p(T)}\frac{\partial s}{\partial z}.$$

The dry-air Gibbs equation can then be used again to write $T\frac{\partial s}{\partial z} = c_p(T)\frac{\partial T}{\partial z} - (1/\rho)\frac{\partial p}{\partial z}$ which is valid for vertical oscillations. If moreover hydrostatic conditions prevail, then $\frac{\partial p}{\partial z} = -\rho g$, leading to

$$N^2 = \frac{g}{T}\left(\frac{\partial T}{\partial z} + \frac{g}{c_p(T)}\right).$$

This equation corresponds to the dry-air version of (22) in MG13, and it is Equation (1a) in the previous famous paper of Durran and Klemp (1982) about computations of the Brunt-Väisälä frequency (a key paper that you do not cite).

An expected result is that $N^2 = 0$ for the dry-air adiabatic lapse rate $\frac{\partial T}{\partial z} = -g/c_p(T)$.

The important finding for your study is that there is no need to use the gradient of any potential temperature for computing N^2 . Really, only the vertical gradient of T has to be calculated in (3), where it is possible to take into account the variations of $c_p(T)$ with the temperature you want to study in your paper. It is thus "possible", but not "mandatory",

to use (2) and a possible entropy formulation $s = c_p \ln(\theta) + const$ for the entropy to get the form (1) $N^2 = (g/\theta)\frac{\partial\theta}{\partial z}$ you have considered in your paper, but if and only if c_p is a constant. And this is not possible if $c_p(T)$ depends on the temperature, with in this case the need to stick with the formulation (3) recalled above in terms of the gradient $\frac{\partial T}{\partial z}$.

The other important result here is that it is the local temperature that is involved in $c_p(T)$, so those between 1004.5 J/K/kg and 1007.5 J/K/kg for 200 K < T < 320 K, and especially not the ones at the higher temperatures that you studied in your paper to calculate θ_{ref} or θ_{real} , which are not needed for computing N^2 by (3).

It therefore seems to me that the application described in your section 7 is inaccurate, since the formulation (1) that you use for N^2 is not the right one (3). If so, can you show another application where values of your formulation of θ_{ref} or θ_{real} would intervene in meteorological science?

We thank the reviewer for this excellent comment. Indeed, we were misled by the often used formula

$$N^2 = \frac{g}{\theta}\frac{\partial\theta}{\partial z} \tag{3}$$

to compute the Brunt-Väisälä frequency, where we substituted our new θ_{ref} without reviewing the precise derivation of formula (3). In fact, after applying the correct formula

$$N^2 = \frac{g}{T}\left(\frac{\partial T}{\partial z} + \frac{g}{c_p(T)}\right), \tag{4}$$

the differences in the Brunt-Väisälä frequency profiles, and therefore also in the gravity wave breaking heights, vanish, which we described in Section 7 of our original submission. To highlight the impact of using formula (4) instead of the incorrect formula (3), we recreated Figure 9 from our manuscript; please find the new version as Figure 1 within this document below. Since the differences in the gravity wave breaking heights disappear, the initially documented changes were an artifact of using the incorrect formula.

This motivated us to offer the reader a warning on simply substituting θ_{ref} into a formula that contains the potential temperature, see the new Section 7.1. Moreover, we rewrote Section 7 completely to highlight other aspects of the use of potential temperature in atmospheric science, where we provide examples of the (dis-)agreement of computations using θ_{ref} instead of θ_{1005}. Please see our general response #3 for further details.

8. My recommendation is that the document deserves acceptance only if the impacts described in section 7 concerning gravity waves are real.

   Therefore, the authors must provide evidence that it is indeed their formulations of θ_{ref} or θ_{real} (obtained by an adiabatic evolution between the pressures p and p_0) that intervenes in the Brunt-Väisälä frequency formula, and not the local vertical gradients of temperature and pressure derived in Durran and Klemp (1982) and Marquet and Geleyn (2013).

   If the authors can provide this evidence, then their paper would merit to be published subject to taking all the major recommendations and specific comments into account, or explaining why they do not need to take them into account.
   Even though the impact on the gravity wave breaking height was not real, we are convinced that our re-assessed potential temperature might prove useful for other upper atmospheric applications, i.e. within the stratosphere and beyond. In our newly written Section 7, we indicate three typical applications of the potential temperature, which might be affected by using the new reference potential temperature. Please see our general response #3 for details on the rewritten Section 7 and our response to your general comment #7 above.

2.3 Response to Specific Comments

- **Line 1:** add *dry* in: "...it is conserved for *dry* air's adiabatic..."
  We added the word "dry".

- **Lines 10 to 22:** I do not have access to Wegener's book (1911) and I confess that I was not aware of Köppen's oral contribution (1888). I have cited only the contributions of von Helmholtz and von Bezold in my papers (Marquet 2011, 2017, 2019b, Marquet and Dauhut 2018). I have been able to verify, however, Kutzbach's sentence (1979, page 143) in which Köppen's (1988) oral contribution is mentioned (see the excerpts in the Figure 1 in section 3 bellow). However, the title of the 1888 lecture of Köppen is written in Kutzbach (1979) as: "Ueber die Luftmischung und potentielle Temperatur", which might be different from the one in your bibliography: "Über Luftmischung..."? Moreover, I have not found the paper (or a copy of this lecture) of Köppen: do you have a copy of this lecture, or are you just citing the sentence of Kutzbach? Finally, I do not understand why you cite the URL: http://snowcrystals.com/?
  An online version of Wegener's book from 1911 (written in german)

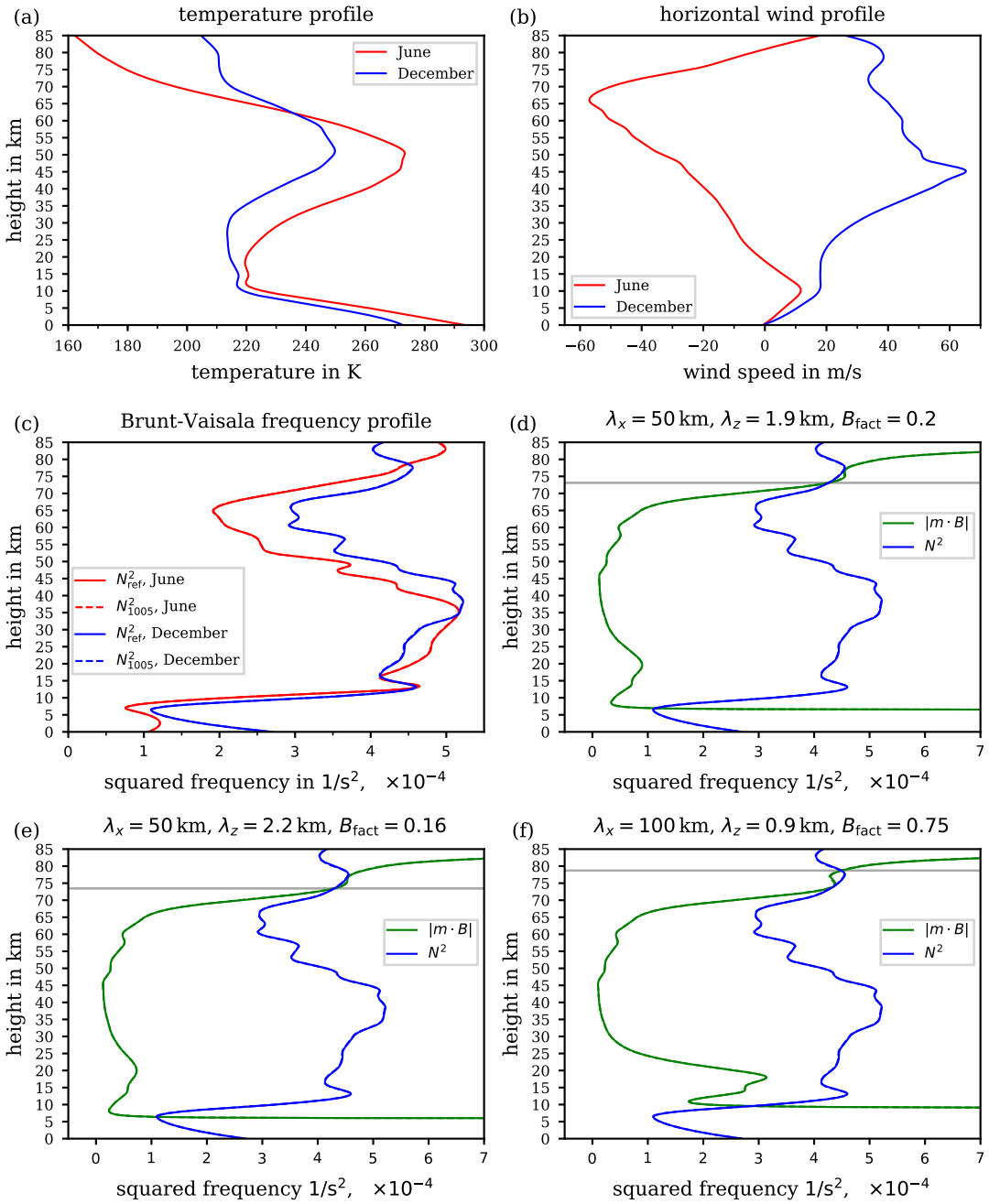

Figure 1: The same as Figure 9 from the originally submitted manuscript, where now the Brunt-Väisälä frequency is computed using the correct equation (4).

is available at `https://ia800404.us.archive.org/24/items/bub_gb_kWtUAAAAMAAJ/bub_gb_kWtUAAAAMAAJ.pdf`. Within the footnote on page 111 of this book, Köppen's oral contribution is mentioned similarly as in Kutzbach's book. Wegener cites the title of Köppens talk as "Über Luftmischung und potentielle Temperatur, in Anlehnung an die neueste Abhandlung von Herrn v. Helmholtz" and we refer to his citation. Given that "die" is a German article which does not modify the meaning of the sentence and we also do not have a copy of Köppen's talk, we prefer to adopt the title as written by Wegener. The citation of the url `http://snowcrystals.com/` is due to a false entry in the BibTeX file; we eliminated this URL.

- **Lines 10 to 28:** It would be useful to refer to the papers by Poisson (1833) and Thomson (1862-65) who had clearly imagined, before von Helmoltz and von Bezold in 1888, this idea of adiabatic variation on the vertical and the calculation of temperature for an air particle brought back to the surface (see section 5 of Marquet and Dauhut, 2018, and Marquet 2019b). I give copies of these articles on Figures 2 and 3.
  We are grateful for the references to the works of Poisson and Thomson which we were not aware of. We added these works to our text.

- **Lines 10 to 28:** It would be useful to refer to Bauer's paper (1908-1910), where the link between entropy and the potential temperature of dry air is made for the first time (see citations in Marquet 2011, Marquet and Dauhut 2018 and Marquet 2019b). I give copies of this paper of Bauer on Figures 4 and 5
  We included the reference to Bauer's work.

- **Lines 53 to 61:** You should mention the basic references for the definition and the use of $PV(\theta)$: Ertel (1940) and Hoskins (1987) at least (see also Schubert et al. 2004 cited in Marquet 2014).
  We added these references.

- **Lines 65-67:** The studies of the moist-air entropy by Hauf and Höller (1987) and Marquet (2011) do not start from the Gibbs' equation "$Tds = dh - dp/\rho - \sum_n n\mu_n dq_n$". On the contrary, they start from the moist-air entropy $s = \sum_n q_n s_n$ expressed as the weighted sum of the entropies s_n for its $n = 0, ..., 3$ constituents (dry air, water vapour, liquid water and ice) with concentrations q_n (specific contents).
  We thank for this clarification. We reformulated the sentence to clarify that the first law of thermodynamics together with Gibbs' equation is

used to derive the equation for the moist-air entropy, as stated in the introduction of Hauf and Höller (1987).

- **Lines 68-69:** The assumption of "local equilibrium" and use of latent heats release (of vaporization L_v and sublimation L_s) are also included in the definition of Hauf and Höller (1987) and Marquet (2011), not only in the formulation of Emanuel (1994).
  We reformulated the sentences accordingly.

- **Lines 69-70:** It is not true that "These formulations always rely on the assumption of reversible processes (i.e. conserved entropy)". On the contrary, the formulation $s(\theta_s)$ of Marquet (2011, ...) makes it possible to measure and quantify the losses or increases in moist-air entropy associated with irreversible processes such as the removal of precipitations that you mention. See in particular Eq.(59) in Marquet and Geleyn (2015), where the change in moist-air entropy associated with pseudo-adiabatic (von Bezold, 1888) processes writes:

$$ds = c_{pd}\frac{d\theta_s}{\theta_s} = (s - s_l)\left(\frac{-dr_{sw}}{1 + r_{sw}}\right).$$

  We reformulated the paragraph accordingly to clarify that also the case of irreversible processes is included in this formulation.

- **Lines 82-83:** You say: "the potential temperature is commonly used as a prognostic variable in numerical models for the formulation of the energy equation". Could you explain in which models θ is used as a prognostic variable? As far as I know, the prognostic variables associated with energy is either the temperature T or the combination c_pT, with the moist-air definition for c_p. In particular, your reference to Richardson et al (2007) on line 105 seems incorrect, since page 25 of this article the equations are: "$DT/Dt = F_q$" or "$\frac{\partial T}{\partial t} = ... + F_q$" or "$\frac{\partial \rho T}{\partial t} = ... + \rho F_q$".
  Indeed, the equations on page 25 of Richardson et al. (2007) are formulated without indicating the potential temperature. However, in their Section 2, the authors refer to the WRF model where the potential temperature is used as a prognostic variable (also see Skamarock et al., 2005; Skamarock and Klemp, 2008). We contacted the developers of the "planetWRF" model and they confirmed that the governing model equations were not changed, thus the symbol T used on page 25 of Richardson et al. (2007) appears to be a typographical error. Apart from the WRF-model, also the governing equations within the ICON model (employed by the German

Weather Service) are based on the (virtual) potential temperature (e.g., Zängl et al., 2015), which, in the case of dry conditions, reduces to the dry air potential temperature. An example of such a case is the upper-atmosphere extension of the ICON model (Borchert et al., 2019). We reformulated the paragraph accordingly and included the references. In addition to these numerical weather forecasting models, we now mention two chemical transport models in our new Section 7, which are Lagrangian models and use a formulation based on potential temperature.

- **Lines 105:** You say: "it was pointed out by Li and Chen (2019) that this approach could suffer from not accounting for the temperature dependence of the isobaric specific heat capacity c_p of the respective atmospheres gas composition". I spent some time checking this out in Li and Chen (2019), and I find (page 2): "Furthermore, the expressions of potential temperature and equivalent potential temperature become complicated when the heat capacity of the atmosphere varies with temperature or when multiple condensing species exist in the atmosphere." Here as elsewhere, could you quote the pages and/or equations corresponding to your citations, to help the reader find his way around in articles or books with very many pages?
  Unfortunately, we erroneously cited the wrong article. The correct article is Li et al. (2018), where the authors characterize the moist adiabats, especially for atmospheres of other planets. Within their derivation, they explicitly take the temperature dependency of the specific heat capacity into account. In addition, they stress the importance to incorporate temperature dependent versions of the heat capacities for Jupiter: "Because the measured absolute brightness temperature is precise to about a few percent and the limb darkening is precise to 0.1 % (Janssen et al. 2017), traditional Jovian thermodynamics—assuming constant heat capacity and small mixing ratios of condensates—needs to be carefully reviewed and refined according to the requirement of the new instrument." We corrected the references and reformulated the paragraph. Moreover, we went again over the manuscript to include numbers of pages or equations for certain references.

- **Lines 117:** It is customary, at the end of the introduction, to present the outline of the article, with a summary of the content of each forthcoming sections. This should be included at the end of your Section 1.
  We followed this suggestion and included an outline of the subsequent sections.

- **Lines 134:** Your value for $R_a = R/M_{\mathrm{mol},a}$ is known with R given up to ± 0.0001 I believe? You could retain the value 8.31446 for example? Anyhow you have to give the resulting value $R_a = 287.115$ at least, with perhaps the associated precision ± 0.005?
  We followed this suggestion and specified an interval within which the value of R_a is contained, when the division is carried with the indicated precision for $M_{\mathrm{mol},a}$.

  Recently, the value of the molar gas constant R was defined to have the indicated value, see `http://physics.nist.gov/constants`, therefore there is no uncertainty in the value of R. We hint the reader on this fact in a footnote.

- **Lines 183:** It was indeed indicating by WMO that the variability of c_p ranges from 994 J/K/kg to 1011 J/K/kg. But the real recommendation is rather a value close to 1005 J/K/kg, in line with the values presently used in most General Circulation (GCM) and Numerical Weather Prediction (NWP) models:

c_p (J/K/kg)	GCM and/or NWP models
1005.0	Unified-Model (UKMO, UK, from Adrian Lock)
1005.0	COSMO (DWD, Germany, from Dmitrii Mironov)
1004.7	IFS (ECMWF, Reading, UK, from "sucst.F90")
1004.7	ARPEGE (Meteo-France, Toulouse, France, from "sucst.F90")
1004.7	AROME (Meteo-France, Toulouse, France, from "sucst.F90")
1004.7	Meso-NH (L.A.+Meteo-France, Toulouse, France, from "sucst.F90")
1004.7	LMD-Z (IPSL, Paris, France, from "suphec.F90")
1004.6	ICON (DWD, Germany, from Dmitrii Mironov)
1004.6	GFS (USA, from "physcons.f")

  We thank for the compilation of the values of c_p used by several General Circulation and Numerical Weather Prediction models. Indeed, the WMO recommends the value $1005\,\mathrm{J\,kg^{-1}\,K^{-1}}$, hence we always compare our results to the resulting potential temperature θ_{1005}, see also our general response #1.

- **Lines 191-192:** These old WMO values of 994 J/K/kg and 1011 J/K/kg are too extreme and unrealistic, because they are not used in any current GCM and NWP model. Or could you indicate the models where these

values might be used?
We refer the reviewer to our response to the previous comment as well as to our general response #1.

- **Page 8, Table 1:** The values of 994 J/K/kg, 1000 J/K/kg, 1003 J/K/kg and 1011 J/K/kg do not seem relevant.
  - The value 994 J/K/kg comes from an old book I couldn't find, and the accuracy of the data obtained before 1933 can be questioned. This is like the measurement of the speed of light, the accuracy of which cannot be the "meeting of all possibilities", including for example the measurements of Romer and Huygens in 1675 (220, 000 km/s), Bradley in 1729 (301, 000 km/s), Fizeau in 1849 (315, 000 km/s) or Foucault in 1862 (298, 000 km/s)? It is the same for the measurement of the numerical values of $\gamma = c_p/c_v$ for diatomic gases, where the value of 1.421 retained by Poisson in 1833 or of 1.41 by Thomson in 1862 cannot be compared with the modern value of $7/5 = 1.40$? It is the same for the measurement of absolute scale of temperature, with a constant corresponding to 267 K in Gay-Lussac (1802) and Carnot (1824), to 273.22 K in Thomson (1848), before to be presently fixed to 273.15 K (see the review in Marquet, 2019a).
  - The value of 1000 J/K/kg attributed to Valis (2009) seems to be easily questionable: see the legend in Figure 6 in section 3 bellow.
  - I don't know where the value of 1003 J/K/kg published in Tripoli and Cotton (1981) comes from. But one can also have doubts about their values of c_p for ice (2100 J/K/kg instead of 2106 J/K/kg) and liquid water (4187 J/K/kg instead of 4218 J/K/kg), with important differences for both dry air, liquid water and ice from the values commonly used in GCM and NWP model.
  - Other than the mention in the WMO recommendations, I have never seen an application of the value 1011 J/K/kg. Could you indicate such an application of the value $c_p = 1011$ J/K/kg for dry air?

  We agree, the value $1000\,\mathrm{J\,kg^{-1}\,K^{-1}}$ from Vallis (2006) seems to be intended as a rough order of magnitude estimate of c_p, therefore we removed this value from our Table. However, the same value $1000\,\mathrm{J\,kg^{-1}\,K^{-1}}$ nevertheless appears in the recent textbook by Roedel and Wagner (2011).

  The value $1003\,\mathrm{J\,kg^{-1}\,K^{-1}}$ from Tripoli and Cotton (1981) appears in their appendix. Since our Table 1 is intended to provide a synopsis of values from literature, we prefer to keep this value within the table.

We cannot provide an application where the value $1011\,\mathrm{J\,kg^{-1}\,K^{-1}}$ is used. However, the document WMO (1966) explicitly states the values $1003\,\mathrm{J\,kg^{-1}\,K^{-1}}$ and $1011\,\mathrm{J\,kg^{-1}\,K^{-1}}$ as the minimum and maximum "range of actual values", hence in our opinion such a range should be part of our synopsis of literature values.

We additionally refer the reviewer to our general response #1.

- **Lines 194-199 and Figure 2:** Assuming new extreme values of 1004.5 J/K/kg and 1007.5 J/K/kg (later demonstrated), I was able to redo your figures 2 (a) and (b) with the same US standard atmosphere profile: see Figure 7 in section 3 bellow, with indeed the same difference $\Delta\theta_{c_p} = \theta_{994} - \theta_{1011}$ (in black) as in your paper. The new differences $\theta_{1004.5} - \theta_{1007.5}$ (in red) are much smaller, by an order of magnitude or so (divided by a factor of about 5 to 7). The new differences are less than 2 K at 20 km, 5 K at 35 km and 14 K (instead of 75 K) at 50 km. These new differences $\theta_{1004.5} - \theta_{1007.5}$ may modified your comments and conclusions in your section 3.
  We appreciate the effort for reproducing this figure. Since the range of extreme values in our Table 1 should only reflect the range provided in the literature, we included the curve for $\theta_{1000} - \theta_{1010}$ in the updated Figure 2b. These curves only serve to illustrate the range of values of θ_{c_p} for the values indicated in the synopsis of Table 1. Moreover, these difference plots also serve to indicate the sensitive response of θ_{c_p} to even small perturbations in the value for c_p. We also refer the reviewer to our general response #1.

- **Section 4, Lines 226-260 and Figure 3:** I disagree with many of the points you've drawn on your figure 3. So I redid your figure 3 by deleting the old and questionable data (see Figure 8 in section 3 bellow). I kept the values of 1004 J/K/kg, 1004.832 J/K/kg, 1005 J/K/kg and 1005.7 J/K/kg, the data of Vassermann et al (1966) and NIST-REFPROP as well as the two curves of Lemmon et al (2000) and Dixon (2007). This new figure shows that constant values of c_p between 1004.5 J/K/kg and 1007.5 J/K/kg agree with the selected points for the range of temperatures observed in the atmosphere (say 200 to 320 K). The two curves of Lemmon et al (2000) and Dixon (2007) are retained here because they are valid for the approximation of ideal gases and allow to measure the differences with formulations for real gases, such as Vassermann et al (1966) and NIST-REFPROP. The impact of real gases properties on c_p increases with decreasing values of T bellow 260 K, and is larger than 4 J/K/kg at 200

K.

We agree that the relatively old measurement data may not be very accurate and we stress this aspect in our text. Apart from the possible limited accuracy of the old measurements, these data are not always given for pressures of "about one atmosphere", i.e. about 1000 hPa, but also include measurement data for lower pressures. In any case, this figure follows two purposes: On the one hand, it provides an impression of the available measurement data, even though these might stem from older sources. On the other hand, even these (maybe more uncertain) measurement data nicely show that c_p should indeed be considered as a function of temperature which is the key aspect of that subsection. We reformulated some sentences to point out our intension more clearly.

We also refer the reviewer to our response to his general comment #5.

- **Lines 245, legend of Fig 3, lines 315-321 and Eqs.(18) and (19):** It should be mentioned that your formula (18) with the coefficients (19) of Lemmon et al (2000) disagrees with the observed values given in Table A2 of the same article Lemmon et al (2000). And indeed, while formula (18) leads to decreasing values of $c_p(T)$ for decreasing T, the values of $c_p(T)$ in Table A2 show a minimum around 250 K and become increasing for decreasing temperatures up to 81.72 K (see Figs.9 and 10 in section 3 bellow). It should also be mentioned that your equation (18) corresponds to equation (18) (page 345) in Lemmon et al (2000).

  We indicated the number of the equation for the parameterization $\frac{C_p^0(T)}{R}$ in the work by Lemmon et al. (2000).

  Table A2 in the Lemmon et al. (2000) paper is computed with the pseudo-pure fluid model (see reply to your major comment #5). It is therefore not directly relevant to compare with ideal-gas calculations (the same is true of the real-gas tables of N_2, O_2, and Ar discussed near the end of the review). We do show real-gas results (at 1013.25 hPa) from the more rigorous of the two models of Lemmon (via REFPROP), which should be close to those from the simpler pseudo-pure model (for example, showing a minimum near 250 K).

- **Lines 246 and 325-329:** You should mention that the equation of Dixon (2007, p.376) used to compute the dry-air value $c_p(T)$ plotted in your Fig.3 is

$$c_p(T) = 1002.5 + 275 \cdot 10^{-6}(T - 200)^2 \text{J/K/kg}$$

(see Figure 11 in section 3 bellow).
We followed the suggestion and included the relevant page in Dixon's book, the stated accuracy and the formula.

- **Lines 356 / Eq.(11):** The gaz constant "R_a" is missing before the integral $\int_{p_0}^{p} dp'/p'$
We added the missing gas constant.

- **Lines 356 / Eq.(21), Lines 359 / Eq.(22), Lines 374 / Eq.(23), Lines 411 / Eq.(25), Line 426 and 429, Line 691 / Eq.(C1), Line 693 / Eq.(C2):** You should used the same dummy variable "T'" as in your Eq.(11) line 153 ($\int_{T_0}^{T} dT'/T'$) to write all the integrals of the kind $\int_{\theta}^{T} c_p(T')dT'/T'$. The use of the dummy variable "z" can lead to unfortunate confusion with the altitude variable, which is then used in the rest of your paper to describe the true vertical coordinate.
We followed this suggestion and used the dummy variable T' instead of z.

- **Page 11 / Fig 3:** I have plotted in Figure 12 (top, see section 3 bellow) the equivalent of your Figure 3, but with different formulations that correspond to observed ("real gases") values of $c_p(T)$, with a zoom (Figure 12 bottom) around the usual atmospheric temperatures.

  I first reported (from your Fig.3) the points of your calculations made with the (paid) application of NIST-REFPROP. These NIST-REFPROP values are comparable to those I have computed with the (free) SIA software (`http://www.teos-10.org/software.htm`) corresponding to the IAPWS-2010 (Feistel et al, 2010) and TEOS-10 (Feistel, 2018) formulations. There is a similar minimum $c_p(T) \approx 1005.5$ to 1005.7 J/K/kg at around 250 K and with the same higher values of about 1007 J/K/kg at 320 K and 1006.7 J/K/kg at 200 K.

  The values published in Table A2 of Lemmon et al. (2000) are fairly comparable to those of NIST-REFPROP and IAPWS-TEOS10, with a similar minimum of $c_p(T)$ at around 250 K.

  The same applies to the values of $c_p(T)$ for N2 and O2 published in Marquet (2015), with the values for dry air completed with the values of $c_p(T)$ for Argon.

  The minimum of $c_p(T)$ for N2 is at around 290 K in both Stewart and Jacobsen (1989, Table 5.73, see Fig.13 bellow) and Span et al. (2000, page 1410, see Fig.14 bellow). The resulting figure 5 for N2 published in Marquet (2015) is recalled in Fig.15 bellow.

The minimum of $c_p(T)$ for O2 is at around 220 K in Jacobsen et al. (1997, Table 5.79, see Figs.16 and 17). The resulting figure 4 for O2 published in Marquet (2015) is recalled in Fig.18 bellow.

Values of $c_p(T)$ for Argon increases for decreasing T for both Tegeler et al. (1999, Table 34, see Fig.19) and Stewart and Jacobsen (1989, Table 15, Figs.20 and 21). The unpublished Fig.22 plotted bellow shows that values for Tegeler et al. (1999) and Stewart and Jacobsen (1989) fairly coincide for $150 < \mathrm{T} < 300$ K.

The unpublished Fig.23 bellow shows that it is equivalent to use $c_p(T)$ computed for N2, O2 and H20 vapour by using Statistical and Quantum Physics (dashed lines) or by the "calorimetric method" (third law and integration of $c_p(T')/T'$ from 0 K to T , sum of $L(T_k)/T_k$ for all changes of phases at T_k , add the Pauling-Nagle residual entropy at 0 K for H2O). It thus appears that it is for these temperature-dependent values of $c_p(T)$ for gases that the agreement between the calorimetric and quantum methods can be obtained, an agreement which is not obtained with "ideal gas" formulations.

I have also plotted on Figure 12 bellow the constant values used in many GCM and NWP models (1004.6, 1004.7, 1005 J/K/kg, depicted by coloured horizontal dashed lines). It appears, considering all these values of c_p constant or dependent on T, and in the range of atmospheric temperatures ($200 < \mathrm{T} < 320$ K), that the imprecision on $c_p(T)$ is between 1004.5 and 1007.5 J/K/kg. These extreme values have been used earlier in this review to plot several figures, instead of the (old) WMO extreme values 994 and 1011 J/K/kg you used in your study.

Regarding the search for an accurate average value $c_p(T) \approx c_p^0$, it appears that $c_p^0 \approx 1005.8 J/K/kg$ could be more realistic (for $200 < \mathrm{T} < 320$ K) than those presently used in GCM and NWP models (1004.6, 1004.7, 1005 J/K/kg).

However, the impact of these new formulations ($c_p(T)$ or c_p^0) should be small in our CMGs and NWP models. Moreover, taking into account the dependence of $c_p(T)$ on temperature, not only for dry air but also for water vapor, liquid water and ice, would greatly complicate the writing of the physical parameterizations of these models, and would greatly increase the cost of these physical parameterizations.
It is true that, if only the heat capacity at atmospheric temperatures (e.g. from 200 K to 320 K) is of interest, a constant value near $1005\,\mathrm{J\,kg^{-1}\,K^{-1}}$ might be adequate. However, for calculations in the upper atmosphere,

the potential temperatures become much larger, and the assumption of the constancy of c_p becomes increasingly erroneous. This may be considered as the main reason for the increasing deviation between θ_{ref} and one of θ_{c_p} at increasing altitude.

The reviewer is correct that accounting for this effect would complicate atmospheric models. We are not advocating that all atmospheric modeling use our more rigorous reference potential temperature. The purpose of our paper is to document the error caused by the typical simplifying assumptions on calculations of the potential temperature so that scientists can make an informed decision about whether it is worthwhile to implement the more rigorous calculation in their particular context. We now emphasize this aspect in the introductory paragraph of the new Section 7.

3 Response to Reviewer #2

- Abstract, line 1: 'changes of state' → should this be changed to or complemented by 'motions'; changes of state in my understanding mostly refers to thermodynamic changes of state, e.g. for a mixture of air and water. Potential temperature is already extremely useful for dry air undergoing displacements in the atmosphere, or even simply experiencing pressure changes.
  We thank for this hint, but as the thermodynamic "state" of a fluid already refers to temperature and pressure, we prefer to leave the formulation as it is.

- l42-44: meaning not clear, although I believe I know what is meant; the formulation is somewhat confusing
  We rephrased this sentence.

- l59: "Occasionally" means "on occasion, now and then", according to the Merriam-Webster dictionnary; it does not seem appropriate for this sentence. Suggestion: "Examples of definitions based on the potential vorticity include..."
  We followed the suggestion and rephrased the sentence to avoid the use of "occasionally".

- l185: has ξ been introduced before, or does it make sense only upon reding Weigel et al 2016? If that is the case, perhaps it is sufficient to mention 'a coefficient factor, cf Weigel et al 2016'?
  The symbol ξ indeed only makes sense upon reading the reference. Therefore, we followed the suggestion and eliminated the symbol.

- l192 and 194: it seems odd that the same reference (WMO, 1966) both suggests the value of 1005 and 1011 J/(kg K)
  The WMO (1966) offers three values in total:
  - a recommended value $1005\,\mathrm{J\,kg^{-1}\,K^{-1}}$,
  - the minimum "range of actual values" $1003\,\mathrm{J\,kg^{-1}\,K^{-1}}$,
  - the maximum "range of actual values" $1011\,\mathrm{J\,kg^{-1}\,K^{-1}}$

  where the indicated "range of actual values" might be interpreted as to highlight the uncertainty on the precise values at that time, although this is not explicitly stated in WMO (1966). We added a subsentence to indicate, that $1011\,\mathrm{J\,kg^{-1}\,K^{-1}}$ represents the upper limit in the reference WMO (1966). We also refer to our general response #1.

- l224: the range of uncertainty displayed in figure 2 is an upper bound, obtained using the extreme values one may find in textbooks for c_p. A more plausible interval is probably 1004 - 1006, with key references like Holton (2004) and Emmanuel (1994) serving as classical references for one and the other extreme. Perhaps the authors could indicate how this more limited range modifies the Δc_p at 50 km (from 75 K down to ..?)
  Following also a comment of Reviewer #1, we included a second curve in Figure 2b, showing the absolute difference $\theta_{1000} - \theta_{1010}$. We agree, that these values of c_p are still quite extreme, but these values are suggested in the literature. In any case, we reformulated the text to emphasize, that these absolute differences only serve to indicate the possible range of deviations between the θ_{c_p} based on the range of values of c_p found in the literature. Moreover, these curves illustrate the sensitive response of θ_{c_p} to even small perturbations in the value of c_p. Moreover, we also emphasize, that all comparisons are made in reference to θ_{1005}, based on the recommended value by WMO (1966).

- l347: seductive → appealing? attractive? tempting?
  We agree that the word "seductive" is not appropriate; we substituted it by "tempting".

- l495: should the authors recall what effects are dominant in the difference between ideal and real gas, or would this be too redundant with the first sections?
  We thank for this suggestion and included a reference to Section 4 where the differences are discussed.

- l618: '...depending on the textbook consulted.' Perhaps recall the range of values, or at least refer to the table so the reader can quickly find the range of values (this table is useful and thought-provoking).
  We followed this suggestion and recalled the minimum and maximum value from recent textbooks. In addition, we included a reference to Table 3.

References

Borchert, S., Zhou, G., Baldauf, M., Schmidt, H., Zängl, G., and Reinert, D. (2019). "The upper-atmosphere extension of the ICON general circulation model (version: ua-icon-1.0)". In: *Geoscientific Model Development* 12.8, pp. 3541–3569.

Brusseau, M., Pepper, I. L., and Gerba, C. P. (2019). *Environmental and Pollution Science*. Third Edition. Elsevier.

Chang, X., Zhao, W., Zhang, Z., and Su, Y. (2006). "Sap flow and tree conductance of shelter-belt in arid region of China". In: *Agricultural and Forest Meteorology* 138.1, pp. 132–141.

Hauf, T. and Höller, H. (Oct. 1987). "Entropy and Potential Temperature". In: *Journal of the Atmospheric Sciences* 44.20, pp. 2887–2901.

Lemmon, E. W., Jacobsen, R. T., Penoncello, S. G., and Friend, D. G. (2000). "Thermodynamic Properties of Air and Mixtures of Nitrogen, Argon, and Oxygen From 60 to 2000 K at Pressures to 2000 MPa". In: *Journal of Physical and Chemical Reference Data* 29.3, pp. 331–385.

Li, C., Ingersoll, A. P., and Oyafuso, F. (2018). "Moist Adiabats with Multiple Condensing Species: A New Theory with Application to Giant-Planet Atmospheres". In: *Journal of the Atmospheric Sciences* 75.4, pp. 1063–1072.

Richardson, M. I., Toigo, A. D., and Newman, C. E. (2007). "PlanetWRF: A general purpose, local to global numerical model for planetary atmospheric and climate dynamics". In: *Journal of Geophysical Research: Planets* 112.E9.

Roedel, W. and Wagner, T. (2011). *Physik unserer Umwelt: Die Atmosphäre*. Springer Berlin Heidelberg.

Skamarock, W. C., Klemp, J. B., Dudhia, J., Gill, D. O., Barker, D. M., Wang, W., and Powers, J. G. (2005). *A Description of the Advanced Research WRF Version 2*. (No. NCAR/TN-468+STR).

Skamarock, W. C. and Klemp, J. B. (2008). "A time-split nonhydrostatic atmospheric model for weather research and forecasting applications". In: *Journal of Computational Physics* 227.7. Predicting weather, climate and extreme events, pp. 3465–3485.

Span, R., Lemmon, E. W., Jacobsen, R. T., Wagner, W., and Yokozeki, A. (2000). "A Reference Equation of State for the Thermodynamic Properties of Nitrogen for Temperatures from 63.151 to 1000 K and Pressures to 2200 MPa". In: *Journal of Physical and Chemical Reference Data* 29.6, pp. 1361–1433.

Tiwary, A. and Williams, I. (2019). *Air Pollution: Measurement, Modelling and Mitigation*. Fourth Edition. CRC Press.

Tripoli, G. J. and Cotton, W. R. (1981). "The Use of lce-Liquid Water Potential Temperature as a Thermodynamic Variable In Deep Atmospheric Models". In: *Monthly Weather Review* 109.5, pp. 1094–1102.

Vallis, G. K. (2006). *Atmospheric and Oceanic Fluid Dynamics*. Cambridge, U.K.: Cambridge University Press, p. 745.

Wegener, A. and Wegener, K. (1935). *Vorlesung über Physik der Atmosphäre*. Leipzig: J. A. Barth.

WMO (1966). *International Meteorological Tables, WMO-No.188.TP97*. Ed. by S. Letestu. Geneva, Switzerland: Secretariat of the World Meteorological Organization.

Zängl, G., Reinert, D., Rípodas, P., and Baldauf, M. (2015). "The ICON (ICOsahedral Non-hydrostatic) modelling framework of DWD and MPI-M: Description of the non-hydrostatic dynamical core". In: *Quarterly Journal of the Royal Meteorological Society* 141.687, pp. 563–579.

Reappraising the appropriate calculation of a common meteorological quantity: Potential Temperature

Manuel Baumgartner[1,2], Ralf Weigel[2], Allan H. Harvey[3], Felix Plöger[4,5], Ulrich Achatz[6], and Peter Spichtinger[2]

[1]Zentrum für Datenverarbeitung, Johannes Gutenberg University Mainz, Germany
[2]Institute for Atmospheric Physics, Johannes Gutenberg University Mainz, Germany
[3]Applied Chemicals and Materials Division, National Institute of Standards and Technology, Boulder, CO, USA
[4]Forschungszentrum Jülich GmbH, Institute of Energy and Climate Research (IEK-7), Jülich, Germany
[5]Institute for Atmospheric and Environmental Research, University of Wuppertal, Wuppertal, Germany
[6]Institut für Atmosphäre und Umwelt, Goethe-Universität Frankfurt, Frankfurt am Main, Germany

Correspondence: Manuel Baumgartner (manuel.baumgartner@uni-mainz.de)

Abstract. The potential temperature is a widely used quantity in atmospheric science since it is conserved for dry air's adiabatic changes of state. Its definition involves the specific heat capacity of dry air, which is traditionally assumed as constant. However, the literature provides different values of this allegedly constant parameter, which are reviewed and discussed in this study. Furthermore, we derive the potential temperature for a temperature-dependent ~~parameterization~~ parameterisation of the specific heat capacity of dry air, thus providing a new reference potential temperature with a more rigorous basis. This new reference shows different values and vertical gradients~~in the upper troposphere and the stratosphere~~ , in particular in the stratosphere and above, compared to the potential temperature that assumes constant heat capacity. The application of the new reference potential temperature ~~to the prediction of gravity wave breaking altitudes reveals that the predicted wave breaking height may depend on the definition of the potential temperature used~~is discussed for computations of the Brunt-Väisälä frequency, Ertel's potential vorticity, diabatic heating rates, and for the vertical sorting of observational data.

1 Introduction

According to the book *Thermodynamics of the Atmosphere* by Alfred Wegener (1911), the first published use of the expression *potential temperature* in meteorology is credited to Wladimir Köppen (1888)[1] and Wilhelm von Bezold (1888), both following the conclusions of Hermann von Helmholtz (1888) ~~(Kutzbach, 2016). Over 130 years ago~~(see also Kutzbach, 2016). Even prior to the introduction of the entropy, Poisson (1833) and Thomson (1862) used the "adiabatic equation", the basis of what is understood today as "potential temperature"[2], to describe adiabatic processes, e.g., the coincident variation of temperature and pressure on the movement of air, which is "independent of the effects produced by the radiation or conduction of heat"

[1] Wegener mentioned a talk given by Köppen in a footnote on page 111. In the publication year (1911) of Wegener's book, Köppen's daughter Else got engaged to Alfred Wegener (Reinke-Kunze, 2013) and they married in the year 1913 (Hallam, 1975).

[2] Cf. Bauer (1908) where, for the first time, the potential temperature and the entropy are set in a relationship.

(Thomson, 1862)[3]. Approximately 26 years later, von Helmholtz perceived that within the atmosphere the heat exchange between air masses of different temperatures, which are relatively moved, is insufficiently explained by heat transfer due only to radiation and convection. He argued that wind phenomena (e.g., the trade winds), storm events, and the atmospheric circulation were more intense, of larger extent, and more persistent than observed if the air's heat exchange within the discontinuity region (the friction surface of the different air masses) was not mainly due to eddy-driven mixing. On his way to analytically describe the heat exchange of different air masses within the atmosphere, in May of 1880, von Helmholtz introduced the air's *immanent heat* while its absolute temperature changes with changing pressure (von Helmholtz, 1888). In essence, von Helmholtz concluded that the temperature gained by a volume of dry air due to its adiabatic descent from a certain initial pressure level (p) to ground pressure (p_0) corresponds to the air's immanent heat. In November of the same year, in agreement with von Helmholtz and probably inspired by a presentation that was given in June by Köppen (1888), this property was renamed and reintroduced as the air's *potential temperature* (θ in the following) by von Bezold (1888) with the following definition for strictly adiabatic changes of state:

$$\theta = T \left(\frac{p_0}{p} \right)^{\frac{\gamma-1}{\gamma}}, \tag{1}$$

where T and p are the absolute temperature and pressure, respectively, of an air parcel at a certain initial (pressure-) altitude level. The quantities θ and p_0 are corresponding values of the same air parcel's absolute temperature and pressure if the air was exposed to conditions at ground level. The dimensionless coefficient γ, nowadays called the isentropic exponent, was specified as 1.41 (von Bezold, 1888).

Moreover, in the same publication, von Bezold concluded that for moist air's adiabatic changes of state, its potential temperature remains unchanged as long as the change of state occurs within dry-adiabatic limits; and further, if there is condensation and precipitation, the potential temperature changes by a magnitude that is determined by the amount of water that falls out of the air parcel. From a modern perspective, it is clear that the air parcel is an isolated thermodynamic system, and adiabatic processes correspond to processes with conserved entropy (i.e., isentropic processes). The description of the immanent heat is then equivalent to the thermodynamic state function entropy, which corresponds to potential temperature of dry air in a one-to-one relationship.

In general, the potential temperature has the benefit of providing a practicable vertical coordinate (equivalent to the pressure level or the altitude above, e.g., sea level) to visualise and analyse the vertical distribution and variability of (measured) data related to any type of atmospheric parameter. Admittedly, the use of the potential temperature as a vertical coordinate is initially less intuitive than applying altitude or pressure coordinates. Indeed, the potential temperature bears a certain abstractness to describe an air parcel's state at a certain altitude level by its imaginary dry-adiabatic descent to ground conditions. However, one major advantage of using the potential temperature as a vertical coordinate is that the (measured) data are sortable with respect to the entropy state at which the atmospheric samples were taken. Thus, ~~the comparison of~~ comparing repeated measurements of an atmospheric parameter on an ~~equipotential surface (isentrope)~~ isentropic surface or layer excludes any diabatic change of the ~~air parcel's state due to an entropy-changing uplift or descent of the~~ probed air mass.

[3] These early applications of entropy in meteorology are also documented in Marquet (2019).

Apart from characterising the isentropes, the vertical profiles of the potential temperature (θ as a function of height z) are used as the reference for evaluating the atmosphere's actual vertical temperature gradient, which allows characterising its static stability. Notably, von Bezold (1888) already proposed the potential temperature as an atmospheric stability criterion. In its basic formulation, the potential temperature exclusively refers to the state of dry air, and thus the potential temperature characterises the atmosphere's static stability with respect to vertical displacements of a dry air parcel. In meteorology, the static stability parameter is expressed in terms of the (squared) Brunt-Väisälä frequency N, often written in the form

$$N^2 = \frac{g}{\theta}\frac{\partial \theta}{\partial z}, \tag{2}$$

where ~~g~~ $g = 9.81\,\mathrm{m\,s^{-2}}$ is the gravitational acceleration. The potential temperature twice enters the formulation of the stability parameter, as the denominator (θ^{-1}) and as the vertical gradient $\frac{\partial \theta}{\partial z}$. In the research field of dynamical meteorology, the potential vorticity (PV) is often used (Ertel, 1942; Hoskins et al., 1985; Schubert et al., 2004). The PV is proportional to the scalar product of the atmosphere's vorticity (the air's local spinning motion) and its stratification (the air's tendency to spread in layers of diminished exchange). More concretely, the PV is the scalar product of the absolute vorticity vector and the three-dimensional gradient of θ, i.e., not only the potential temperature's vertical gradient but also its partial derivatives on the horizontal plane add to the resulting PV, although, particularly at stratospheric altitudes, the vertical gradient constitutes the dominant contribution. For the analytical description of a fluid's motion within a rotational system, as is the atmosphere, the PV provides a quantity that varies exclusively due to diabatic processes. ~~Occasionally, by means of the dynamical parameter PV ,~~ Frequently, the PV is used to define the tropopause height ~~is defined~~ (usually at 2 PV units, see, e.g., Gettelman et al., 2011) ~~as is, e.g.,~~ or the edge of a large-scale cyclone such as the polar winter vortex on specific θ levels (cf. Curtius et al., 2005).

While for a dry atmosphere (i.e., with little or no water vapour) the potential temperature is the correct conserved quantity (corresponding to entropy) for reversible processes, for an atmosphere containing water in two or more phases (vapour, liquid, and/or solid phases) energy transfers due to phase changes play a major role. Thus, the formulation of the potential temperature has to be extended ~~(~~since entropy is still the right quantity for reversible processes, including phase changes~~)~~. Starting from ~~Gibbs' equation , some formulations are available, e.g., the entropy potential temperature defined by Hauf and Höller (1987) or more general versions as derived by Marquet (2011). In these formulations,~~ the equation for the moist specific entropy, as derived from the first law of thermodynamics and the Gibbs equation, further extensions of the dry air potential temperature have been developed (Hauf and Höller, 1987; Emanuel, 1994; Marquet, 2011; Marquet and Geleyn, 2015) to account for phase changes and deviations from thermodynamic equilibrium~~are included. An approximation to these more general formulations is~~, e.g., ~~the equivalent potential temperature, which includes latent heat release, assuming thermodynamic equilibrium (e.g., Emanuel, 1994) . These formulations always rely on the assumption of~~ by irreversible processes. By assuming only reversible processes (i.e., conserved entropy)~~.~~, approximate formulas can be derived (e.g., Emanuel, 1994). However, in the case of large hydrometeors, liquid or solid particles are removed due to gravitational acceleration, leading to an irreversible process, hence the formulas based on the assumption of a reversible process are no longer applicable. Sometimes for this situation a so-called pseudo adiabatic potential temperature is defined, assuming instantaneous removal of hydrometeors from the air parcel; usually, mean-

ingful approximations to this quantity are given, since generally it cannot be derived from first principles. ~~In a strict sense, this is not a conserved quantity, since an irreversible process is considered.~~ Equivalent potential temperature including phase changes for vapour and liquid water is often used for the determination of convective instabilities. The general formulation can be easily adapted for an ice equivalent potential temperature, i.e., for reversible processes in pure ice clouds (see, e.g., Spichtinger, 2014). Although the latent heat of sublimation is larger than the latent heat of vaporisation, the absolute mass content of water vapour decreases exponentially with decreasing temperature, leading to only small corrections due to phase changes in pure ice clouds.

At altitudes above the clouds' top, within the upper troposphere and across the tropopause, the air is substantially dried out compared to tropospheric in-cloud conditions. Therefore, above clouds and further aloft, e.g., within the stratosphere, the conventional dry-air potential temperature may suffice to provide a meaningful vertical coordinate. Moreover, the potential temperature ~~is~~ or the virtual potential temperature, which includes water vapour, are commonly used as ~~a prognostic variable~~ prognostic variables in numerical models for the formulations of the energy equation (e.g., Skamarock et al., 2005; Skamarock and Klemp, . Thereby, very often both variants, the potential temperature as well as the equivalent potential temperature, are involved to account for dry air situations and cloud conditions.

In any case, the use of the potential temperature requires the following preconditions to be fulfilled:

1. θ should be based on a rigorous derivation to ensure its validity as a function of atmospheric altitude in order not to corrupt its character as a vertical coordinate that allows for appropriately comparing (measured) atmospheric parameters, and

2. θ should approximate to the greatest possible extent the true entropy state of a probed air mass and should preferably account for the implied dependencies on atmospheric variables, even under the assumption that air behaves as an ideal gas,

with the aim that the potential temperature behaves as a rational physical variable. Thus, still abiding by the ideal gas assumption, a re-assessment of the fundamental atmospheric quantity θ is suggested, which is based on the state-of-knowledge of air's thermodynamic properties, and this re-assessed θ is comprehensively examined concerning its ability to hold also for atmospheric conditions above the troposphere.

In principle, the concept of the potential temperature is transferable to all systems of thermally stratified fluids ~~as is~~ such as a planetary gas atmosphere or an ocean, to investigate heat fluxes (advection or diffusion) or the static stability of the fluid. In astrophysics, the potential temperature is used almost identically as in atmospheric sciences to describe dynamic processes and thermodynamic properties (e.g., static stability or vorticity) in the atmosphere of planets other than the Earth. Here, the same value $p_0 = 1000\,\mathrm{hPa}$, as applied to the Earth's atmosphere, is frequently used as a reference pressure for the atmosphere of other planets (Catling, 2015, Table 4), whereby the formulations of the specific heat capacity require adaptations to account for the individual gas composition of the respective planetary atmosphere. ~~The~~ In order to simulate the weather in the atmosphere of other planets, the Weather Research and Forecasting model (WRF) was extended to "planetWRF" ~~to simulate the weather in the atmosphere of other planets. Here,~~ (Richardson et al., 2007) and the governing equations considered within

the WRF model include a prognostic equation for the potential temperature ~~is included in the prognostic model equations (Richardson et al., 2007), while it was pointed out by Li and Chen (2019) that this approach could suffer from not accounting for the temperature dependence~~ (Skamarock et al., 2005; Skamarock and Klemp, 2008). However, the temperature dependency of the isobaric ~~specific~~ heat capacity c_p ~~of the respective atmosphere's gas composition~~is not generally negligible, especially when taking "deep atmospheres, such as on Venus" (Catling, 2015, p. 436) into account or the temperature lapse rates on other planets (Li et al., 2018). The atmosphere of ~~Jupiter~~Saturn's moon Titan, the only known moon with a substantial atmosphere, was comprehensively studied with frequent application of the potential temperature based on profile measurement of temperature and pressure in Titan's atmosphere by the ~~Huygens-probe (Müller-Wodarg et al., 2014).~~ Huygens probe (Müller-Wodarg et al., 2014).

Moreover, the potential temperature is a frequently used quantity in oceanography (e.g., McDougall et al., 2003; Feistel, 2008), while here the consideration of sea water's salinity and its impact on the specific heat capacity of sea water implies additional complexity. In particular, McDougall et al. (2003) suggests a re-assessment of the potential temperature as applied in oceanography to approximate the adiabatic lapse rate, thus this study bears certain parallels to the present investigation aiming at the reappraisal of the potential temperature for atmosphere-related purposes. These studies from other disciplines motivate the need for a re-assessment of the potential temperature for the atmospheric sciences. Thus, the approach provided herein proposes a modified calculation of the widely used quantity of the potential temperature by additionally accounting for the current state of knowledge concerning air's properties.

The study is organised as follows: The derivation of the potential temperature for an ideal gas with constant specific heat capacity c_p is recalled in Section 2. In Section 3 the assumption of a constant c_p is discussed together with a synopsis of various c_p values as provided in the literature. The temperature dependency of c_p is examined in Section 4 and a parameterisation is given. Section 5 is devoted to the definition and computation of a new reference potential temperature θ_{ref} based on the temperature-dependent specific heat capacity, while Section 6 focuses on the influence of real-gas effects on the resulting potential temperature. Section 7 presents some implications of the use of θ_{ref} and concluding remarks are given in Section 8.

2 Derivation of the potential temperature for an ideal gas

The Gibbs equation (see, e.g., Kondepudi and Prigogine, 1998) is a general thermodynamic relation to describe the state of a system with m components and reads as

$$T\,\mathrm{d}S = \mathrm{d}H - V\,\mathrm{d}p - \sum_{k=1}^{m} \mu_k\,\mathrm{d}M_k, \tag{3}$$

where T denotes the absolute temperature in K, S the entropy in $\mathrm{J\,K^{-1}}$, H the enthalpy in J, V the volume in $\mathrm{m^3}$, μ_k the chemical potential of component k in $\mathrm{J\,kg^{-1}}$, M_k the mass of component k in kg, and p the static pressure in Pa. Assuming no phase conversion or chemical reaction within the system, the mass of each component does not change, hence $\mathrm{d}M_k = 0$ for each component k.

In the following, dry air is assumed to be the single component in the system. Expressing the Gibbs equation in its specific form (i.e., division by the total mass M_a of dry air; note, lowercase letters indicate specific variables, e.g., $h = H/M_a$, etc.) leads to

$$T\,\mathrm{d}s = \mathrm{d}h - \frac{V}{M_a}\,\mathrm{d}p \quad \Leftrightarrow \quad \mathrm{d}s = \frac{1}{T}\,\mathrm{d}h - \frac{V}{M_a T}\,\mathrm{d}p. \tag{4}$$

Furthermore, approximating dry air as an ideal gas leads to the following simplifications:

- The ideal gas law

$$pV = M_a R_a T \tag{5}$$

can be applied with the specific gas constant R_a of dry air, which is

$$\begin{aligned} R_a &= \frac{R}{M_{\mathrm{mol},a}} \\ &= \frac{8.31446261815324\,\mathrm{J\,mol^{-1}K^{-1}}}{0.0289586\,\mathrm{kg\,mol^{-1}} \pm 0.0000002\,\mathrm{kg\,mol^{-1}}} \\ &\in \left[287.11350\,\mathrm{J\,kg^{-1}K^{-1}}, 287.11748\,\mathrm{J\,kg^{-1}K^{-1}}\right], \end{aligned} \tag{6}$$

~~where R is~~ with the molar gas constant R in $\mathrm{J\,mol^{-1}K^{-1}}$ (Tiesinga et al., 2020; Newell et al., 2018) and $M_{\mathrm{mol},a}$ ~~is~~ the molar mass of dry air (Lemmon et al., 2000), composed of nitrogen $\mathrm{N_2}$, oxygen $\mathrm{O_2}$, and argon Ar.

- The specific enthalpy is given by

$$\mathrm{d}h = c_p\,\mathrm{d}T \tag{7}$$

with c_p the specific heat capacity of dry air.

Based on these assumptions, the change of the specific entropy (within the fluid *dry air*) is given by

$$\mathrm{d}s = \frac{c_p}{T}\,\mathrm{d}T - R_a\frac{\mathrm{d}p}{p}. \tag{8}$$

For isentropic changes of state, i.e., $\mathrm{d}s = 0$, equation (8) reduces to

$$\frac{c_p}{T}\,\mathrm{d}T = R_a\frac{\mathrm{d}p}{p}. \tag{9}$$

Note that the assumption of dry air being an ideal gas does not imply that in (9) the specific heat capacity c_p is constant. While statistical mechanics excludes any pressure dependence in the ideal-gas heat capacity, the general derivation (cf. Appendix A) permits a temperature dependence of c_p. However, usually the temperature dependence is neglected in atmospheric physics and, instead, c_p is assumed as constant (see, e.g., Ambaum, 2010, page 48/49, where vibrational modes of the air molecules are neglected). Immediately below and in Section 3, the treatment of c_p as a temperature-independent constant is discussed. The introduction of the temperature dependence then follows in Section 4.

Treating c_p as a constant, rearrangement of (9) leads to

$$\frac{\mathrm{d}T}{T} = \frac{R_a}{c_p}\frac{\mathrm{d}p}{p}. \tag{10}$$

Integration of (10) over the range from ground-level pressure and temperature (p_0, T_0) to the pressure and temperature at a specific height (p, T) yields

$$\ln\left(\frac{T}{T_0}\right) = \int_{T_0}^{T} \frac{\mathrm{d}T'}{T'} = \frac{R_a}{c_p}\int_{p_0}^{p} \frac{\mathrm{d}p'}{p'} = \frac{R_a}{c_p}\ln\left(\frac{p}{p_0}\right), \tag{11}$$

and, after another straightforward conversion, one arrives at

$$\ln\left(\frac{T_0}{T}\right) = \frac{R_a}{c_p}\ln\left(\frac{p_0}{p}\right). \tag{12}$$

With the definition $\theta_{c_p} = T_0$, equation (12) is transformed into the commonly used expression for determining the potential temperature

$$\theta_{c_p} = T\left(\frac{p_0}{p}\right)^{\frac{R_a}{c_p}}, \tag{13}$$

for which the ground-level pressure p_0 is arbitrary but usually set to $p_0 = 1000\,\mathrm{hPa}$. This choice coincides with the definition of the World Meteorological Organisation (WMO, 1966) and the standard-state pressure (Tiesinga et al., 2020), but should not be confused with the standard atmosphere $101325\,\mathrm{Pa}$ (Tiesinga et al., 2020). In the following, θ_{c_p} denotes the potential temperature based on a constant c_p and, when a specific value of c_p is applied, the subscript c_p in the potential temperature's notation is replaced by the corresponding c_p value.

3 Examining the assumption of constant c_p for dry air

The general theory of thermodynamics, assuming dry air as an ideal gas, gives the expression

$$c_p = \left(1 + \frac{f}{2}\right) R_a \tag{14}$$

for the constant specific heat capacity, which is based on the results of statistical mechanics and the equipartition theorem (e.g., Huang, 1987). In (14), the parameter $f = f_{\mathrm{trans}} + f_{\mathrm{rot}} + f_{\mathrm{vib}}$ is equal to the total number of degrees of freedom of the gas molecules of which dry air consists. The individual contributions to f comprise the degrees of freedom of translation f_{trans}, rotation f_{rot}, and vibration f_{vib}. Assuming further that dry air exclusively consists of the linear molecules $\mathrm{N_2}$ and $\mathrm{O_2}$ (implying $f_{\mathrm{trans}} = 3$ and $f_{\mathrm{rot}} = 2$, while the contribution of Ar remains disregarded) and additionally neglecting the vibrational degrees of freedom ($f_{\mathrm{vib}} = 0$), the general relation (14) reduces to

$$c_p = \left(1 + \frac{3+2}{2}\right) R_a = \frac{7}{2} R_a. \tag{15}$$

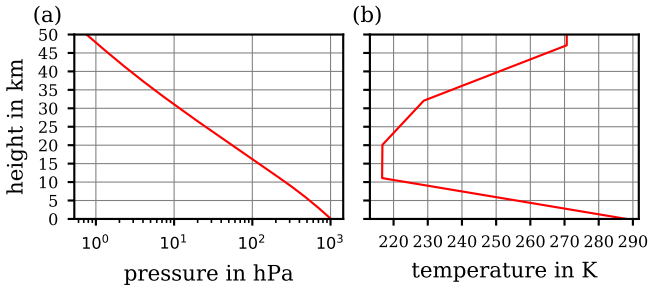

Figure 1. Vertical profiles of (a) atmospheric pressure and (b) temperature as functions of height, corresponding to the US Standard Atmosphere.

Although the neglect of vibrational excitation, particularly at very low temperatures, seems plausible and appropriate, errors are already introduced by this assumption for the temperature range relevant in the atmosphere.

In atmospheric sciences, for the majority of computations that require the specific heat capacity of dry air, a constant value of c_p may be appropriate. According to the WMO (1966), the recommended value for c_p of dry air is $1005\,\mathrm{J\,kg^{-1}K^{-1}}$ and, furthermore (*ibid.*), it is defined that $\gamma = \frac{c_p}{c_v} = \frac{7}{5} = 1.4$, cf. (1). This definition is consistent with the general thermodynamic theory together with all aforementioned additional assumptions and results in (15) as well.

Even assuming a universally valid constant c_p, a single consistently used value of c_p was not found. Instead, the specified values of c_p vary among different textbooks and other sources. In Table 1, some of the available values of constant specific heat capacity for dry air are compiled, indicating a variability of c_p that ranges from $994\,\mathrm{J\,kg^{-1}K^{-1}}$ to $1011\,\mathrm{J\,kg^{-1}K^{-1}}$. However, the extremes in Table 1 are from old references of historical interest only; to reflect recently stated values the narrower range $1000\,\mathrm{J\,kg^{-1}K^{-1}}$ to $1010\,\mathrm{J\,kg^{-1}K^{-1}}$ is considered.

These different values of constant c_p scatter within a small range (below $\pm 1.1\,\%$) around the WMO's recommendation $1005\,\mathrm{J\,kg^{-1}K^{-1}}$, which may seem negligible if c_p contributes only as a linear coefficient within an equation ~~(e.g., in the expression of the c~~ ~~. Unfortunately, however~~(e.g., in the expression of a correction factor, cf. Weigel et al., 2016). However, in the formulation of the potential temperature θ_{c_p}, cf. (13), the specific heat capacity c_p does not contribute linearly but rather as the denominator in the exponent. Thus, the variety of different c_p values, although scattering within a small range, ~~impacts~~ impact the resulting θ_{c_p} significantly. To ~~quantify~~ illustrate this impact, a computation of θ_{c_p} by using (13) was based on the values of static pressure (p, cf. Figure 1a) and absolute temperature (T, cf. Figure 1b) corresponding to the US Standard Atmosphere (United States Committee on Extension to the Standard Atmosphere, 1976).

~~Vertical profiles of (a) atmospheric pressure and (b) temperature as functions of height, corresponding to the US Standard Atmosphere.~~

From the list of the different ~~c_p (cf. Table 1), two~~ c_p in Table 1, the extreme values were selected ~~, namely $994\,\mathrm{J\,kg^{-1}K^{-1}}$ (Wegener and Wegener, 1935) and $1011\,\mathrm{J\,kg^{-1}K^{-1}}$ (WMO, 1966),~~ in order to initially illustrate the sensitivity of the resulting θ_{c_p} to variations in c_p in the range of ~~$\sim 1\%$, as referenced by literature. Specific distinctions will be discussed at a later stage, then mainly in relationship to the commonly used recommendation of the WMO ($c_p = 1005\,\mathrm{J\,kg^{-1}K^{-1}}$, WMO, 1966)~~ $\sim 1\,\%$,

constant dry air's specific heat capacity c_p in $\mathrm{J\,kg^{-1}K^{-1}}$	literature source
994	~~Wegener and Wegener (1935) (converted from units other than SI)~~Wegener and Wegener (1935, converted from units other than SI)
1000	~~Vallis (2006)~~~~Roedel and Wagner (2011)~~ Roedel and Wagner (2011, page 66)
1003	"minimum of range of actual values" (WMO, 1966) ~~Tripoli and Cotton (1981)~~ Tripoli and Cotton (1981, the appendix therein)
1004	~~Holton (2004)~~Holton (2004, page 491) ~~Wallace and Hobbs (2006)~~Wallace and Hobbs (2006, page 75) Schumann (2012) ~~Wendisch and Brenguier (2013)~~ Wendisch and Brenguier (2013, page 24) Liou (2002, appendix F) Ambaum (2010, table "Useful Data")
1004.8	~~Pruppacher and Klett (2010)(converted from units other than SI)~~ Pruppacher and Klett (2010, converted from units other than SI; p. 489)
1004.86	Curry and Webster (1998, page 62)
1005	recommended by WMO (1966) ~~Bohren et al. (1998)~~Bohren et al. (1998, page 384) ~~Houghton (2002)~~Houghton (2002, page 275) ~~Zdunkowski and Bott (2003)~~Zdunkowski and Bott (2003, page 705) ~~Brasseur and Solomon (2005)~~Brasseur and Solomon (2005, page 426) ~~Seinfeld and Pandis (2006)~~Seinfeld and Pandis (2006, page 1178) ~~Cotton et al. (2011)~~ Cotton et al. (2011, table 2.1)
1005.7 ± 2.5	Bolton (1980) ~~Emanuel (1994)~~ Emanuel (1994, appendix 2)
1006	~~Wendisch and Brenguier (2013)~~Wendisch and Brenguier (2013, page 69) ~~(potential typo on p.69, a smaller value, cf. above, is given on p.24 and in the list of constants)~~ Stamnes et al. (2017, page 14)
1010	Chang et al. (2006) Tiwary and Williams (2019, beneath eq. 8.8; possibly a typo, as indicated by inconsistencies on reproducing t Brusseau et al. (2019, page 59)

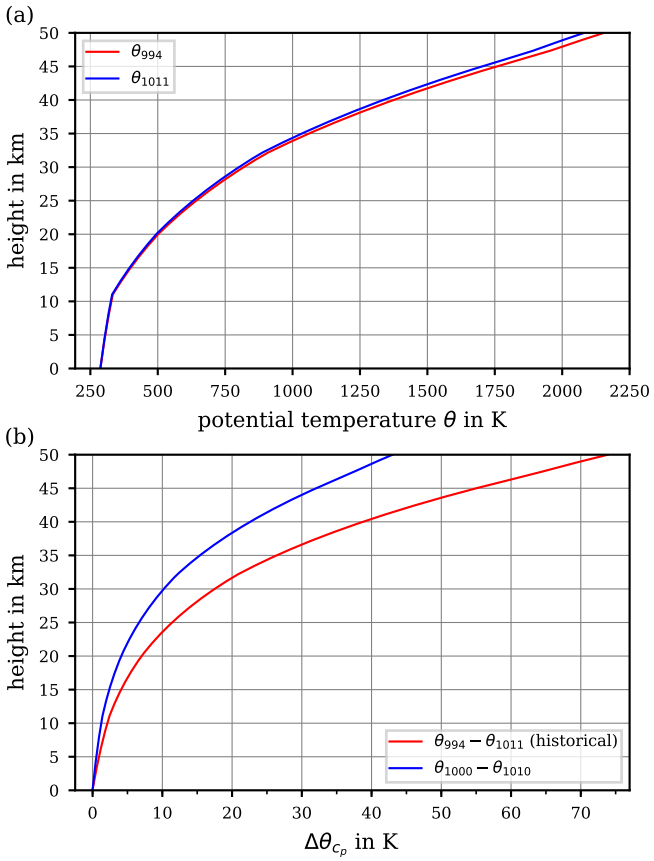

Figure 2. Computed vertical course of the potential temperature θ_{c_p} based on the two extremes of constant values for the specific heat capacity c_p provided in the literature including the historical extreme values (panel (a); cf. Table 1), and (b) the absolute differences $\Delta\theta_{c_p} = \theta_{994} - \theta_{1011}$ and $\Delta\theta_{c_p} = \theta_{1000} - \theta_{1010}$ between the two resulting curves of θ_{c_p}.

as seen in the literature. In Figure 2a, the individual profiles of ~~θ_{c_p} are shown , and panel (b)exhibits the absolute difference $\Delta\theta_{c_p} = \theta_{994} - \theta_{1011}$, based on the~~ θ_{c_p} are shown for the extremes of the historic c_p ~~values selected.~~ values (Table 1), while Figure 2b illustrates the absolute differences $\Delta\theta_{c_p} = \theta_{1000} - \theta_{1010}$ (blue curve) and $\Delta\theta_{c_p} = \theta_{994} - \theta_{1011}$ (red curve). The absolute error exhibited with the blue curve in Figure 2b ~~shows the sensitive response of calculated θ_{c_p} to a small variability in c_p~~is based on the extremes of most recently referred c_p values in the literature (Table 1). At an altitude of ~~5 km~~8.5 km, the difference $\Delta\theta_{c_p}$ already exceeds 1 K (blue curve). The values of $\Delta\theta_{c_p}$ reach approximately ~~2.5 K~~ 1.2 K at 10 km ~~altitude~~ and rise further, above ~~7 K~~4 K, with increasing altitude up to 20 km. At 50 km, approximately where the stratopause is located, which is the chosen upper height limit for this investigation, the computed $\Delta\theta_{c_p}$ reaches ~~almost 75 K~~43 K.

Figure 2 illustrates the possible spread of θ_{c_p} based on a range of c_p values from different literature references; hence, if one uses a different value for c_p from the literature than that defined by WMO (1966), the difference $\theta_{1005} - \theta_{c_p}$ might be significant. Since the c_p values provided by some literature references are close to the recommended value $c_p = 1005\,\mathrm{J\,kg^{-1}K^{-1}}$

by the WMO (1966), the subsequent comparisons will be made to θ_{1005}. The θ_{c_p}, which are based on the computation with c_p values other than $1005\,\mathrm{J\,kg^{-1}K^{-1}}$ are only used to illustrate respective deviations. Although the curves in Figure 2b depict extremes in the deviation of potential temperatures, as they are based on the extremes of c_p values (cf. Table 1), they nevertheless illustrate the sensitive response of θ_{c_p} to even small variations in c_p, on the order of $\sim 1\,\%$. Further proof of this sensitivity from the mathematical perspective is provided in Appendix B. The impact of this sensitivity becomes important at altitudes of $\sim 10\,\mathrm{km}$ and above, thus, where the use of the potential temperature becomes increasingly meaningful. Here, and in particular above the cloud tops, the small-scale and comparatively fast tropospheric dynamics (causing vertical transport and implying diabatic processes) become diminished, while further above, towards the stratosphere, an increasingly layered vertical structure of the atmosphere is taking over.

~~Computed vertical course of the potential temperature θ_{c_p} based on the two extremes of constant values for the specific heat capacity c_p provided in the literature (panel (a); cf. also Table 1), and (b) the absolute difference $\Delta\theta_{c_p} = \theta_{994} - \theta_{1011}$ between the two resulting curves of θ_{c_p}.~~

~~As discussed~~ As indicated above, the ~~potential temperature is remarkably sensitive~~ reason for this sensitivity to small variations ~~(within the per-cent range)~~ of air's specific heat capacity ~~, as these variations affect~~ is that it affects the exponent of the equation for θ_{c_p}~~; further proof of this, from the mathematical perspective, is provided in Appendix B~~. The studies of Ooyama (1990, 2001) document an interesting attempt to formulate, e.g., the energy balance equations for the moist atmosphere, wherein entropy replaces the more common formulation using the potential temperature. This substitution avoids the use of the potential temperature, which "is merely an exponential transform of the entropy expressed in units of temperature" (Ooyama, 2001), thus, within this equation, air's specific heat capacity is implied exclusively as a linear coefficient. Consequently, a parameterisation for the temperature dependence of the specific heat capacity ($c_p(T)$, cf. Section 4) may be easily adopted. However, the crucial drawback of the entropy-based equations is that to gain a numerical model for, e.g., weather forecast purposes, the parameterisations of most of the physical processes within the atmosphere would require a reformulation.

It should be noted that not only do literature values of air's specific heat capacity c_p vary, but also the values of the gas constant R_a vary slightly due to different historical approximations for the molar gas constant[4] R and for the composition of dry air. The variation of values for R_a is typically only on the order of ~~$10^{-1}\,\mathrm{J\,kg^{-1}K^{-1}}$~~$0.1\,\mathrm{J\,kg^{-1}K^{-1}}$, whereas the variability in c_p is on the order of a few $\mathrm{J\,kg^{-1}K^{-1}}$ (cf. Table 1). Therefore, within the exponent of the expression (13) for θ_{c_p}, the variability of c_p has by far a stronger impact on the resulting θ_{c_p} value than the variability of R_a.

However, accepting for a moment the WMO's definition (15) of c_p (WMO, 1966), the variability of air's c_p should naturally be constrained to certain limits. With the specific gas constant $R_a = 287.05\,\mathrm{J\,kg^{-1}K^{-1}}$ (WMO, 1966), the WMO's definition leads to $c_p = 1004.675\,\mathrm{J\,kg^{-1}K^{-1}}$. In contrast, taking into account the uncertainty introduced in R_a by the molar mass of dry air, cf. Equation (6), the resulting range for air's specific heat capacity is $1004.897\,\mathrm{J\,kg^{-1}K^{-1}} \leq c_p \leq 1004.912\,\mathrm{J\,kg^{-1}K^{-1}}$. It may be surmised that the rounded value $c_p = 1005\,\mathrm{J\,kg^{-1}K^{-1}}$ as recommended by the WMO (1966) had the main goal to simplify certain calculations, which at the time may have been mostly done by hand.

[4] The value of R is now defined exactly, cf. Tiesinga et al. (2020); Newell et al. (2018) and is used in Equation (6).

4 Accounting for the temperature dependence of air's specific heat capacity

Next, while retaining the ideal-gas assumption, we consider the dependence of air's c_p on temperature, mainly over the atmospherically relevant range (180 K to 300 K). The temperature dependence of c_p is, of course, not a new finding. Experimental approaches for determining the calorimetric properties of air and the temperature dependence of a fluid's specific heat capacity are described by Witkowski (1896), who investigated the change of the mean c_p as a function of temperature intervals between room temperature (as a fixed reference) and various warmer and colder temperatures, for atmospheric pressures and slightly beyond. Despite the potentially high uncertainty of the experimental results from these times, Witkowski (1896) already indicated that with decreasing temperature the experimentally determined c_p values initially decline, then pass a minimum, and subsequently increase again at lower temperatures ($T < 170$ K). The description of refined experiments and ascertainable data of air's $c_p(T)$ for temperatures below 293 K is summarised by Scheel and Heuse (1912), Jakob (1923), and Roebuck (1925, 1930), illustrating in comprehensive detail the experimental effort and providing the resulting data. The review by Awano (1936) compiled and compared the data of $c_p(T)$ of dry air ("*air containing neither carbon-dioxide nor steam*", Awano, 1936) and he attested—at that time—the previously mentioned studies to constitute "*the most reliable experiments*". During the decades following these experiments, further insights were gained and landmarks were reached which are summarised in the comprehensive survey by Lemmon et al. (2000) of the progress of modern formulations for the thermodynamic properties of air and about the experiments the previous formulations were based on.

Figure 3 illustrates the range of suggested constant values for the specific heat capacity ~~(see Table 1~~ as indicated in Table 1 (dashed curves) together with the measurements that were made to obtain air's behaviour as a function of temperature and pressure. Note, Figure 3 includes data at other atmospheric pressures, indicated by squares, diamonds, and triangles. In the same figure, calculated values of $c_p(T)$ of dry air are displayed resulting from the equation of state which was derived from experimental p, V, and T data by Vasserman et al. (1966), who provided an extensive review of previous experimental and theoretical works and of the state of knowledge at that time. In addition, Figure 3 exhibits two different parameterisations, by Lemmon et al. (2000) and by ~~Dixon (2007)~~Dixon (2007, see page 376 in his book, the accuracy is "within 0.1 % from 200 K to 450 K"), which account for the temperature dependence of the specific heat capacity $c_p(T)$. The parameterisation by Lemmon et al. (2000), to be discussed in detail in Section 4.2, is valid for dry air assumed as an ideal gas whereas this distinction is not explicitely made in Dixon (2007). Moreover, Figure 3 contains discrete values of dry air's $c_p(T)$ extracted from the database *REFPROP* (Reference Fluid Thermodynamic and Transport Properties Database by NIST, the National Institute of Standards and Technology, Lemmon et al., 2018), which is based on parameterisations resulting from thermodynamic considerations discussed later.

The measurement data, as well as the parameterisations, clearly indicate a dependence of air's specific heat capacity on the temperature. At temperatures above 300 K, the data points by Jakob (1923) are surprisingly well captured by the parameterisations, while below 270 K the course of the parameterised and measured $c_p(T)$ diverge significantly. Possible reasons for this include:

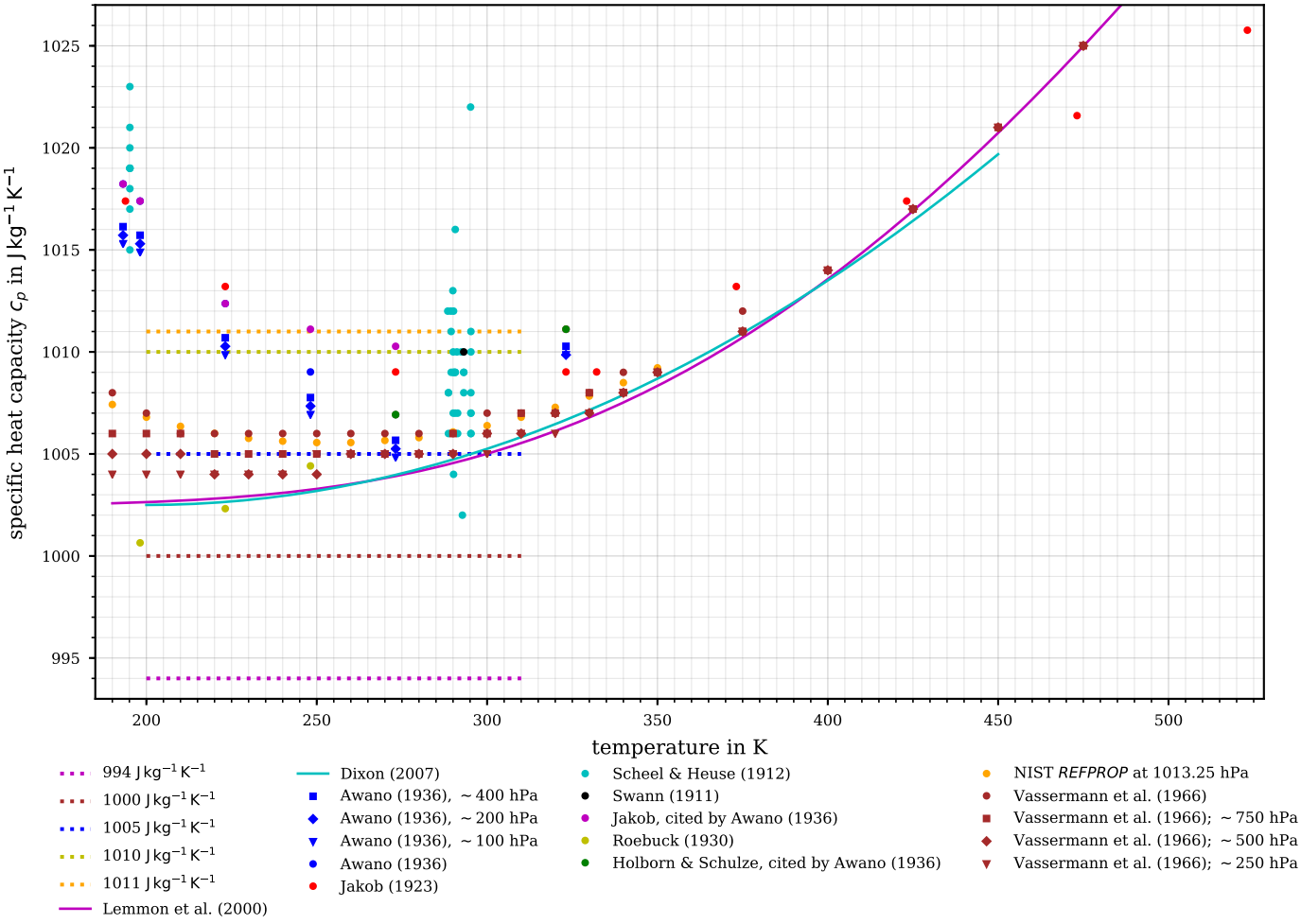

Figure 3. Variety of suggested values for the specific heat capacity of air. ~~Constant values~~ Ranges of constant values for c_p (including the historical) together with the recommended value by the WMO (1966) are displayed ~~over the range documented~~ as given in Table 1 (dashed lines). The parameterisations of air's ~~$c_p(T)$~~ $c_p^0(T)$, assuming dry air as an ideal gas, accounting for its temperature dependence by Lemmon et al. (2000, solid magenta curve) and by Dixon (2007, solid cyan curve) are displayed. Discrete measurement and literature data at about 1000 hPa (i.e., as often specified, at *about one atmosphere*) are indicated by dots. In addition, the studies by Awano (1936) and Vasserman et al. (1966) provide data at other atmospheric pressures, as indicated by squares, diamonds, and triangles.

- the measurements of $c_p(T)$ have a precision likely no better than $1\,\%$ (in particular the historical measurements), and there could be systematic errors, especially at low temperatures;

- the measured data reflect the true thermodynamic behaviour of the real gas, rather than that of an ideal gas.

However, it is immediately obvious from Figure 3 that a good agreement among (i) the experimentally determined $c_p(T)$ data, (ii) a constant c_p (e.g., $1005\,\mathrm{J\,kg^{-1}K^{-1}}$; WMO (1966)), and (iii) the parameterised $c_p(T)$ is found only for a temperature interval ranging from $270\,\mathrm{K}$ to ~~290 K. For all~~ 300 K. For air temperatures below $270\,\mathrm{K}$, the constant value $c_p = 1005\,\mathrm{J\,kg^{-1}K^{-1}}$ is only comparable with the values from Vasserman et al. (1966), but fails to coincide with ~~either the parameterised or the~~ other parameterised or experimentally determined values of $c_p(T)$.

4.1 The temperature dependence of the ideal-gas specific heat capacity

As already indicated by the data depicted in Figure 3, the specific heat capacity c_p depends on the gas temperature. With regard to measured values, the lack of constancy may be due to real-gas effects or to a dependence of the ideal-gas heat capacity on temperature. In this section, we focus on the latter effect, denoting the ideal-gas isobaric specific heat capacity by $c_p^0(T)$, where the superscript 0 indicates the underlying ideal-gas assumption. For an individual gas, there is always a contribution from the three translational degrees of freedom, $c^0_{p,\mathrm{trans}} = \frac{5}{2}R_i$, where R_i is the specific gas constant of the gas. If the molecule is assumed to be a rigid rotor, there is also a rotational contribution given by

$$c^0_{p,\mathrm{rot}} = \begin{cases} R_i, & \text{for linear (e.g., diatomic) molecules,} \\ \frac{3}{2}R_i, & \text{for nonlinear molecules.} \end{cases} \tag{16}$$

As mentioned previously, at finite temperatures molecules also have contributions to $c_p^0(T)$ from intramolecular vibrations (and, at high temperatures, excited electronic states). To arrive at a temperature-dependent parameterisation for the ideal-gas specific heat capacity of dry air, the compounds' individual contributions, considering all degrees of freedom, need to be parameterised and then combined according to each compound's proportion in the mixture. For the following, dry air is considered a three-component mixture: the diatomic gases nitrogen ($\mathrm{N_2}$) and oxygen ($\mathrm{O_2}$) and the monatomic gas argon (Ar).

To determine the contribution of $\mathrm{N_2}$ to $c_p^0(T)$, both Bücker et al. (2002) and Lemmon et al. (2000) use the ideal-gas heat capacity from the reference equation of state of Span et al. (2000) that compares well with the findings from other studies within an uncertainty Δc_p^0 of less than $0.02\,\%$.

For the contribution of $\mathrm{O_2}$, Lemmon et al. (2000) use the formulation given by Schmidt and Wagner (1985). Alternatively, Bücker et al. (2002) provide a slightly different formulation from the International Union of Pure and Applied Chemistry (IUPAC, Wagner and de Reuck, 1987), after refitting it to more recently obtained data, thereby achieving an overall uncertainty Δc_p^0 of less than $\pm 0.015\,\%$ for $\mathrm{O_2}$ (Bücker et al., 2002). However, the difference in the resulting specific heat capacity contribution by $\mathrm{O_2}$ between the two approaches (Lemmon et al. (2000) or Bücker et al. (2002)) is comparatively small.

For a monoatomic gas such as Ar, vibrational and rotational contributions to the heat capacity do not exist, and Bücker et al. (2002) consider that argon's excited electronic states are relevant only at temperatures above $3500\,\mathrm{K}$. Hence, the contribution of ~~argon~~ Ar to the specific heat capacity of air reduces to $c_p^0 = \frac{5}{2} R_{\mathrm{Ar}}$.

The approach by Bücker et al. (2002) additionally considers the contribution of further constituents of air, such as water, carbon monoxide, carbon dioxide, and sulfur dioxide. These authors provide an analytical expression for specific heat capacity, accounting for this more complex but proportionally invariant air composition which is specified to deviate from the used reference by $\Delta c_p^0 \leq \pm 0.015\,\%$ in the temperature range of $200\,\mathrm{K} \leq T \leq 3300\,\mathrm{K}$. At atmospheric altitudes above the clouds' top, i.e., on average above $\sim 11\,\mathrm{km}$, the air is assumed to have lost most of its water and is deemed as dry. Furthermore, for the following, trace gases that contribute to air's composition by molar fractions of less than that of Ar are neglected.

4.2 NIST's parameterisation of $c_p^0(T)$

Besides a comprehensive survey of the available experimental data for the specific heat capacity of air, Lemmon et al. (2000) also provide state-of-the-art knowledge for other thermodynamic properties (isochoric heat capacity, speed of sound, vapour-liquid-equilibrium, etc.). Additionally, they give two approaches to derive air's thermodynamic properties, including the vapour-liquid equilibrium:

1. an empirical model-based *equation of state* for standard (dry) air considered as a pseudo-pure fluid, and
2. assembly of a *mixture model* from equations of state for each pure fluid.

Each approach allows calculating the thermodynamic properties, e.g., c_p, of gas mixtures such as dry air, and both are real-gas models with the ideal-gas behaviour as a boundary condition. The major difference between the models is that the first approach considers air as a pseudo-pure fluid while the second, more rigorous approach treats air as a mixture composed of $\mathrm{N_2}$, $\mathrm{O_2}$, and Ar, in molar fractions of 0.7812, 0.2096, and 0.0092, respectively, following Lemmon et al. (2000, their table 3). This fractional composition of dry air is assumed to be constant from ground level up to $80\,\mathrm{km}$ height (United States Committee on Extension to the Standard Atmosphere, 1976) and its fractional composition would have to be shifted significantly to cause a serious deviation of the resulting potential temperature. The contribution to the composition by carbon dioxide ($\mathrm{CO_2}$) and of any other trace species was assumed to be negligible. The validity of both approaches is specified for various states of dry air, from its solidification point ($59.75\,\mathrm{K}$) up to temperatures of $1000\,\mathrm{K}$, and for pressures up to $100\,\mathrm{MPa}$ and even much further beyond the pressure range that is relevant for atmospheric investigations. Both the pseudo-pure fluid model and the mixture model are implemented in NIST's *REFPROP* database (cf. https://www.nist.gov/srd/refprop) for various physical properties of fluids over a wide range of temperatures and pressures. ~~Lemmon et al. (2000) suggest that their mixture models allow calculation of the specific heat capacity of a gas mixture within an estimated uncertainty of $1\,\%$.~~

Both the pseudo-pure fluid model and the mixture model of Lemmon et al. (2000) use the same expression for the ideal-gas heat capacity, which is rigorously given as a sum of the pure-component contributions:

$$\begin{aligned}\frac{C_p^0(T)}{R} = x_{\mathrm{N_2}} \left(\frac{C_p^0(T)}{R}\right)_{\mathrm{N_2}} + x_{\mathrm{Ar}} \left(\frac{C_p^0(T)}{R}\right)_{\mathrm{Ar}} \\ + x_{\mathrm{O_2}} \left(\frac{C_p^0(T)}{R}\right)_{\mathrm{O_2}},\end{aligned} \tag{17}$$

where x_i denotes the molar fraction of species i, and C_p^0 as well as the molar gas constant R are given in units of $\mathrm{J\,mol^{-1}K^{-1}}$.

Like Bücker et al. (2002), Lemmon et al. (2000) use the expression of Span et al. (2000) for the contribution of $\mathrm{N_2}$ to the heat capacity and adopt $C_p^0 = \frac{5}{2}R$ for Ar. Together with the contribution by $\mathrm{O_2}$ according to the formulation by Schmidt and Wagner (1985), the expression provided by ~~Lemmon et al. (2000)~~ Lemmon et al. (2000, equation 18 therein) for the ideal-gas heat capacity of dry air is

$$\begin{aligned}\frac{C_p^0(T)}{R} = N_1 + N_2 T + N_3 T^2 + N_4 T^3 + N_5 T^{-\frac{3}{2}} \\ + N_6 \frac{\frac{N_9^2}{T^2}\exp\left(\frac{N_9}{T}\right)}{\left(\exp\left(\frac{N_9}{T}\right)-1\right)^2} + N_7 \frac{\frac{N_{10}^2}{T^2}\exp\left(\frac{N_{10}}{T}\right)}{\left(\exp\left(\frac{N_{10}}{T}\right)-1\right)^2} \\ + \frac{2N_8}{3} \frac{\frac{N_{11}^2}{T^2}\exp\left(-\frac{N_{11}}{T}\right)}{\left(\frac{2}{3}\exp\left(-\frac{N_{11}}{T}\right)+1\right)^2},\end{aligned} \tag{18}$$

with the scalar coefficients N_i for dry air (*ibid.*),

$$\begin{aligned} N_1 &= 3.490888032, & N_2 &= 2.395525583 \cdot 10^{-6}, \\ N_3 &= 7.172111248 \cdot 10^{-9}, & N_4 &= -3.115413101 \cdot 10^{-13}, \\ N_5 &= 0.223806688, & N_6 &= 0.791309509, \\ N_7 &= 0.212236768, & N_8 &= 0.197938904, \\ N_9 &= 3364.011, & N_{10} &= 2242.45, \\ N_{11} &= 11580.4, \end{aligned} \tag{19}$$

which is specified as valid for temperatures from 60 K to 2000 K. Because the underlying calculations are based on rigorous statistical mechanics and accurate spectroscopic data, $\frac{C_p^0(T)}{R}$ should be accurate to within 0.01 % throughout this range, as discussed by Span et al. (2000).

The parameterisation (18) provides the isobaric specific heat capacity of dry air, considered as a mixture of ideal gases. This represents a more rigorous and accurate behaviour than assuming it to be a constant.

4.3 The parameterisation of $c_p^0(T)$ from an engineer's perspective

The parameterisation from Dixon (2007)

$$c_p(T) = 1002.5 + 275 \cdot 10^{-6} \cdot (T - 200)^2 \tag{20}$$

for $200\,\mathrm{K} \leq T \leq 450\,\mathrm{K}$ is not explicitly described to be based on particular assumptions or data sets. The author indicates his suggested parameterisation to hold within $0.1\,\%$ for temperatures between $200\,\mathrm{K}$ and $450\,\mathrm{K}$. For elevated air temperatures, the deviation between the ideal-gas limit $c_p^0(T)$ (Lemmon et al., 2000) and Dixon's parameterisation substantially increases. This is most likely due to the chosen type of polynomial approximation (Dixon, 2007), which increasingly departs from the reference $c_p^0(T)$ for gas temperatures exceeding $450\,\mathrm{K}$.

Concerning the thermophysical properties of humid air, the study by Tsilingiris (2008) provides further insight. Its purpose was to evaluate the transport properties as a function of different levels of the relative humidity and as a function of temperature (from $273\,\mathrm{K}$ to $373\,\mathrm{K}$) for the gas mixture of air with water vapour at a constant pressure ($1013\,\mathrm{hPa}$). The atmospherically relevant pressure range below $1013\,\mathrm{hPa}$ and temperatures smaller than $273\,\mathrm{K}$ were not considered. Although this study focused on providing a comprehensive account of moisture within air, mainly for technical purposes and engineering calculations, the possible usefulness of these findings to atmospheric investigations is also apparent. However, the impact of water vapour on the resulting gas mixture's $c_p(T)$ is significantly larger (cf. Tsilingiris, 2008) than the uncertainty of dry air's $c_p(T)$ that is discussed in the present work. Furthermore, the consideration of water vapour as a component of air requires very individual and case-specific computations of $c_p(T)$ of moist air, as water vapour is among the most variable constituents of the atmosphere.

The effort required to produce an analytical formulation for gas properties which best reflects the true gas behaviour may indicate that for engineering purposes (pneumatic shock absorbers, engines' combustion efficiency, improvements of turbofan/-prop propulsion, aerodynamics, material sciences, etc.), especially where pressures exceed atmospheric, the assumption of ideal-gas behaviour introduces excessive uncertainty.

5 The $\theta_{c_p(T)}$ from the temperature-dependent specific heat capacity of air

Previously introduced approaches for computing the specific heat capacity of dry air call for a brief discussion on how to use the obtained $c_p(T)$ to derive the potential temperature. In the following, $\theta_{c_p(T)}$ denotes the derived potential temperature that accounts for the temperature dependence of dry air's specific heat capacity. Furthermore, it should be noted that simply substituting any $c_p(T)$ value into the conventionally used and defining equation (13) for θ_{c_p} (WMO, 1966) may appear ~~seductive~~ tempting but definitely leads to results inconsistent with $\theta_{c_p(T)}$ that is based on the reference parameterisation of dry air's $c_p(T)$. Therefore, the thermodynamically consistent use of $c_p(T)$ in the derivation of θ is described in the following.

5.1 Derivation of $\theta_{c_p(T)}$ based on the temperature-dependent specific heat capacity of dry air

In the derivation of the potential temperature (cf. Section 2), we note that, until reaching the expression for isentropic changes of state (9), no specific assumption was made about the specific heat capacity. As soon as the temperature dependence of the specific heat capacity comes into play, the re-assessment of (9) leads to

$$\frac{c_p(T)}{T}\,\mathrm{d}T = R_a \frac{\mathrm{d}p}{p}. \tag{21}$$

Integration of (21) from the basic state $(p_0, \theta_{c_p(T)})$ to any other state (p, T) yields

$$R_a \ln\left(\frac{p}{p_0}\right) = R_a \int_{p_0}^{p} \frac{\mathrm{d}p'}{p'} = \int_{\theta_{c_p(T)}}^{T} \frac{c_p(z)}{z} \frac{c_p(T')}{T'} \,\mathrm{d}z T', \tag{22}$$

where $\theta_{c_p(T)}$ is the desired potential temperature.

The rearrangement of (22) makes evident that the desired potential temperature is a zero of the function $F(x)$, given by

$$F(x) = \int_{x}^{T} \frac{c_p(z)}{z} \frac{c_p(T')}{T'} \,\mathrm{d}z - T' - R_a \ln\left(\frac{p}{p_0}\right). \tag{23}$$

To arrive at the desired potential temperature $\theta_{c_p(T)}$ for any given temperature and pressure, the equation $0 = F(x)$ must be solved for the variable x, which is the desired $\theta_{c_p(T)}$. Equation (23) has at most only one real zero, since its integrand is strictly positive which means $F(x)$ is strictly monotonic.

In the following, the ideal-gas reference potential temperature θ_{ref} is introduced, based on the formulation of the ideal-gas limit of dry air's specific heat capacity $c_p^0(T)$ in accordance with (18) as formulated by Lemmon et al. (2000). This reference potential temperature θ_{ref} represents the zero of $F(x)$ in (23), wherein ~~$c_p(z)$~~ $c_p(T')$ is to be replaced by ~~$c_p^0(T)$~~ $c_p^0(T')$. The parameterisation of $c_p^0(T')$ is stated to give accurate values for temperatures from 60 K to 2000 K (cf. Section 4.2), thus values of θ_{ref} should not exceed 2000 K, since otherwise $c_p^0(T')$ within the integrand in (23) is evaluated outside of its range of validity. However, due to the division by T', the value of the integrand $\frac{c_p^0(T')}{T'}$ may be expected to give nevertheless a good approximation even if the accuracy of $c_p^0(T')$ is decreased, hence values $\theta_{\mathrm{ref}} > 2000\,\mathrm{K}$ should not be discarded.

It may be noted that further variants of a reference potential temperature are derivable by replacing ~~$c_p(z)$~~ $c_p(T')$ in (23) by any other expression of the specific heat capacity of air which may appear sufficiently accurate. The steps to compute or approximate the zero of the function (23), described in this study, are independent of the chosen heat capacity formulation.

Unfortunately, for a straightforward solution of the integral (23), the suggested parameterisation of c_p is too complex and an analytically insolvable nonlinear equation $0 = F(x)$ could result. Thus, an approximation of the equation's desired zero is required. Newton's method (cf., e.g., Deuflhard, 2011) provides a standard approach to numerically approximate the zero of a nonlinear equation. Proceeding from an initial guess x_0, Newton's method constructs a sequence $\{x_k\}_{k\in\mathbb{N}}$ defined by the recursion

$$\begin{aligned} x_{k+1} &= x_k - \frac{F(x_k)}{F'(x_k)} = x_k - \frac{F(x_k)}{-\frac{c_p(x_k)}{x_k}} \\ &= \frac{x_k}{c_p(x_k)} \left[c_p(x_k) + F(x_k)\right] \\ &= \frac{x_k}{c_p(x_k)} \left[c_p(x_k) - R_a \ln\left(\frac{p}{p_0}\right) + \int_{x_k}^{T} \frac{c_p(T')}{T'} \,\mathrm{d}T'\right]. \end{aligned} \tag{24}$$

The constructed sequence $\{x_k\}_{k\in\mathbb{N}}$ converges to the equation's desired zero. For the herein described computations, the iteration is stopped as soon as the absolute difference $|x_{k+1} - x_k|$ of two consecutive iterations falls below $10^{-8}\,\mathrm{K}$.

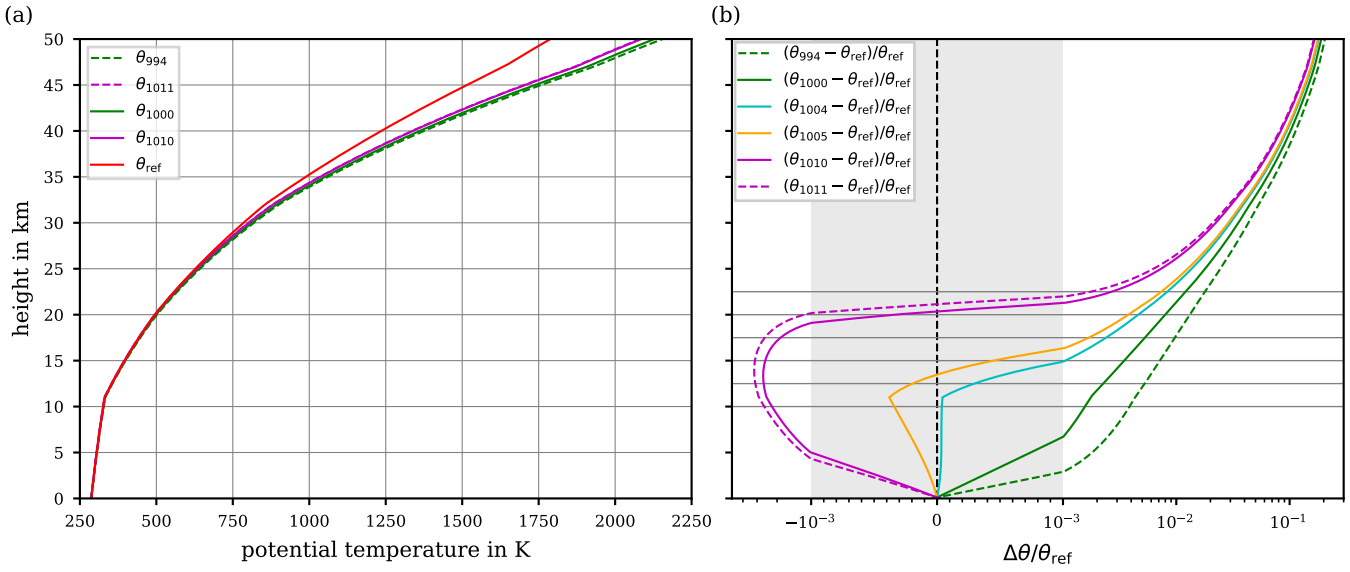

Figure 4. (a) Reference potential temperature θ_{ref} together with the potential temperatures ~~θ_{994}~~ $\theta_{994}, \theta_{1000}, \theta_{1010}$ and θ_{1011} relying on constant c_p values (~~e.g. 994 and 1011 J kg^{-1}K^{-1}~~ the dashed lines depict the historical extremes for c_p, cf. Table 1). (b) Relative differences ~~$(\theta_{994}-\theta_{\mathrm{ref}})/\theta_{\mathrm{ref}}$ and $(\theta_{1011}-\theta_{\mathrm{ref}})/\theta_{\mathrm{ref}}$~~ $(\theta_{c_p}-\theta_{\mathrm{ref}})/\theta_{\mathrm{ref}}$ for the same choices $c_p \in \{994\,\mathrm{J\,kg^{-1}K^{-1}}, 1000\,\mathrm{J\,kg^{-1}K^{-1}}, 1010\,\mathrm{J\,kg^{-1}K^{-1}}, 1011\,\mathrm{J\,kg^{-1}K^{-1}}\}$ as in the left panel between the reference potential temperature and the potential temperatures relying on constant c_p values. For comparison, ~~also~~ the relative difference $(\theta_{1005}-\theta_{\mathrm{ref}})/\theta_{\mathrm{ref}}$ is displayed, for which $c_p = 1005\,\mathrm{J\,kg^{-1}K^{-1}}$ corresponds to the WMO recommendation. In addition, also a comparison with θ_{1004} is included. All profiles are based on the values for temperature and pressure according to the US Standard Atmosphere. Note the linear axis-scaling inside and the logarithmic scaling outside of the grey-shaded area in panel (b).

For the reference of air's specific heat capacity, $c_p^0(T)$, the integral (23) turns out not to be explicitly solvable. Therefore, with each iteration, the solution of the integral $\int_{x_k}^{T} \frac{c_p^0(z)}{z}\,\mathrm{d}z$ ~~$\mathrm{d}z$~~ $\int_{x_k}^{T} \frac{c_p^0(T')}{T'}\,\mathrm{d}T'$ is approximated by subdividing the entire integration range, $[x_k, T]$, into intermediate intervals with respective size of at most $0.1\,\mathrm{K}$, and by applying Simpson's rule on each subinterval.

As a first guess x_0 for the Newton iteration, the conventional definition of θ_{c_p} based on a constant specific heat capacity (WMO, 1966) is inserted:

$$x_0 = T\left(\frac{p_0}{p}\right)^{\frac{R_a}{1005\,\mathrm{J\,kg^{-1}K^{-1}}}} = \theta_{1005}. \tag{25}$$

In the course of Newton's method, the sequence $\{x_k\}_{k\in\mathbb{N}}$ will converge to the unique zero for any initial guess x_0 due to the monotonicity of $F(x)$. However, the right choice of the initial guess x_0 substantially decreases the error of the first iteration x_1, speeding up convergence to the desired zero of the function $F(x)$. Therefore, it may be comprehensible to use the conventional definition of θ_{c_p} as the first guess for the Newton iteration (24).

Solving the previously described root-finding problem by Newton's method over the comprehensive range of iteration steps (until the set requirement, i.e., $|x_{k+1}-x_k| < 10^{-8}\,\mathrm{K}$, is fulfilled) finally leads to the reference potential temperature θ_{ref}.

This θ_{ref} is based on the ideal-gas limit of dry air's specific heat capacity $c_p^0(T)$, which refers to the current thermodynamic state-of-knowledge and, thus, we use θ_{ref} as our reference for the potential temperature in the following. For evaluating the results, the air temperature and pressure from the US Standard Atmosphere are used once more to set up the vertical profiles of the potential temperature. Figure 4a exhibits the resulting reference profile, i.e., θ_{ref} (red curve). Additionally, for comparison with the reference, further potential temperature profiles θ_{c_p} are shown based on ~~two extremes~~ the two (historical) extremes $c_p = 994\,\mathrm{J\,kg^{-1}K^{-1}}$ and $c_p = 1011\,\mathrm{J\,kg^{-1}K^{-1}}$ (dashed curves), and based on the range limits of more recent values $c_p = 1000\,\mathrm{J\,kg^{-1}K^{-1}}$ and $c_p = 1010\,\mathrm{J\,kg^{-1}K^{-1}}$ (solid green and magenta curves) of given constant values of air's specific heat capacity (cf. Table 1)~~, $c_p = 994\,\mathrm{J\,kg^{-1}K^{-1}}$ and $c_p = 1011\,\mathrm{J\,kg^{-1}K^{-1}}$~~. Clearly, in particular at elevated altitudes, the courses of ~~θ_{994} and θ_{1011}~~ θ_{1000} and θ_{1010} significantly deviate from the reference. To quantitatively evaluate the match between the different profiles, the relative difference of the ~~four profiles , θ_{994}, θ_{1004}, θ_{1005} and θ_{1011},~~ profiles based on a constant c_p, with respect to the reference, i.e., $\Delta\theta/\theta_{\mathrm{ref}} = \left(\theta_{c_p} - \theta_{\mathrm{ref}}\right)/\theta_{\mathrm{ref}}$, is depicted in Figure 4b. The comparison ~~impressively~~ demonstrates that the θ_{c_p} profiles significantly depart from the reference by ~~up to $\sim 250\,\mathrm{K}$~~ about $\sim 300\,\mathrm{K}$ at $50\,\mathrm{km}$ altitude, corresponding to a relative difference of about ~~10 %~~16 %. With both extremes of ~~constant c_p~~ the recent constant values $c_p \in \left\{1000\,\mathrm{J\,kg^{-1}K^{-1}}, 1010\,\mathrm{J\,kg^{-1}K^{-1}}\right\}$, the relative error level of $0.1\,\%$ is exceeded at altitudes ~~below~~ about $5\,\mathrm{km}$. While ~~θ_{994}~~ θ_{1000} continues to increasingly deviate from the reference, ~~θ_{1011}~~ θ_{1010} re-enters and crosses the $0.1\,\%$ relative error interval (grey-shaded area) at altitudes between ~~$\sim 20\,\mathrm{km}$ and $22.5\,\mathrm{km}$~~ $\sim 19\,\mathrm{km}$ and $21\,\mathrm{km}$, before it reaches similar errors to the other θ_{c_p} profiles that are based on a constant c_p. Notably, up to an altitude of $15\,\mathrm{km}$, the reference potential temperature is comparably well matched by both the recommended θ_{1005} (WMO, 1966) and θ_{1004} (based on the frequently used alternative $c_p = 1004\,\mathrm{J\,kg^{-1}K^{-1}}$, cf. Table 1). Until $15\,\mathrm{km}$ altitude, both constant c_p values lead to errors of calculated θ_{c_p} which remain comparatively small within the $0.1\,\%$ relative error interval. However, above $\sim 17.5\,\mathrm{km}$, both θ_{1004} and θ_{1005} exceed the $0.1\,\%$ relative error interval, and further aloft their relative error with respect to the reference θ_{ref} increases rapidly.

In the context of numerical models of the atmosphere, the energy balance equation is occasionally formulated based on the potential temperature θ, thus θ constitutes a prognostic model variable. In such a case, the temperature T needs to be calculated from a given pair of values of pressure p and potential temperature θ. Using once more the defining equation (22), for given θ a zero of the function

$$0 = -\int_T^\theta \frac{c_p(z)}{z}\,\frac{c_p(T')}{T'}\,\mathrm{d}z - RT' - R_a \ln\left(\frac{p}{p_0}\right) \tag{26}$$

is to be computed. Since (26) corresponds to the function F defined in (23) with the exception of a negative sign, the identical approximation procedure as outlined above in this section for the calculation of $(T, p) \mapsto \theta$ may be applied ~~mutatis mutandis~~ *mutatis mutandis* to calculate the transformation $(\theta, p) \mapsto T$.

In any case, a certain effort is required to implement the new formulation of the potential temperature in an atmospheric model, as this equation should be based on the implicit definition (22) and such a goal may be subject of future endeavours.

5.2 Approximations of the reference potential temperature

Of course, the previously described procedure to compute the potential temperature may appear to be anything but practical. Indeed, due to the complications inherent with:

- the requirement to numerically solve the integral in the function $F(x)$ and
- the need to use Newton's method for an iteration sequence to approach the zero of $F(x)$,

a convenient approach to re-assess the conventional definition of the potential temperature is not provided at all. This motivates the development of a more practical approximation of the reference potential temperature. To arrive at a practicable approximation procedure, the two principal steps in the suggested procedure are briefly outlined in the following, whereas the comprehensive details and intermediate derivation steps are found in Appendix C.

Proceeding from the definition (23) of the function $F(x)$, the computation of the integral $\int_x^T \frac{c_p^0(z)}{z}\,\mathrm{d}z$ $\int_x^T \frac{c_p^0(T')}{T'}\,\mathrm{d}T'$ becomes the first obstacle to a practical approximation. Therefore, a plausible initial step is to replace the integral by an expression that is easier to treat. This expression may be proposed as $f(T) - f(x)$, where the function f is defined as $f(x) = b_0 + b_1 \ln(x - b_2) + b_3 x + b_4 x^2$ and which is recognisable as an approximated primitive of $\frac{c_p^0(z)}{z}\frac{c_p^0(T')}{T'}$, see Appendix C1. The choice of the functional form of f is motivated by the exact primitive of the integral in the case of a constant c_p.

As previously discussed (cf. Section 5.1), the formulation of a new expression for the potential temperature based on the temperature-dependent specific heat capacity $c_p(T)$ requires finding the zero of the equation $0 = F(x)$, where the function $F(x)$ is defined in (23). Replacing the exact integral in (23) by the difference $f(T) - f(x)$ means that $F(x)$ is substituted by the function

$$\widehat{F}(x) = f(T) - f(x) - R_a \ln\left(\frac{p}{p_0}\right). \tag{27}$$

Consequently, the resulting approximated reference potential temperature, i.e., the respective zero of the function $\widehat{F}(x)$, is denoted as $\theta_{\mathrm{ref}}^{\mathrm{approx}}$.

The difference between the approximation result and the reference, i.e.,

$$\theta_{\mathrm{ref}} - \theta_{\mathrm{ref}}^{\mathrm{approx}}, \tag{28}$$

is then referred to as the basic error of the approximation. Note that the replacement of the function F by $\widehat{F}$ only circumvents the integration in F; the root-finding problem $0 = \widehat{F}(x)$ for the approximated reference potential temperature $\theta_{\mathrm{ref}}^{\mathrm{approx}}$ remains analytically not solvable.

Therefore, the second move towards a practical approximation procedure is to construct approximations $\theta^{(k)}$ to the zero of $\widehat{F}(x)$ by using Newton's method, see Appendix C2. Newton's method is an iterative procedure; the notation $\theta^{(k)}$ refers to the k-th computed iterate. Hence, $\theta^{(k)}$ constitutes an approximation to $\theta_{\mathrm{ref}}^{\mathrm{approx}}$, and, in the limit $k \to \infty$, the approximation error

$$\theta_{\mathrm{ref}}^{\mathrm{approx}} - \theta^{(k)} \tag{29}$$

vanishes. Two formulations of Newton's method are distinguished in Appendix C2, i.e., the principal application of Newton's method, and its further derivative, called Householder's method. Both formulations require the stipulation of one of the iterates $\theta^{(k)}$ as sufficient to obtain a result of appropriate accuracy. The higher the number of iterations, of course, the smaller is the error (29), whereas the basic error (28) remains unaffected by the number of iterations. Hence, in any case, the basic error (28) is to be accepted as at least implied in the final approximation, even though a well-chosen $\theta^{(k)}$ could result in an approximation error $\theta_{\mathrm{ref}} - \theta^{(k)}$ that is smaller than the basic error.

The various errors implied in the proposed approximation procedure combining for the approximation's total error, as well as accompanying details, are discussed in Appendix D. In brief, Figure 5a illustrates the basic error (28) based on the pressure and temperature profiles of the US Standard Atmosphere, as these provide atmospherically meaningful averages of realistic temperature-pressure data pairs. Based on the parameters of the US Standard Atmosphere, the basic error inherent with the approximation remains below $1.25\,\mathrm{K}$ up to altitudes of $50\,\mathrm{km}$. Thus, regarding the subsequent iteration process, a substantial improvement of the error compared to $\sim 1.5\,\mathrm{K}$ is not to be expected for the total error of approximating the reference potential temperature.

An error analysis exclusively based on the US Standard Atmosphere is constrained to specific combinations of the air's pressure and temperature, potentially suppressing latent errors that may emerge if certain fluctuations of the real atmosphere's temperature and pressure profiles are considered. Thus, the error analysis is extended to an atmospheric pressure (p) and temperature (T) range, from $1000\,\mathrm{hPa}$ to $0.5\,\mathrm{hPa}$ and from $180\,\mathrm{K}$ to $300\,\mathrm{K}$, such that the conditions within the entire troposphere and stratosphere, including the stratopause, are covered. Figure 5b illustrates the absolute basic error (28) for the extended ranges of pressure and temperature while Figure 5c illustrates the relative basic error $|\theta_{\mathrm{ref}} - \theta_{\mathrm{ref}}^{\mathrm{approx}}|\,/\theta_{\mathrm{ref}}$. The contours in Figures 5b and 5c mainly highlight two regions: at $\sim 100\,\mathrm{hPa}$ where $\Delta\theta$ never rises above $0.75\,\mathrm{K}$ which corresponds to a maximum relative basic error of $0.15\,\%$, and in a pressure range from $\sim 5\,\mathrm{hPa}$ to $1\,\mathrm{hPa}$ where a $\Delta\theta$ of $1.25\,\mathrm{K}$ is never exceeded, corresponding to relative errors of at most $0.1\,\%$. Note that the entire $\Delta\theta$ scale ranges up to $3\,\mathrm{K}$, which may only be reached at pressures below $0.8\,\mathrm{hPa}$ combined with temperatures above $280\,\mathrm{K}$.

As previously discussed, the basic error is unavoidable and is to be accepted when applying the suggested substitution for the integral in the definition of the function $F(x)$ in (23). However, as outlined in Appendix C2, the second iterate $\theta^{(2)}$ of Newton's method (principal application), may thoroughly suffice for the final approximation to the reference potential temperature θ_{ref}, as this iteration level already features an approximation error (29) which is negligibly small. Figure 6a illustrates the total relative error of the suggested approximation $\theta^{(2)}$ with respect to the ultimate reference θ_{ref} for the extended ranges of pressure and temperature. Indeed, the contour pattern in Figure 6a and the basic relative approximation error shown in Figure 5c are remarkably similar. Thus, the iteration process itself imparts only a minor contribution to the total error compared to the basic approximation error.

The total approximation error, which is

$$\theta_{\mathrm{ref}} - \theta^{(2)} = (\theta_{\mathrm{ref}} - \theta_{\mathrm{ref}}^{\mathrm{approx}}) + \left(\theta_{\mathrm{ref}}^{\mathrm{approx}} - \theta^{(2)}\right), \tag{30}$$

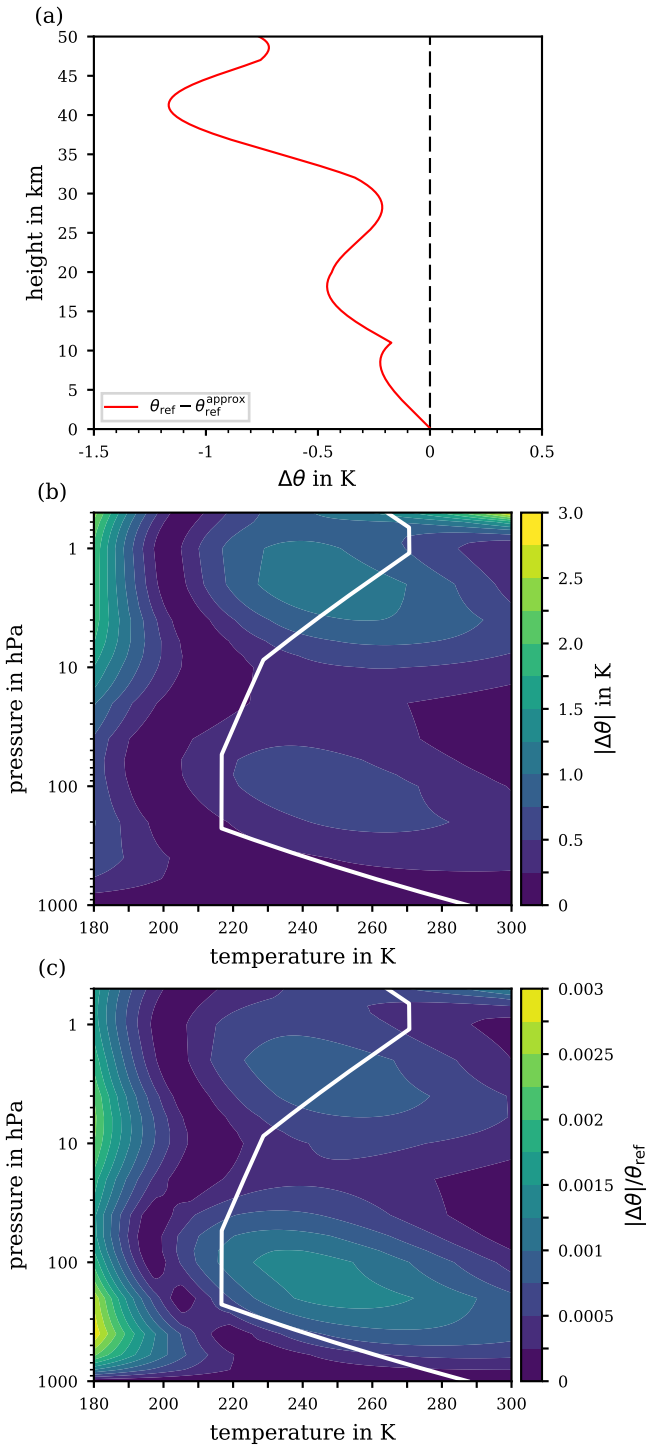

Figure 5. Absolute basic error $\Delta\theta = \theta_{\mathrm{ref}} - \theta_{\mathrm{ref}}^{\mathrm{approx}}$, cf. (28), from approximating the reference potential temperature along the US Standard Atmosphere (a) and for the extended pressure range $1000\,\mathrm{hPa}$ to $0.5\,\mathrm{hPa}$ and temperature range $180\,\mathrm{K}$ to $300\,\mathrm{K}$ (b). For orientation, the white solid line indicates the p-T-profile from the US Standard Atmosphere. The relative basic error $|\Delta\theta|/\theta_{\mathrm{ref}}$ is shown in panel (c) for the extended pressure and temperature range.

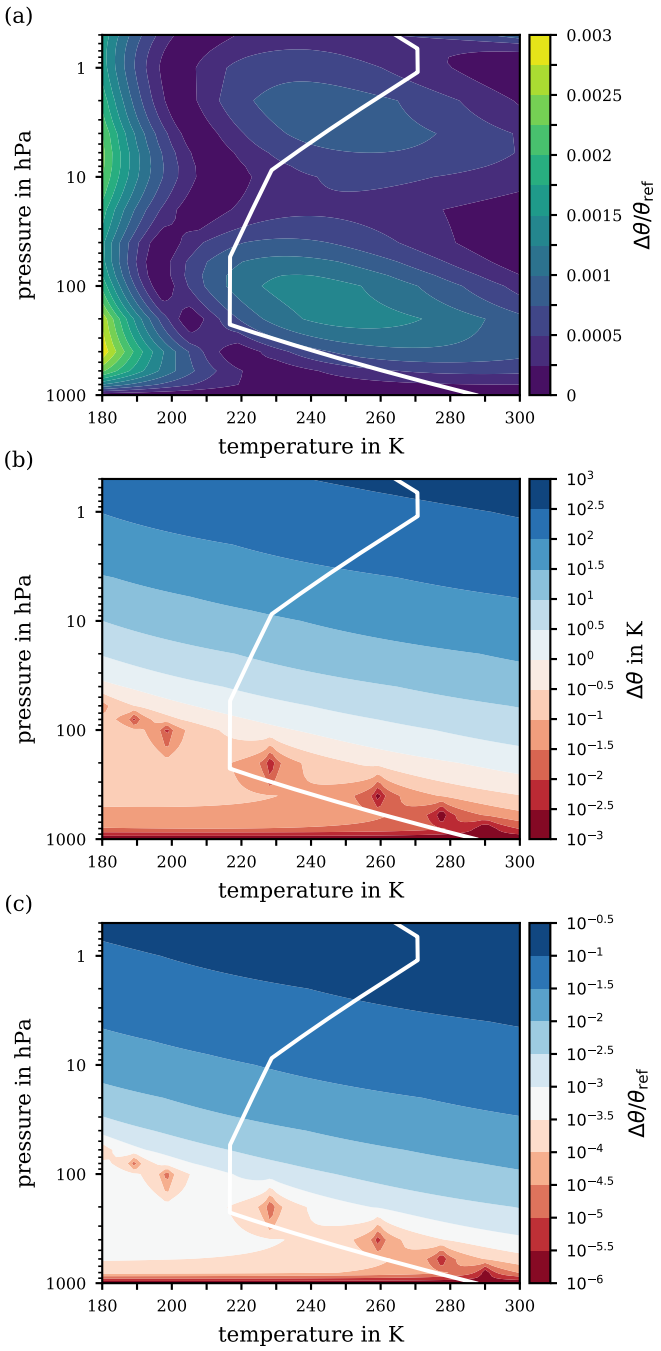

Figure 6. (a) Relative error $\Delta\theta/\theta_{\mathrm{ref}} = \left|\theta^{(2)} - \theta_{\mathrm{ref}}\right|/\theta_{\mathrm{ref}}$ of the second iterate $\theta^{(2)}$, obtained with Newton's method for the ranges of pressure and temperature from 1000 hPa to 0.5 hPa and from 180 K to 300 K, respectively. Panels (b) and (c) exhibit the difference $\Delta\theta = |\theta_{1005} - \theta_{\mathrm{ref}}|$ and relative difference $\Delta\theta/\theta_{\mathrm{ref}}$, respectively, on a logarithmic scale between the reference potential temperature θ_{ref} and the potential temperature θ_{1005} based on a constant specific heat capacity ($c_p = 1005\,\mathrm{J\,kg^{-1}K^{-1}}$). For orientation, the white solid line indicates the p-T-profile from the US Standard Atmosphere.

is dominated by the unavoidable basic error (first bracket) and augmented by a negligible error inherent to the iteration (second bracket), also supporting the conclusion that the second iterate of Newton's method is an appropriate approximation procedure. Figure 7 presents step-wise instructions for the computation of the second iterate approximation to the reference potential temperature, and may serve as a guide to follow the numerous equations and intermediate analytical steps described throughout the derivations in Appendix C.

For completeness, Figures 6b and 6c exhibit a final comparison by means of the logarithmic difference and the logarithmic relative difference between the reference potential temperature θ_{ref} and the conventional definition θ_{c_p} (WMO, 1966) based on a constant specific heat capacity $c_p = 1005\,\mathrm{J\,kg^{-1}K^{-1}}$. Notably, over a wide altitude range within the troposphere (i.e., for atmospheric pressures greater than $\sim 100\,\mathrm{hPa}$), the absolute error $\Delta\theta = |\theta_{1005} - \theta_{\mathrm{ref}}|$ remains below $1\,\mathrm{K}$, cf. Figure 6b, corresponding to a relative error $\Delta\theta/\theta_{\mathrm{ref}}$ of at most $0.1\,\%$. However, in the pressure range below $\sim 100\,\mathrm{hPa}$, deviations of the real atmospheric conditions from those of the US Standard Atmosphere could increase the absolute error $\Delta\theta$ from a few K to up to $10\,\mathrm{K}$, corresponding to an increase of the relative error to $1\,\%$. Further critical pressure levels are at $\sim 20\,\mathrm{hPa}$ and $\sim 5\,\mathrm{hPa}$, where the error's magnitude increases to several tens and several hundreds of K, respectively. At a pressure of $0.5\,\mathrm{hPa}$, an absolute error $\Delta\theta$ of up to $500\,\mathrm{K}$ is reached, which corresponds to a relative error of $10\,\%$ or even more.

5.3 Implementation aspects

The use of the new reference potential temperature θ_{ref} in a numerical model requires additional computational effort to perform corresponding calculations. Hereafter, two aspects are briefly discussed: (i) the formulation of the model equations, which include θ_{ref} and (ii) the calculation of θ_{ref}.

Although it is beyond the scope of the present study to provide a general derivation of an appropriate energy equation based on θ_{ref} for atmospheric models, a formulation of the total derivative of θ_{ref} is given by

$$c_p(\theta_{\mathrm{ref}})\frac{\mathrm{d}\theta_{\mathrm{ref}}}{\theta_{\mathrm{ref}}} = c_p(T)\frac{\mathrm{d}T}{T} - R_a\frac{\mathrm{d}p}{p}, \tag{31}$$

where the details of its derivation are given in Appendix E. The total derivative of θ_{ref} may be useful, since the governing equations are commonly formulated as differential equations.

The calculation of both the reference potential temperature θ_{ref} and its approximation $\theta_{\mathrm{ref}}^{\mathrm{approx}}$ on the basis of given values of pressure p and temperature T requires an iterative procedure. The additional computational effort inherent with these calculations depends on the number of iterations. If, however, the second iteration $\theta^{(2)}$ already represents an appropriate approximation of θ_{ref} (cf. Section 5.2), then the flowchart in Figure 7 immediately conveys the additional computational effort to be expected. The calculation of the starting value x_0 is identical to computing θ_{1005}. An additional effort results from the evaluation of the functions f (three times) and f' (two times), respectively, and the combination (two times) of obtained values to determine x_1 and x_2. Since each of these evaluations causes additional numerical steps, the computational effort to obtain $\theta^{(2)}$ is in total about seven times more than the calculation of the conventional θ_{1005}, while the algorithmic complexity is constant.

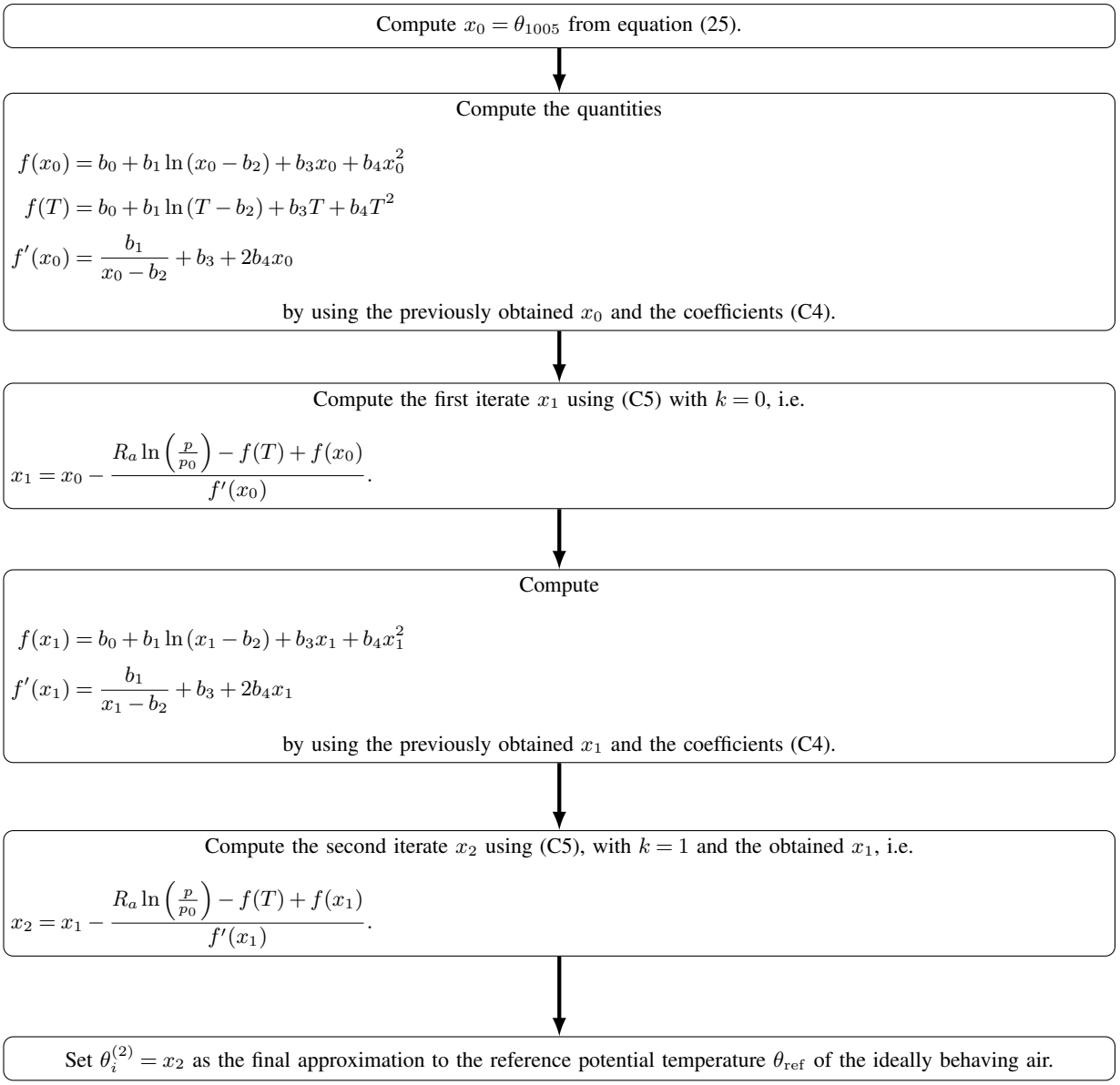

Figure 7. Flowchart guiding through the process of computing the approximation $\theta^{(2)}$ by using Newton's formulation (C5) until its second iteration, wherein T (in K) and p (in hPa) are the atmospheric air conditions in terms of temperature and pressure, respectively, and p_0 is set to $1000\,\mathrm{hPa}$ (WMO, 1966). Table C1 collects values of θ_{ref} and the approximation $\theta^{(2)}$ together with intermediate results for selected pairs of temperature and pressure to verify a computation according to this instruction.

6 The potential temperature for air as a real gas

To ~~calculate~~ account for real-gas effects (that cause a behaviour other than that of an ideal gas cf. Section 4) on the potential temperature, we use the model embedded in *REFPROP* (Lemmon et al., 2018), a standard reference database from NIST. This model treats air as a mixture and employs state-of-the art reference equations of state for pure nitrogen (Span et al., 2000), oxygen (Schmidt and Wagner, 1985), and argon (Tegeler et al., 1999). The mixing rule and binary interaction parameters are taken from the GERG-2008 model (Kunz and Wagner, 2012). From its definition in terms of an isentropic process, the potential temperature $\theta_{\mathrm{real}}(T, p)$ is defined implicitly by

$$s(\theta_{\mathrm{real}}, p_0) = s(T, p), \tag{32}$$

where s is the specific entropy. Calculating $\theta_{\mathrm{real}}(T, p)$ is a two-step process. First, the specific entropy s is computed at temperature T and pressure p. Then, the temperature θ_{real} is found that gives the same entropy s at the ground pressure p_0. This is an iterative calculation, but it is accomplished automatically within the *REFPROP* software (Lemmon et al., 2018).

One caveat should be mentioned regarding the computed potential temperatures. The range of validity of the equations of state for the air components (Span et al., 2000; Schmidt and Wagner, 1985; Tegeler et al., 1999) extends only up to 2000 K. At very high altitudes, computed values of θ_{real} exceed this limit. While all the equations extrapolate in a physically realistic way, their quantitative accuracy is less certain above 2000 K. This caveat also applies to the ideal-gas calculations; the correlations for $c_p^0(T)$ for N_2 and O_2 are extrapolations beyond 2000 K. However, since the same ideal-gas values are used in the real-gas calculations, any inaccuracy in $c_p^0(T)$ will cancel when evaluating the difference between ideal-gas and real-gas values of θ.

Figure 8 illustrates the comparison between the real-gas potential temperature θ_{real} and the ideal-gas reference potential temperature θ_{ref}. Figure 8a shows the difference $\theta_{\mathrm{real}} - \theta_{\mathrm{ref}}$ ~~, once more~~ along the p-T-profile of the US Standard Atmosphere ~~.~~ and Figure 8b accounts ~~again~~ for any p-T-combination of extended range but shows the relative difference instead. The difference between θ_{real} and θ_{ref} never exceeds 0.1 K for the absolute difference or $30 \cdot 10^{-5} = 0.03\,\%$ for the relative difference. As may be anticipated from the deviation of c_p^0 shown in Figure 3 at low temperatures both from the experimentally determined values (which may be inaccurate) as well as from the *REFPROP* data, the real-gas effect on the specific heat capacity of dry air tends to increase towards the coldest gas temperatures. However, the difference between the real- and ideal-gas approaches results in essentially no substantial difference between the resulting θ's, neither at ground conditions (for any temperature at $\sim 1000\,\mathrm{hPa}$) nor at very high altitudes (at pressures below $\sim 1\,\mathrm{hPa}$). While the negligible difference between θ_{real} and θ_{ref} near ground levels is less surprising, the diminished difference at higher altitudes reflects that in this region the potential temperature reaches such high values that the difference between the real-gas and the ideal-gas specific heat capacity becomes insignificant. Within the intermediate (stratospheric) region, the low pressures (and thus the low air densities) cause the ideal-gas assumption to be an accurate approximation even at low temperatures. In general, the degree to which a gas can be treated as an ideal gas is primarily a function of the (molar) density. For an ideal gas, the density is proportional to the quotient $\frac{p}{T}$; this is almost true also for real air. Hence, declining pressures together with rising temperatures both make the air's behaviour increasingly close to ideal.

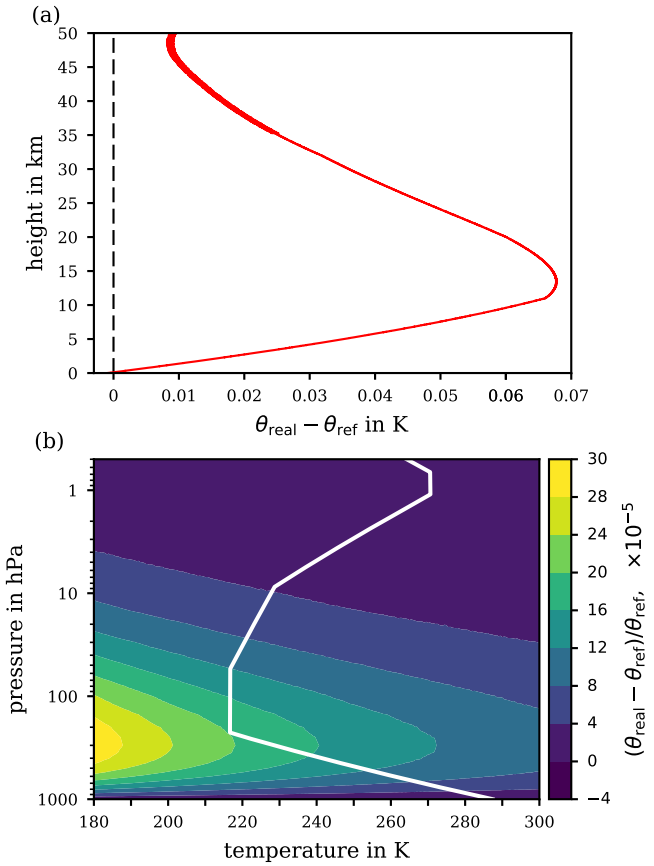

Figure 8. Difference $\theta_{\mathrm{real}} - \theta_{\mathrm{ref}}$ reflecting the deviation of the potential temperature θ_{real}, based on the properties of air behaving as a real gas under variable temperature and pressure, from the herein derived potential temperature expression θ_{ref} for the ideal-gas limit of the air's specific heat capacity $c_p^0(T)$. (a) Difference along the profile of the US Standard Atmosphere. (b) Relative difference in p-T-coordinates covering any combination of atmospherically relevant temperatures and pressures.

7 Implications on the use of the potential temperature~~on the prediction of gravity waves' breaking~~

As previously shown, the newly defined reference potential temperature θ_{ref} deviates most from the WMO-defined potential temperature θ_{1005} at ~~high altitudes~~ stratospheric altitudes and above (cf. Figure 6). More particularly, not only do the values from both θ definitions differ, but also their vertical derivatives, i.e., $\frac{\partial \theta_{\mathrm{ref}}}{\partial z}$ and $\frac{\partial \theta_{1005}}{\partial z}$. ~~As the~~ Whether such deviations have a significant effect on an application is very case-dependent and requires detailed examination and specific appraisal. Below, four typical applications of the potential temperature were selected and are examined regarding the quantitative effect on the results due to deviations of the introduced reference potential temperature compared to the conventional and commonly used θ_{1005}. The purpose of this examination is to document the magnitude of errors to allow a well-founded, individual decision

for each application of the potential temperature whether it is worth applying the more rigorous calculation in the particular context.

7.1 The Brunt-Väisälä frequency

The formula for the (squared) Brunt-Väisälä frequency N^2 ~~depends on both the potential temperature and its vertical derivative, cf.~~ is often given in the form of (2), i.e., a formula involving the potential temperature θ. The substitution of θ in equation (2) ~~, the resulting N^2, a measure of atmospheric stability, is affected by the definition of θ. This may have implications for the investigation of upward propagating gravity waves, which are emitted from the upper troposphere or lower stratosphere by various processes~~by the new reference potential temperature θ_{ref} may be tempting, but it is erroneous and the resulting quantity is denoted as N^2_{false}. The Brunt-Väisälä frequency is not defined by equation (2), since this formula results from various simplifications in its derivation, e.g., ~~spontaneous imbalance (Plougonven and Zhang, 2014), flow over mountains (Palmer et al., 1986), or convection (Choi and Chun, 2011). Various properties of gravity waves directly depend on the vertical profile of~~ by assuming hydrostatic conditions and a constant specific heat capacity. Consequently, the substitution of θ_{ref} in equation (2) leads to a wrong formula for the Brunt-Väisälä frequency ~~N^2. Specifically, the altitude of gravity wave breaking, if due to static instability, depends on N^2. To explore the implication of the θ definition on gravity wave breaking~~that does not correctly consider the temperature dependence of dry air's specific heat capacity.

The Brunt-Väisälä frequency is the oscillation frequency of an air parcel due to a local density perturbation (see, e.g., Durran and Klemp, . Retaining the assumption of hydrostatic conditions, the defining formula yields

$$N^2 = \frac{g}{T}\left(\frac{\partial T}{\partial z} + \frac{g}{c_p(T)}\right) \tag{33}$$

where the temperature-dependent specific heat capacity $c_p(T)$ was implied, and which factually describes the balance between the actual temperature stratification $\frac{\partial T}{\partial z}$ and the dry adiabatic lapse rate $-\frac{g}{c_p(T)}$ (e.g., Holton, 2004).

To illustrate the deviation of N^2_{false} from N^2, vertical profiles of ~~temperature and horizontal wind speed are used as shown in panels (a) and (b) of Figure **??**. These are typical for mid-latitudes for the months June and December, respectively, and they have been~~ both variables were calculated based on the temperature profiles shown in Figure 9a. The temperature data are taken from the Upper Atmosphere Research Satellite Reference Atmosphere Project ~~(URAP) data (Swinbank and Ortland, 2003).~~

~~Note that these~~ (URAP, see Swinbank and Ortland, 2003) data and are assumed as typical at mid-latitudes during June and December. The temperature profiles extend up to altitudes of $85\,\mathrm{km}$ ~~, thus covering~~ and thus cover the entire stratosphere and most of the mesosphere~~, compared to the previously used vertical range reaching at most to $50\,\mathrm{km}$ (up to approximately stratopause level). Nevertheless, both the parameterised specific heat capacity of ideal-gas dry air and the general derivation of the reference potential temperature (Section 5.1) are valid also at altitudes above $50\,\mathrm{km}$. Consequently, the new reference potential temperature also remains valid up to mesospheric altitudes, even though the approximate~~ . The hydrostatic assumption allowed for computing pressure profiles along the URAP values for the vertical temperature distribution. Subsequently, the reference potential temperature $\theta_{\mathrm{ref}}^{\mathrm{approx}}$ ~~may not match very well with θ_{ref} for altitudes above $50\,\mathrm{km}$.~~

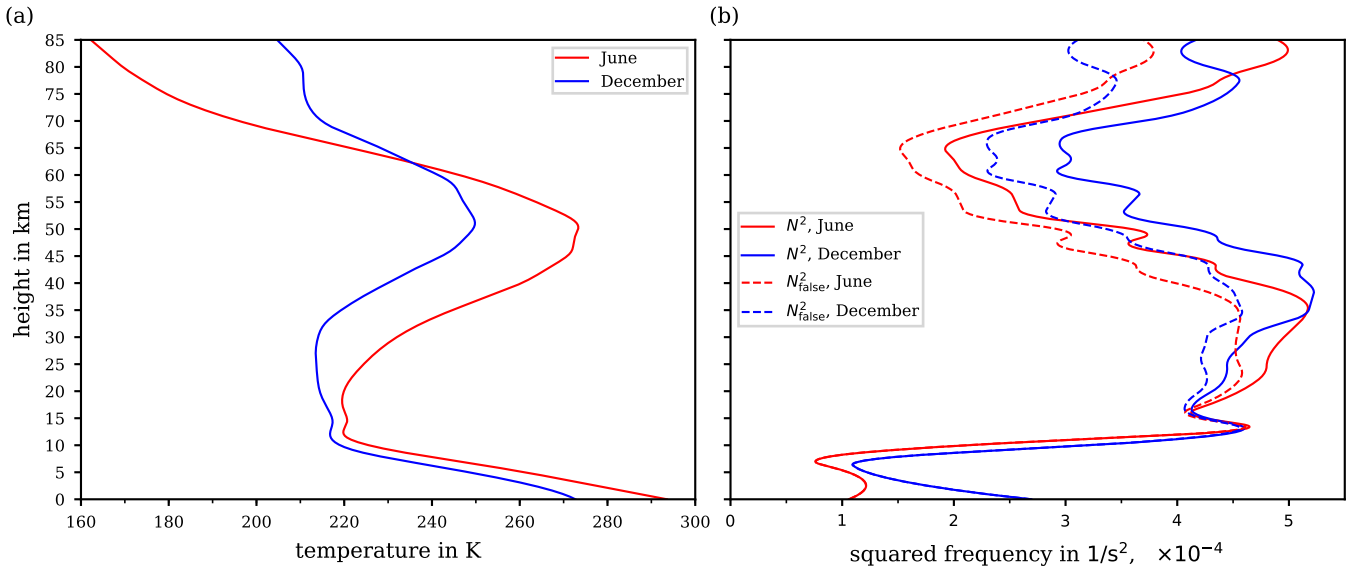

Figure 9. Vertical profiles of (a) the temperature up to 85 km altitude as typical for mid-latitudes in June (red curve) and December (blue curve). (b) Resulting wrong Brunt-Väisälä frequency N^2_{false} (dashed lines) and the true Brunt-Väisälä frequency N^2 (solid lines) for the two temperature profiles from panel (a).

~~Based on the temperature profiles in Figure ??a and considering the hydrostatic assumption as fulfilled, the Brunt-Väisälä frequencies are determined as~~

$$N^2_{\text{ref}} = \frac{g}{\theta_{\text{ref}}} \frac{\partial \theta_{\text{ref}}}{\partial z} \quad \text{and} \quad N^2_{1005} = \frac{g}{\theta_{1005}} \frac{\partial \theta_{1005}}{\partial z},$$

~~where $g = 9.81\,\text{m}\,\text{s}^{-2}$ is the gravitational acceleration~~and its vertical derivative were calculable. The resulting vertical profiles ~~of the~~ for N^2_{false} and the true Brunt-Väisälä ~~frequencies are depicted in Figure ??c~~frequency N^2 are shown in Figure 9b. Evidently, the values of ~~N^2_{ref} and N^2_{1005} deviate from each other and , thus, lead to different predictions of the atmosphere's actual stability. Notably, the difference $N^2_{\text{ref}} - N^2_{1005}$ increases with altitude as already implied by the increase of the difference $\theta_{\text{ref}} - \theta_{1005}$ with altitude, shown in Figure 6b~~N^2_{false} (dashed lines) deviate significantly from N^2 (solid lines) and increasingly so towards higher altitudes above 15 km. However, the absolute deviation $|N^2 - N^2_{1005}|$, using N^2_{1005} as calculated with θ_{1005} in accordance with Equation (2), does not exceed $1.6 \cdot 10^{-6}\,\text{s}^{-2}$ (not shown), indicating that N^2_{1005} is a good representation of N^2 along these temperature profiles.

For equations involving the potential temperature, however, it should be emphasised that the substitution of θ by θ_{ref} rarely succeeds and that instead the entire derivation of the equations requires careful consideration of the assumptions, such as the constancy of c_p, to avoid aberrations and erroneous conclusions.

~~Vertical profiles of (a) temperature and (b) horizontal wind speed as typical for mid-latitudes in June and December, up to 85 km altitude. Resulting Brunt-Väisälä frequency N^2 (c), either based on θ_{ref} (solid lines) or on θ_{1005} (dashed lines). Panels~~

(d), (e), and (f): vertical profiles of N^2_{ref} and N^2_{1005} for December (solid and dashed blue lines, respectively) with the modulus $|m(z) \cdot B(z)|$ (green lines), either based on θ_{ref} (solid lines) or on θ_{1005} (dashed lines), cf. text for further details. The panels' titles document the individually chosen values of the parameters λ_x, λ_z and B_{fact}. The thin grey horizontal lines indicate the altitude of the predicted wave breaking altitude, i.e. where $|m(z) \cdot B(z)|$ first coincides with $N^2(z)$ above the initiation height.

7.2 The Potential Vorticity

Following Lindzen (1981), static instability due to a gravity wave occurs whenever it can lead to an overturn of potential temperature, which is expressed as (e.g., Bölöni et al., 2016) Ertel's potential vorticity (e.g., Ertel, 1942; Hoskins et al., 1985; Schubert et a may be defined as the potential vorticity of the dry air potential temperature by

$$m(z)B(z) > N^2 PV(z\theta) = \frac{1}{\rho}\left(2\boldsymbol{\Omega} + \nabla \times \boldsymbol{u}\right) \cdot \nabla\theta. \tag{34}$$

Here $m(z)$ is a gravity wave's vertical wave number at the altitude z, and $B(z)$ denotes the vertically varying buoyancy amplitude of the same wave. Thus, the (minimum) gravity wave breaking altitude $z_{\mathrm{b}} > z_0$ is predicted as In this definition, $2\boldsymbol{\Omega} + \nabla \times \boldsymbol{u}$ is the absolute vorticity, $\boldsymbol{\Omega}$ denotes Earth's angular velocity, $\boldsymbol{u}$ the three-dimensional wind vector, and ρ the air density (see, e.g., Hoskins et al., 1985; Cotton et al., 2011; Marquet, 2014). Since (34) represents the defining equation for Ertel's potential vorticity, the two potential vorticities

$$\begin{aligned} PV_{\mathrm{ref}} &= PV(\theta_{\mathrm{ref}}), \\ PV_{1005} &= PV(\theta_{1005}) \end{aligned} \tag{35}$$

based on the new reference potential temperature θ_{ref} and θ_{1005}, respectively, are considered. To provide a first comparison of these potential vorticities, $\boldsymbol{u} = 0$ is assumed, i.e., an atmosphere at rest. Additionally, the potential temperature is assumed as horizontally constant. Consequently, (34) reduces to

$$PV(\theta) = \frac{2\sin(\phi)}{\rho}\frac{2\pi}{t_E}\frac{\partial\theta}{\partial z} \tag{36}$$

for a position on Earth with geographical latitude ϕ and $t_E = 24\,\mathrm{h}$, the duration of one rotation of the Earth.

Using the temperature profiles from Figure 9a together with the values of the lowermost altitude where the condition $m(z_{\mathrm{b}})B(z_{\mathrm{b}}) = N^2(z_{\mathrm{b}})$ is satisfiedpotential temperatures θ_{ref} and θ_{1005}, the evaluation of the two potential vorticities (35) and (36) yields the potential vorticity profiles shown in Figure 10a while their relative deviations are shown in Figure 10b. Since the temperature profiles are representative for the north-hemispheric mid-latitudes, the geographical latitude ϕ in (36) was set to 52°N. At tropospheric altitudes, the relative deviation between θ_{ref} and θ_{1005} is small and never exceeds $\sim 1\,\%$, while it continuously increases towards higher altitudes. According to these profiles, the relative deviation exceeds $10\,\%$ at $30\,\mathrm{km}$ and reaches $100\,\%$ at the highest altitudes.

It is noteworthy, however, that the computations of both N^2 (cf. Section 7.1 and Figure 9b) and PV (Figure 10b) are based on the specific temperature profiles from URAP (cf. Section 7.1 and Figure 9a) and thus are not of general validity. The selection

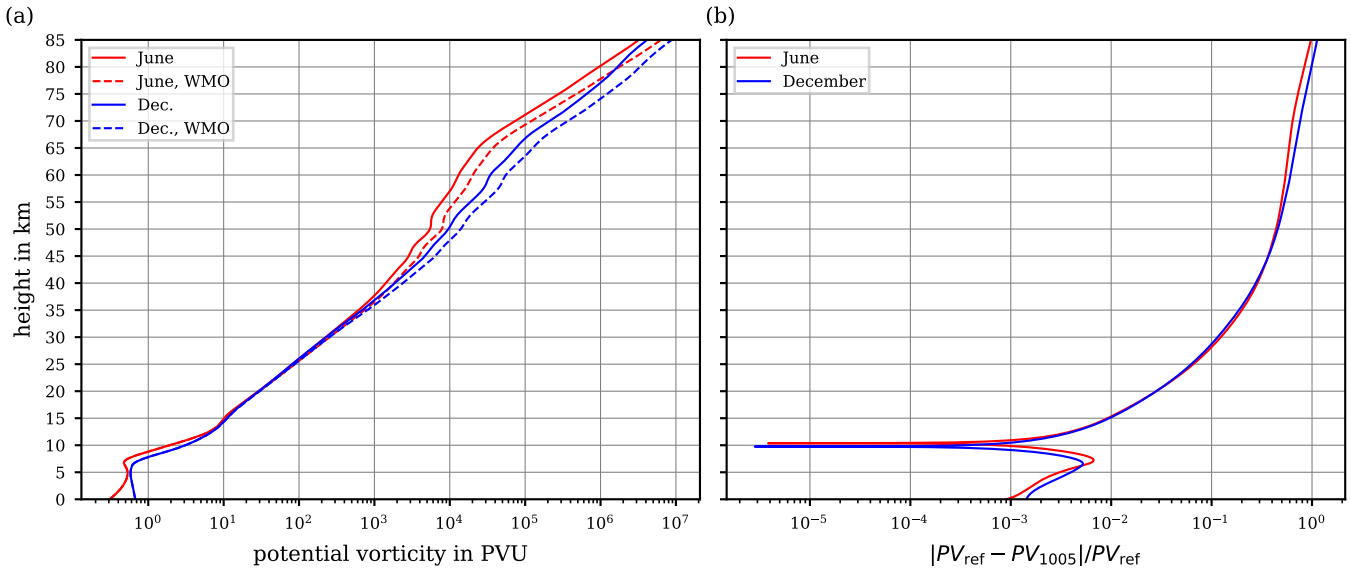

Figure 10. (a) Vertical profiles of the potential vorticitiy PV_{ref} computed with θ_{ref} (solid lines), and PV_{1005} computed with θ_{1005} (dashed lines), for an atmosphere at rest along the temperature profiles from Figure 9a for June (red lines) and December (blue lines). Since the temperature profiles are representative for mid-latitudes on the northern hemisphere, the geographical latitude in (36) was set to 52°N. (b) Relative deviation $|PV_{\mathrm{ref}} - PV_{1005}|/PV_{\mathrm{ref}}$ of the potential vorticity profiles from panel (a).

of these temperature profiles was entirely arbitrary and exclusively aimed at illustrating possible implications inherent with the use of the developed reference potential temperature. The resulting and indicated deviations are ultimately subject to individual assessment on applying θ_{ref}.

7.3 Vertical sorting of data

~~To explore the implications of using the new reference potential temperature instead of the WMO-defined potential temperature on the predicted altitude of gravity wave breaking, a typical altitude of $z_0 = 17.5\,\mathrm{km}$ is chosen as the initiation level of a gravity wave with horizontal wave number $k(z_0) = \frac{2\pi}{\lambda_x}$ and vertical wave number $m(z_0) = \frac{2\pi}{\lambda_z}$. The initial buoyancy amplitude $B(z_0)$ is set to~~

$$B(z_0) = B_{\mathrm{fact}} \frac{N^2(z_0)}{m(z_0)},$$

~~with a scaling factor $0 < B_{\mathrm{fact}} < 1$ defining the wave amplitude at the initiation level with respect to static instability. The dependence of m and B on altitude is then determined by the classic steady-state approach as outlined~~For atmospheric

investigations, e.g., ~~by Bölöni et al. (2016). The selected parameter values for the scaling factor B_{fact} are~~

~~$B_{\mathrm{fact}} \in \{0.05, 0.06, 0.08, 0.1, 0.12, 0.14, 0.16, 0.18,$~~
~~$0.2, 0.22, 0.24, 0.25, 0.3, 0.5, 0.75, 0.9\}$,~~

~~while the selected horizontal wave lengths λ_x at initiation height are~~

$\lambda_x \in \{\pm 100\,\mathrm{km}, \pm 50\,\mathrm{km}, \pm 10\,\mathrm{km}, \pm 5\,\mathrm{km}, \pm 1\,\mathrm{km}\}$,

~~and the vertical wave length is varied between 100 m and 4000 m with 100 m increment. The aforementioned parameter values are used to compute the vertical profiles of $|mB|$ and N^2 based on the mid-latitude December profiles which are displayed in panels (d), (e), and (f) in Figure **??**. The green lines illustrate the modulus $|mB|$ of the product of~~ in the region of the upper troposphere and lower stratosphere (UT/LS), it is common practice to set vertical profiles of atmospheric parameters in relation to the potential temperature as vertical coordinate. This way, the increasingly isentropic stratification of the atmosphere above the UT is taken into account. The transport of an air mass along isentropic surfaces, i.e., surfaces of constant potential temperature and entropy, is to be regarded as adiabatic. Hence, the air's composition and properties within the same isentrope interval, regardless of the observation location, is better comparable than it would be if based on other isopleths (i.e., height or pressure coordinates). Investigations of air mass compositions over time and from different regions at the same θ-level largely exclude that, during its transport history, the air had experienced vertical displacement and/or diabatic processes (radiative heating, condensation/evaporation) which would result in energy conversion. The tropopause height is often used as a reference height in the θ coordinate system in connection with the vertical sorting of observational data, whereby the assignment of tropospheric and stratospheric processes is made, or exchanges across the tropopause are investigated (Holton et al., 1995; Stohl et al., 2003). Consequently, the ~~vertical wave number and~~ tropopause height is also determined by the potential vorticity (e.g., Gettelman et al., 2011, and cf. Section 7.2), if the conventional tropopause definitions (cold point or lapse rate, do not allow for clearly determining the tropopause height, e.g., in the Asian Monsoon Anticyclone (cf. Höpfner et al., 2019) or in the polar winter vortex (Wilson et al., 1989; Weigel et al., 2014). The conventional definition of θ implies a systematic error in the vertical sorting of observational data in the θ coordinate system, independently of the used measurement platform. Investigations with high-altitude research aircraft such as the G-550 HALO (e.g., Wendisch et al., 2016; Voigt et al., 2017), the NASA WB-57 or ER-2 (e.g., Murphy et al., 2007; Dessler, 2002), the ~~buoyancy amplitude, while the blue lines exhibit the altitude dependence of the Brunt-Väisälä frequency N^2. The results shown as solid lines are based on the new reference potential temperature θ_{ref}; the results of the computations using θ_{1005} are represented by dashed lines. The predicted altitude of wave breaking is indicated by the first crossover of $|mB|$ and N^2 above the wave's initiation height, indicated by the thin grey horizontal lines. Apparently, the predicted altitudes of wave breaking differ by more than about 5 km, depending on the definition of~~ M-55 Geophysica (Curtius et al., 2005; Borrmann et al., 2010; Frey, 2011), balloon-borne platforms (Lary et al., 1995; Vernie , or satellite-based vertical profiles (e.g., Davies et al., 2006; Spang et al., 2005), require consideration of the systematic error in θ ~~used (cf. panels (d) , (e), (f) of Figure **??**) . Note that deviations of this scale are only found for the mid-latitude December vertical profiles of temperature~~ if calculated as θ_{c_p} in compliance with the definition by the WMO (1966). The possibly

inconsistent use of a constant c_p value of $1004\,\mathrm{J\,kg^{-1}K^{-1}}$ or $1005\,\mathrm{J\,kg^{-1}K^{-1}}$ (or any other) in different and compared data sets, which could be due to different literature references for this value (cf. Table 1), will not be explored here. At altitudes between 15 and ~~wind speed employed here, and hydrostatic gravity waves with initial horizontal wave lengths $\lambda_x \in \{100\,\mathrm{km}, 50\,\mathrm{km}\}$ and initial vertical wave lengths between approximately $1\,\mathrm{km}$ and $3\,\mathrm{km}$.Significant differences of predicted wave breaking altitudes were most frequently observed with initiation height amplitude scaling factors B_{fact} between 0.1 and 0.2, but larger values can also lead to significant differences, see Figure **??**f. In essence, the improvement from the use of a more accurate potential temperature for predicting~~ $20\,\mathrm{km}$ (ceiling of high-altitude research aircraft) an overestimation by about $0.1 - 0.5\,\%$ is to be expected for the potential temperature according to the conventional definition, cf. Figure 4b. At altitudes of $30 - 35\,\mathrm{km}$, an overestimation by up to $2 - 5\%$ results. Whether this error is significant or small compared to the uncertainty of ambient temperature and pressure measurement aboard the respective aircraft is left to individual judgement in the course of data processing. In the case of spacecraft-bound vertical soundings (e.g., from ASTROSPAS, SCIAMACHY, or ENVISAT), the error in the potential temperature determined by θ_{c_p} exceeds $10\,\%$ at altitudes above $40\,\mathrm{km}$, as shown in Figure 4b. Finally, we note that the specified errors apply exclusively along the vertical profile of the US standard atmosphere, and that deviations of the actual temperature profile from the US standard atmosphere, e.g., warmer temperatures, could lead to larger errors (cf. Figure 6).

7.4 Diabatic heating rates

Diabatic heating rates refer to the rate of energy $\frac{\mathrm{d}q}{\mathrm{d}t}$ supplied to a given air parcel, e.g., by radiative heating, and are given in units of $\mathrm{J\,kg^{-1}s^{-1}}$. This energy supply causes a temperature change of an air parcel at rate, which, hereafter, is referred to as *absolute heating rate*,

$$\begin{aligned} \mathrm{AHR_{ref}}\left(\frac{\mathrm{d}q}{\mathrm{d}t}\right) &= \frac{\mathrm{d}T}{\mathrm{d}t} = \frac{1}{c_p^0(T)}\frac{\mathrm{d}q}{\mathrm{d}t}, \\ \mathrm{AHR_{1005}}\left(\frac{\mathrm{d}q}{\mathrm{d}t}\right) &= \frac{\mathrm{d}T}{\mathrm{d}t} = \frac{1}{1005\,\mathrm{J\,kg^{-1}K^{-1}}}\frac{\mathrm{d}q}{\mathrm{d}t}. \end{aligned} \tag{37}$$

Again, the distinction was made between the temperature-dependent $c_p^0(T)$ and the constant $c_p = 1005\,\mathrm{J\,kg^{-1}K^{-1}}$ specific heat capacity. From the defining equations (37), the relative difference between these absolute heating rates, where x designates an arbitrary diabatic heating rate, is

$$\frac{\mathrm{AHR_{1005}}(x) - \mathrm{AHR_{ref}}(x)}{\mathrm{AHR_{ref}}(x)} = \frac{c_p^0(T)}{1005\,\mathrm{J\,kg^{-1}K^{-1}}} - 1. \tag{38}$$

Apart from the absolute heating rates for the change of absolute temperature, the change of potential temperature due to a diabatic heating rate $\frac{\mathrm{d}q}{\mathrm{d}t}$ is of interest. As an example, it is the change of potential temperature that modifies the altitude of ~~gravity wave breaking is non-negligible, although not excessive. Nonetheless, these improvements may be of particular relevance for individual investigations, e. g. , concerning the mesopause altitude, which involve specific vertical profiles at concrete atmospheric conditions and at locations other than the mid-latitudes. It needs to be emphasised, however, that~~

~~predictions of the gravity wave breaking altitude are highly sensitive to variations along the vertical profiles of both the temperature and wind speed. Furthermore, the results of such predictions strongly depend on the chosen parameters at the gravity waves' initiation height~~modelled trajectories in Lagrangian chemical transport models based on isentropic coordinates rather than the change in absolute temperature (e.g., the SLIMCAT (Chipperfield, 2006) or CLaMS model (Pommrich et al., 2014)).

Taking the relation $T\,\mathrm{d}s = \mathrm{d}q$ for the specific entropy into account, Gibbs' equation (8) may be rewritten as

$$\frac{\mathrm{d}q}{T} = \frac{c_p(T)}{T}\,\mathrm{d}T - R_a\frac{\mathrm{d}p}{p}. \tag{39}$$

Comparing the right-hand side of this equation to the total derivative of the new reference potential temperature θ_{ref} (see Appendix E for the detailed computation and Equation (E6) for the result) equation (39) amounts to

$$\frac{\mathrm{d}q}{T} = c_p(\theta_{\mathrm{ref}})\frac{\mathrm{d}\theta_{\mathrm{ref}}}{\theta_{\mathrm{ref}}}. \tag{40}$$

Consequently, the following two diabatic heating rates

$$\begin{aligned}\frac{\mathrm{d}\theta_{\mathrm{ref}}}{\mathrm{d}t} &= \frac{\theta_{\mathrm{ref}}}{c_p^0(\theta_{\mathrm{ref}})T}\frac{\mathrm{d}q}{\mathrm{d}t} = \mathrm{HR}_{\mathrm{ref}}\left(\frac{\mathrm{d}q}{\mathrm{d}t}\right),\\ \frac{\mathrm{d}\theta_{1005}}{\mathrm{d}t} &= \frac{\theta_{1005}}{(1005\,\mathrm{J\,kg^{-1}K^{-1}})\cdot T}\frac{\mathrm{d}q}{\mathrm{d}t} = \mathrm{HR}_{1005}\left(\frac{\mathrm{d}q}{\mathrm{d}t}\right)\end{aligned} \tag{41}$$

for the potential temperatures θ_{ref} and θ_{1005} may be defined. Denoting again by x an arbitrary diabatic heating rate, the relative difference between the heating rates (41) is

$$\frac{\mathrm{HR}_{1005}(x) - \mathrm{HR}_{\mathrm{ref}}(x)}{\mathrm{HR}_{\mathrm{ref}}(x)} = \frac{\theta_{1005}}{\theta_{\mathrm{ref}}}\,\frac{c_p^0(\theta_{\mathrm{ref}})}{1005\,\mathrm{J\,kg^{-1}K^{-1}}} - 1. \tag{42}$$

In order to judge the magnitudes of the relative differences (38) and (42), the monthly averaged temperature profiles from ERA-Interim (Dee et al., 2011) data for 52°N geographical latitude are used, see Figure 11a. The relative differences of the absolute heating rates (38) are shown in Figure 11b and the difference appears to be small. However, the relative differences of the heating rates (42) in Figure 11c are much larger as relative deviations by more than 50 % are reached in the upper stratosphere and lower mesosphere (at pressures below 1 hPa). Additionally, those temperatures were computed, which resulted after 24 h of heating with a constant heating rate $\frac{\mathrm{d}q}{\mathrm{d}t}$ as given in the (averaged) dataset, where a constant pressure is assumed for simplicity. As may be anticipated from the small deviations in Figure 11b, the difference in the final absolute temperatures by using the absolute heating rates AHR_{1005} or $\mathrm{AHR}_{\mathrm{ref}}$ are smaller than 0.044 K. However, the differences in the potential temperatures θ^*_{1005}, θ^*_{ref}, computed with the heating rates $\mathrm{HR}_{\mathrm{ref}}$, HR_{1005} are much larger (Figure 11d), and amount to about 3 % at 10 hPa and about 15 % at 1 hPa. For transport calculations done in isentropic coordinates, these differences are of the same order of magnitude as the deviations resulting from the use of the temperature-dependent instead of the constant c_p. It remains to be decided on individual application whether this additional effect in the calculation is significant.

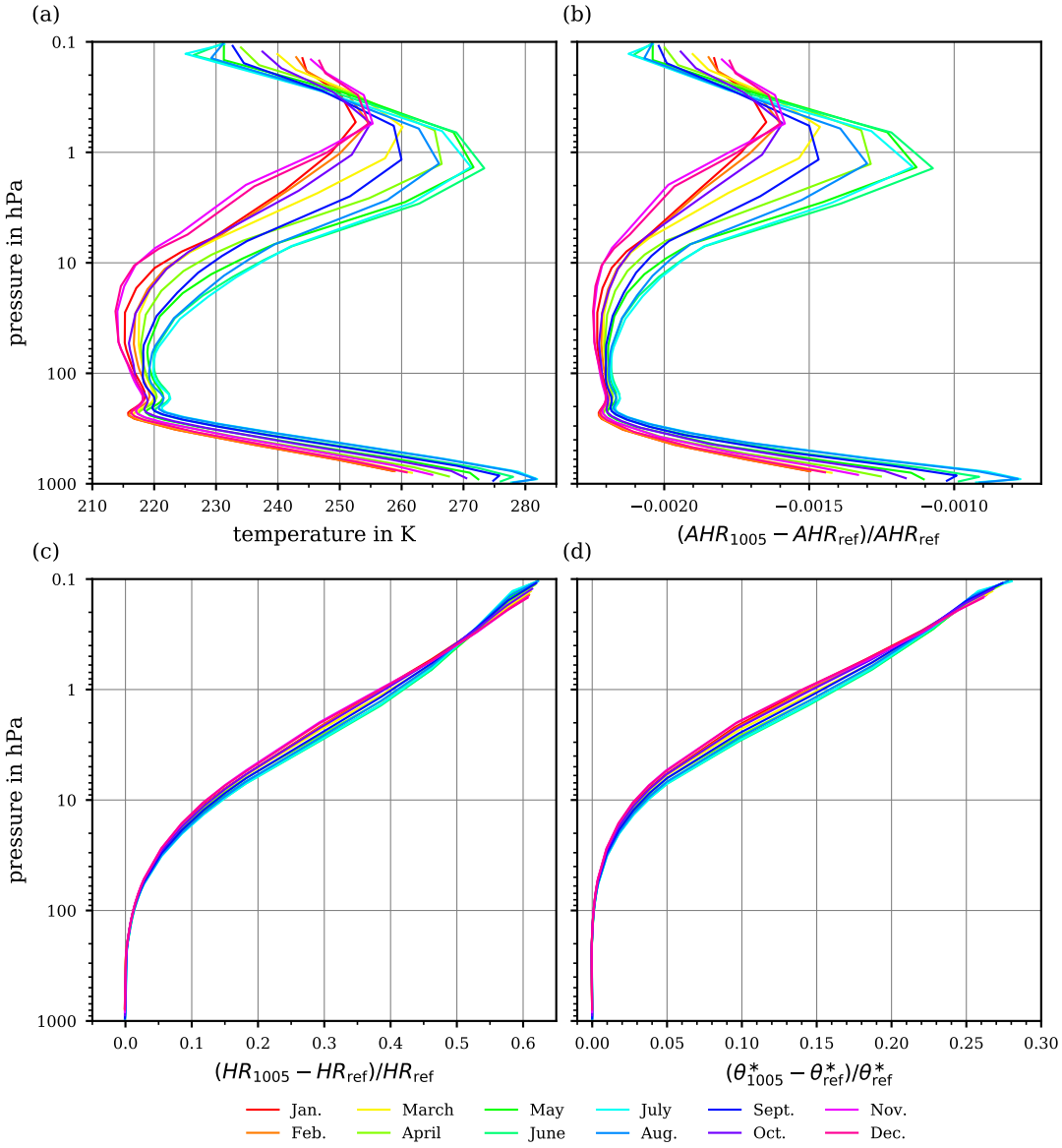

Figure 11. (a) Monthly averaged temperatures profiles for 52°N. (b) The relative differences between the absolute heating rates, defined in (38). (c) The relative differences between the heating rates (42) for the potential temperatures θ_{1005} and θ_{ref}. (d) The resulting potential temperatures θ^*_{1005}, θ^*_{ref} after 24 h of heating with constant diabatic heating $\frac{dq}{dt}$ and the resulting heating rates HR_{ref}, HR_{1005} at constant pressure.

A standard diagnostic for the speed of the stratospheric circulation is the time lag of the upward propagating seasonal signal in tropical stratospheric water vapour (the so-called tape recorder, Mote et al., 1996). Here, differences between calculations (done in isentropic coordinates) based on different current meteorological reanalysis data sets amount to about $10-30\,\%$ for the signal's upward propagation below about $10\,\mathrm{hPa}$ (Tao et al., 2019), such that the additional deviation from using the temperature-dependent c_p is comparably small. However, in cases of smaller inter-model differences the additional c_p-related uncertainty needs to be assessed.

Note, the determination of absolute temperatures $T^*_{1005}, T^*_{\mathrm{ref}}$ which correspond to the resulting potential temperatures $\theta^*_{1005}, \theta^*_{\mathrm{ref}}$ after $24\,\mathrm{h}$ differ by less than $0.014\,\mathrm{K}$ (not shown).

8 Summary and Conclusions

Under the assumption that dry air is an ideal gas, a re-assessment of computing the potential temperature was introduced that accounts for the hitherto unconsidered temperature dependence of air's specific heat capacity. The new reference potential temperature θ_{ref} was introduced, which is thermodynamically consistent and based on a state-of-the-art parameterisation of the ideal-gas specific heat capacity of dry air from the National Institute of Standards and Technology (NIST). This reference potential temperature was compared to a potential temperature θ_{real} wherein the real-gas behaviour of dry air is considered. In the range of temperatures from $180\,\mathrm{K}$ to $300\,\mathrm{K}$ and the range of pressures from $1000\,\mathrm{hPa}$ to $0.5\,\mathrm{hPa}$, covering the atmospheric conditions of roughly the entire troposphere and stratosphere, the relative differences between θ_{ref} and θ_{real} are smaller than $0.03\,\%$ and may be considered negligible. Consequently, θ_{ref} even provides a reasonable approximation to the potential temperature of the real gas.

The difference between the newly derived reference potential temperature θ_{ref} and the conventionally determined potential temperature θ_{c_p} (with constant $c_p = 1005\,\mathrm{J\,kg^{-1}K^{-1}}$, as recommended by the World Meteorological Organisation, WMO, 1966) increases with altitude, e.g., $\Delta\theta \geq 1\,\mathrm{K}$ at pressures $p \leq 60\,\mathrm{hPa}$.

Derivation of a potential temperature that is consistent with thermodynamics and that accounts for the ideal-gas properties of dry air requires the integration of Gibbs' equation and the subsequent solution of the resulting nonlinear equation. With a constant c_p, both analytical steps are straightforward, resulting in the conventional expression (13) as suggested by WMO (1966). However, if instead the temperature dependence of air's specific heat capacity $c_p(T)$ is considered, the integrals as well as the equations are not analytically solvable and, thus, the solution must be approximated. Both approximations were performed and described in detail. The integral was treated with the basic approximation and the solution of the nonlinear equation was ~~approached~~ approximated by using the second iterate of Newton's method. As an alternative to Newton's classical method, a modified formulation of Householder's iteration method is provided, featuring accelerated convergence properties.

The suggested approximation steps to obtain a reference potential temperature have two main sources of error: the error $\theta_{\mathrm{ref}} - \theta_{\mathrm{ref}}^{\mathrm{approx}}$ inherent in the integral's basic approximation and the error $\theta_{\mathrm{ref}}^{\mathrm{approx}} - \theta^{(k)}$ of the k-th Newton iterate. The latter error approaches zero as $k \to \infty$, whereas the error resulting from the basic approximation remains well below $0.1\,\%$ (along

the US Standard Atmosphere) for values of θ_{ref} of up to $\sim 2000\,\mathrm{K}$, hence up to stratopause altitudes. To keep this low error level also for $\theta_{\mathrm{ref}} > 2000\,\mathrm{K}$, the approximation may require an extension by means of a higher-order polynomial.

One of the foremost implications of the re-assessed potential temperature's definition concerns the use of θ as a vertical co-ordinate for the sorting, grouping, and comparison of (measured) data, e.g., along or across isentropes. Thereby, the re-assessed potential temperature constitutes a more accurate consideration of the air's actual properties. This particularly concerns, e.g., the specific heat capacity which is conventionally assumed as constant and for which various values are given depending on the textbook consulted (offering a range from $1000\,\mathrm{J\,kg^{-1}K^{-1}}$ to $1010\,\mathrm{J\,kg^{-1}K^{-1}}$, see Table 1).

Significant errors and biases may arise if, for instance, the conventional derivation of θ (WMO, 1966) is used together with values for air's specific gas constant (R_a) or air's specific heat capacity (c_p), which better comply with the most recent state-of-knowledge. Moreover, the use of the standard pressure $1013.25\,\mathrm{hPa}$ instead of $1000\,\mathrm{hPa}$ as defined by WMO (1966) and consistently used herein as ground level pressure (p_0), may cause an additional deviation of the resulting θ. Thus, the re-assessment of θ's definition could largely diminish such errors and biases and improve the comparability of data.

Concerning ~~investigations of the propagation of gravity waves within the upper atmosphere, one further implication was investigated that arises from using the re-assessed potential temperature~~the implications on the use of the new reference potential temperature, several other applications were discussed alongside the vertical sorting of data, which frequently involve computations using the potential temperature. On the one hand, results may appear mostly unaffected by using θ_{ref} instead of the ~~conventional definition. For predictions concerning the altitude of a gravity wave's breaking, the atmosphere's static stability is analysed, which is a function of both~~ convential θ_{1005}, such as the values of the Brunt-Väisälä frequency or the temperature change of air parcels due to diabatic heating. On the other hand, it was illustrated that any formula which involves the potential temperature needs to be carefully reviewed to see if its derivation relies on the assumed constancy of the specific heat capacity. If this is the case, substituting θ_{ref} for all occurrences of θ ~~and its vertical derivative $\frac{\partial\theta}{\partial z}$. Using the re-assessed reference potential temperature instead of its conventional definition can result in a shift of predicted altitudes where the wave breaking occurs. The analysed cases revealed the prediction's high sensitivity to variations in the initiation conditions and the vertical profiles of temperature and wind. Moreover, the predictions concerning the presence of critical layers within the atmosphere may be impacted by using~~ within the particular formula may lead to a wrong computation.

In contrast, examples were shown where the computation of Ertel's potential vorticity and the rate of change of potential temperature in response to diabatic heating yields different results by the use of θ_{ref} instead of ~~the conventional θ. Of all studied cases, a limited number of predictions produced a vertical deviation on the order of $5\,\mathrm{km}$. Of course, a comprehensive sensitivity study concerning these altitude predictions of gravity waves' breaking should be based on a larger variety of initiation parameters and vertical profiles of the temperature and wind fields from different geographical latitudes. However, such an investigation is beyond the scope of this study. The evaluation of the quantitative and/or qualitative significance of identified vertical shifts and deviations may be left to the reader~~θ_{1005}. The differences increased for increasing altitudes, hence they become more important for applications within the stratosphere and above.

It should be emphasised that all these examples were based on assuming particular profiles of temperature and pressure together with other assumptions. Moreover, only a limited number of examples could be investigated, while the applications of

potential temperature are numerous. Consequently, a well-founded, individual decision is required for each application of the potential temperature as to whether it is worth applying the more rigorous calculation in the particular context.

On the one hand, such a re-assessment could take into account the current state of knowledge regarding the accuracy of thermodynamic variables and substance-related properties. On the other hand, this way, the conceptional abstractness already inherent in θ is not further complicated by a misleading selection of parameters or reputed constants. There is no doubt that the conventional method is suitable for the description of most processes occurring within the troposphere. However, at stratospheric or even mesospheric altitudes, the neglect of the temperature dependence of the ideal-gas heat capacity in the ~~convential~~ conventional definition increasingly distorts the resulting absolute values as well as the vertical course of the potential temperature. Ultimately, it seems obvious to profit from the computing capacities available today and from the known higher accuracy of physical variables and atmospheric parameters to carry out a reappraisal of the potential temperature, a useful (but not always consistently used) meteorological quantity.

Appendix A: Derivation of the specific heat capacity from thermodynamics

In the following, the derivation of the air's specific heat capacities C_V, C_p (capital letters indicate molar units) at constant volume and pressure, respectively, is summarised, mainly following the textbook exposition by Kondepudi and Prigogine (1998). We start with the ideal gas law

$$pV = NRT, \tag{A1}$$

with p the pressure, V the volume of the system, N the amount of gas within the volume, T the temperature, and R the universal gas constant. Additionally, the first law of thermodynamics is

$$\mathrm{d}U = \mathrm{d}Q - p\,\mathrm{d}V, \tag{A2}$$

with the internal energy U of the system and $\mathrm{d}Q$ specifies the change of heat. Insertion of the total derivative of the internal energy U in (A2), and assuming the system as thermodynamically closed, i.e., the molar amount N remains conserved ($\mathrm{d}N = 0$), leads to

$$\mathrm{d}Q - p\,\mathrm{d}V = \left.\frac{\partial U}{\partial T}\right|_{V,N} \mathrm{d}T + \left.\frac{\partial U}{\partial V}\right|_{T,N} \mathrm{d}V, \tag{A3}$$

and subsequently

$$\mathrm{d}Q = \left.\frac{\partial U}{\partial T}\right|_{V,N} \mathrm{d}T + \left(p + \left.\frac{\partial U}{\partial V}\right|_{T,N}\right) \mathrm{d}V. \tag{A4}$$

If the system's volume is held constant, equation (A4) represents the definition of the constant-volume heat capacity C_V in molar units, i.e.,

$$\mathrm{d}Q = \left.\frac{\partial U}{\partial T}\right|_{V,N} \mathrm{d}T = C_V(p,T)\,\mathrm{d}T. \tag{A5}$$

Alternatively, assuming the system's pressure as constant, its volume is variable with total derivative

$$\mathrm{d}V = \left.\frac{\partial V}{\partial T}\right|_{p,N} \mathrm{d}T + \left.\frac{\partial V}{\partial p}\right|_{T,N} \underbrace{\mathrm{d}p}_{=0} = \left.\frac{\partial V}{\partial T}\right|_{p,N} \mathrm{d}T \tag{A6}$$

and, therefore ~~, it results,~~

$$\begin{aligned}
\mathrm{d}Q &= \left.\frac{\partial U}{\partial T}\right|_{V,N} \mathrm{d}T + \left(p + \left.\frac{\partial U}{\partial V}\right|_{T,N}\right) \mathrm{d}V \\
&= \left.\frac{\partial U}{\partial T}\right|_{V,N} \mathrm{d}T + \left(p + \left.\frac{\partial U}{\partial V}\right|_{T,N}\right) \left(\left.\frac{\partial V}{\partial T}\right|_{p,N} \mathrm{d}T\right) \\
&= \left[\left.\frac{\partial U}{\partial T}\right|_{V,N} + \left(p + \left.\frac{\partial U}{\partial V}\right|_{T,N}\right) \left.\frac{\partial V}{\partial T}\right|_{p,N}\right] \mathrm{d}T \\
&= C_p(p,T)\,\mathrm{d}T,
\end{aligned} \tag{A7}$$

defining the isobaric molar heat capacity C_p. In general, this quantity depends on pressure as well as on temperature. However, if the gas is assumed as ideal, an important conclusion from the statistical description of an ideal gas is the fact that the internal energy U must be independent of the pressure (see, e.g., Fay, 1965).

Using this result, together with (A7) and the ideal gas law (A1), it follows

$$\begin{aligned}
C_p &= \left.\frac{\partial U}{\partial T}\right|_{V,N} + \left(p + \left.\frac{\partial U}{\partial V}\right|_{T,N}\right) \left.\frac{\partial V}{\partial T}\right|_{p,N} \\
&= \left.\frac{\partial U}{\partial T}\right|_{V,N} + p \left.\frac{\partial V}{\partial T}\right|_{p,N} \\
&= \left.\frac{\partial U}{\partial T}\right|_{V,N} + \left.\frac{\partial}{\partial T}(pV)\right|_{p,N} \\
&= \left.\frac{\partial U}{\partial T}\right|_{V,N} + \left.\frac{\partial}{\partial T}(NRT)\right|_{p,N} \\
&= \left.\frac{\partial U}{\partial T}\right|_{V,N} + NR.
\end{aligned} \tag{A8}$$

In the previous computations, there is no restriction on the temperature dependence of the internal energy $U(T)$. Therefore, even ~~under the assumption of~~ by assuming ideal-gas behaviour, the specific heat capacity C_p in (A8) is in general a function of temperature.

Appendix B: Sensitivity of the conventional definition of θ to perturbations of c_p

This section explores, from a mathematical perspective, the sensitivity of the potential temperature formulation (13) based on a constant specific heat capacity. Considering the specific heat capacity c_p as a variable, the sensitivity of θ_{c_p} (13) to a small

perturbation δ of c_p is described by ~~the~~ its Taylor expansion

$$\begin{aligned}\theta_{c_p+\delta} &= \theta_{c_p} + \frac{\partial \theta_{c_p}}{\partial c_p}\delta + \mathcal{O}\left(\delta^2\right) \\ &= \theta_{c_p} - \theta_{c_p}\frac{R_a}{c_p^2}\ln\left(\frac{p_0}{p}\right)\delta + \mathcal{O}\left(\delta^2\right).\end{aligned} \tag{B1}$$

For any constant value of the specific heat capacity c_p and for a minor perturbation δ, the second summand within the expansion (B1) remains small for small values of $\ln\left(\frac{p_0}{p}\right)$. If the interval between the two pressure levels is very narrow, i.e., $p \approx p_0$, the expression $\ln\left(\frac{p_0}{p}\right)$ ~~approximates~~ approximately equals $\ln(1) = 0$. Contrarily, if the pressure approaches very low values, i.e., $p \to 0\,\mathrm{Pa}$, the logarithmic expression diverges to negative infinity, i.e., $\ln\left(\frac{p_0}{p}\right) \to -\infty$, implying that the impact of the second summand intensifies with decreasing pressure, i.e., for increasing altitudes. Moreover, this may explain why the deviation between ~~θ_{994} and θ_{1011}~~ θ_{1000} and θ_{1010}, as illustrated in Figure 2b, remains comparatively small within the troposphere and systematically increases with rising altitude, i.e., decreasing pressure levels.

Appendix C: Approximate computation of the reference potential temperature

This section summarises the detailed steps of approximating the function $F(x)$, defined in (23), by $\widehat{F}(x)$, defined in (27) (Section C1), as well as the approximations of the solutions of the resulting nonlinear equations by Newton's method (Section C2).

C1 Reformulating the function $F(x)$

Proceeding from the definition of a function $h(x)$

$$h(x) = \int_{T_1}^{x} \frac{c_p(z)}{z}\frac{c_p(T')}{T'}\,\mathrm{d}zT', \tag{C1}$$

with $T_1 = 180\,\mathrm{K}$, the function $F(x)$ may be rearranged as

$$\begin{aligned}F(x) &= \int_{x}^{T} \frac{c_p(T')}{T'}\,\mathrm{d}T' - R_a\ln\left(\frac{p}{p_0}\right) \\ &= h(T) - h(x) - R_a\ln\left(\frac{p}{p_0}\right).\end{aligned} \tag{C2}$$

The advantage of this reformulation of $F(x)$ is the inclusion of $h(x)$ ~~which consists~~, consisting of an integral with fixed lower bound and a sole variable ~~as~~ upper bound. This way, the function $h(x)$ is numerically solvable, and subsequently $h(x)$ can be substituted by an approximation $f(x)$ that is defined as

$$f(x) = b_0 + b_1\ln(x - b_2) + b_3 x + b_4 x^2. \tag{C3}$$

Notably, if c_p is constant, this function reduces to an exact primitive of the integrand $\frac{c_p}{z}$ $\frac{c_p}{T'}$ with $b_3 = b_4 = 0$. Moreover, in this case, the resulting root-finding problem $0 = F(x)$ is exactly solvable and finally leads to the known conventional definition (13) of the potential temperature.

As a further step, the function $h(x)$ is numerically approximated, while $c_p(T)$ in (C1) is replaced by the ideal-gas limit of air's specific heat capacity $c_p^0(T)$. The integration interval $[T_1, x]$ with $T_1 \leq x \leq 2000\,\mathrm{K}$ is traversed in steps of at most $0.001\,\mathrm{K}$ while each step of the integration process is carefully approximated by using Simpson's rule.

By solving a least-squares problem, the coefficients in (C3) for the approximation of $h(x)$ by the function $f(x)$ are estimated as

$$\begin{aligned} b_0 &= -4072.2121328563667, \\ b_1 &= 797.09247926609601, \\ b_2 &= 29.587047521428016, \\ b_3 &= 0.41981158226925142, \\ b_4 &= -5.1008025097060311 \cdot 10^{-5}. \end{aligned} \tag{C4}$$

In Figure C1a the function $h(x)$ is graphed ~~,~~together with the approximation $f(x)$, as well as the respective deviations $h(x) - f(x)$ in Figure C1b. Evidently, the absolute error inherent to the approximations is comparatively small as, over the entire temperature range above $190\,\mathrm{K}$, the approximation error never exceeds $\pm 1\,\mathrm{J\,kg^{-1}K^{-1}}$. ~~Thus, the approximation error remains even smaller than the error caused by the scatter of given constant values of the specific heat capacity.~~ Exclusively at temperatures below $190\,\mathrm{K}$, the approximation error rapidly rises above $1\,\mathrm{J\,kg^{-1}K^{-1}}$, bearing in mind that such absolute temperatures are only occasionally found in the atmosphere within a relatively narrow altitude interval at the cold point tropopause. Moreover, the deviation of $f(x)$ and $h(x)$ from each other appears negligible as the profiles almost ideally coincide (cf. Figure C1a).

C2 Finalised approximation of the reference potential temperature

As discussed in Section 5.1, the new formulation ~~for~~ of the potential temperature based on the temperature-dependent specific heat capacity $c_p(T)$ requires solving the root-finding problem $0 = F(x)$, where the function $F(x)$ is defined in (23). However, since $F(x)$ contains an integral that complicates the root-finding process, this integral is substituted by the difference $f(T) - f(x)$, where f is given in Section C1. Therefore, $F(x)$ is replaced by the function $\widehat{F}(x)$ as defined in (27) and the zero of the equation $0 = \widehat{F}(x)$ is denoted as $\theta_{\mathrm{ref}}^{\mathrm{approx}}$.

The equation $0 = \widehat{F}(x)$ is still not analytically solvable, so Newton's method is once more required. Using again $x_0 = \theta_{1005}$ as the initial guess, cf. (25), the iteration sequence for Newton's method is given by the recursion

$$\begin{aligned} x_{k+1} &= x_k - \frac{\widehat{F}(x_k)}{\widehat{F}'(x_k)} = x_k - \frac{f(T) - f(x_k) - R_a \ln\left(\frac{p}{p_0}\right)}{-f'(x_k)} \\ &= x_k - \frac{R_a \ln\left(\frac{p}{p_0}\right) - f(T) + f(x_k)}{f'(x_k)}. \end{aligned} \tag{C5}$$

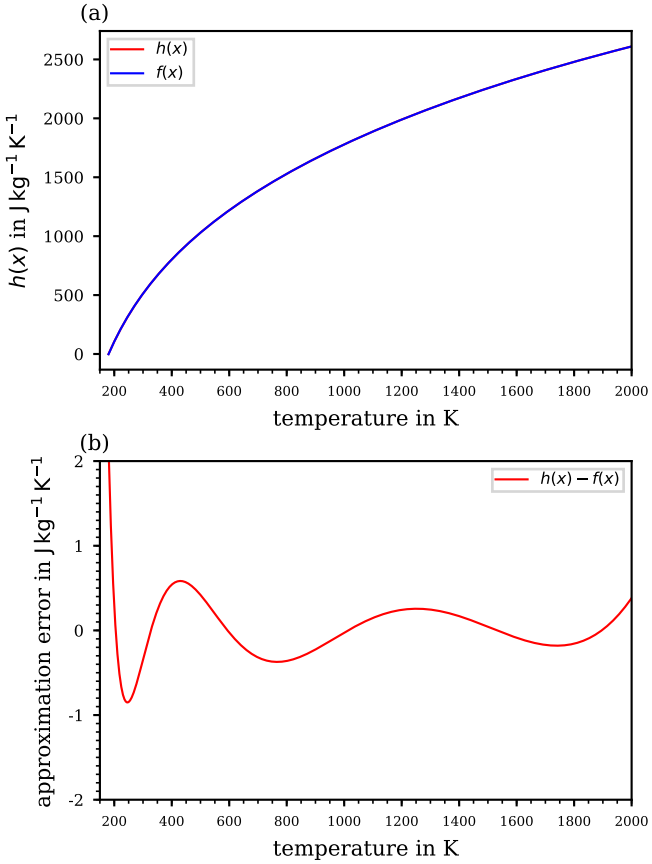

Figure C1. (a) Numerically evaluated function $h(x)$ together with its approximation $f(x)$; (b) the absolute approximation error $h(x) - f(x)$.

Instead of this standard formulation of Newton's method (C5), Householder's formulation

$$\begin{aligned} x_{k+1} &= x_k - \frac{\widehat{F}(x_k)}{\widehat{F}'(x_k)} - \frac{\widehat{F}''(x_k)}{2\widehat{F}'(x_k)} \left[\frac{\widehat{F}(x_k)}{\widehat{F}'(x_k)}\right]^2 \\ &= x_k - \frac{R_a \ln\left(\frac{p}{p_0}\right) - f(T) + f(x_k)}{f'(x_k)} \\ &\quad - \frac{f''(x_k)}{2f'(x_k)} \left[\frac{R_a \ln\left(\frac{p}{p_0}\right) - f(T) + f(x_k)}{f'(x_k)}\right]^2 \end{aligned} \tag{C6}$$

may be used, which allows for reducing the computation time due to its accelerated convergence speed. For completeness, the required derivatives f', f'' in the recursion formulas (C5) and (C6) are

$$\begin{aligned} f'(x) &= \frac{b_1}{x - b_2} + b_3 + 2b_4 x, \\ f''(x) &= 2b_4 - \frac{b_1}{(x - b_2)^2}. \end{aligned} \tag{C7}$$

z in m	T in K	p in Pa	θ_{ref} in K	$\theta^{(1)}$ in K	$\theta^{(2)}$ in K	$\theta^{(1)}_{\mathrm{Householder}}$ in K
5500	252.4	50506.8	306.837	307.016	307.016	307.016
11000	216.65	22632.1	331.337	331.510	331.510	331.510
20000	216.65	5474.89	494.940	495.376	495.378	495.378
32000	228.65	868.019	855.324	855.172	855.656	855.660
47000	270.65	110.906	1637.052	1620.463	1637.726	1638.974

Table C1. Values of the new reference potential temperature θ_{ref}, together with the first two iterates $\theta^{(1)}$, $\theta^{(2)}$ using Newton's method and the first iterate $\theta^{(1)}_{\mathrm{Householder}}$ using Householder's method for five pairs of temperature and pressure along the US Standard Atmosphere. The computed values are rounded to three digits.

The final step on the way to formulate a new expression for the potential temperature requires defining one of the iterates x_k as appropriate enough for the approximations that result from applying the different methods:

- the standard of Newton's method (C5), simply referred to as Newton's method in the sequel, or
- Householder's method (C6).

While the mathematical expressions in (C5) and (C6) are of increasing complexity, the convergence rate of the approximating sequence increases with rising mathematical complication. The preferred method is determined by the accuracy required, i.e., an elevated accuracy level is necessarily associated with elevated computational effort for the approximation method. A discussion of the approximation errors is found in Appendix D.

Table C1 collects values of the new reference potential temperature θ_{ref}, together with the first two iterates $\theta^{(1)}$, $\theta^{(2)}$ using Newton's method (C5) and the first iterate $\theta^{(1)}_{\mathrm{Householder}}$ using Householder's method (C6) for five pairs of temperature and pressure along the US Standard Atmosphere, cf. Figure 1, which allows ~~to verify a computation~~verification of computations. The first height is chosen midway along the linearly decreasing temperature profile within the troposphere, while the other heights correspond to the kinks of the temperature profile.

Appendix D: Approximation error for the reference potential temperature

The following aims at a comprehensive investigation of the errors inherent with approximating the ultimate reference potential temperature θ_{ref}. As discussed in Section 5.2, the total error is a combination of the basic error $\theta_{\mathrm{ref}} - \theta^{\mathrm{approx}}_{\mathrm{ref}}$ and, furthermore, the approximation error that results from the approximation sequence $\theta^{\mathrm{approx}}_{\mathrm{ref}} - \theta^{(k)}$, where $\theta^{(k)}$ denotes the k-th iterate of the approximation sequence which is computed in accordance with either Newton's or Householder's method. The formulations of Newton's (C5) and Householder's (C6) method require replacing the function $F(x)$ by $\widehat{F}(x)$, and the approximation sequences $\theta^{(k)}$ converge to $\theta^{\mathrm{approx}}_{\mathrm{ref}}$ for $k \to \infty$. Consequently, the approximation error $\theta^{\mathrm{approx}}_{\mathrm{ref}} - \theta^{(k)}$ tends to zero for $k \to \infty$.

The analysis of the approximation error is initially based on the pressure and temperature profiles of the US Standard Atmosphere. Figure D1 shows the total relative errors $\left(\theta_{\mathrm{ref}} - \theta^{(1)}\right)/\theta_{\mathrm{ref}}$ of the first iterate (Figure D1a) and $\left(\theta_{\mathrm{ref}} - \theta^{(2)}\right)/\theta_{\mathrm{ref}}$

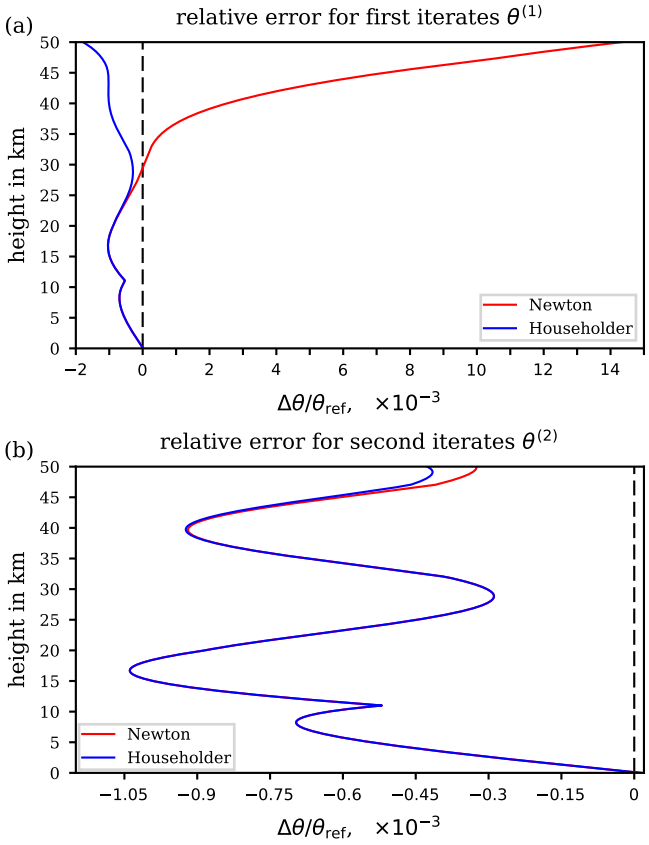

Figure D1. Total relative error along the US Standard Atmosphere arising from the iteration process by declaring (a) the first iterate $\theta^{(1)}$ or (b) the second iterate $\theta^{(2)}$ as the final approximation to the reference potential temperature θ_{ref}. Red curves: iterates computed using Newton's method (C5); blue curves: iterates computed using Householder's method (C6). Note the different range of the abscissae.

of the second iterate (Figure D1b), computed with Newton's or Householder's method. The first iterate still causes the approximation to have significant errors, especially at altitudes above $35\,\mathrm{km}$. However, the second iterate with either Newton's or Householder's method yields results with negligible approximation error. Hence, the total error of the approximation procedure is dominated by the unavoidable basic error, and may be deduced from the provided figures whenever the total error profile nearly congruently follows the profile of the basic error (cf. Figures D1b and 5a).

It may be noted that Householder's method achieves a significantly lower error level than Newton's method due to its accelerated rate of convergence. Compared to the first iterate approximations, computation up to the second iterate (cf. Figure D1b) achieves, in general, a considerable improvement for both methods, and both second iterate approximations approach the basic error quite closely (cf. Figure D1b). As is also evident from Figure D1b, compared to Householder's method, the second iterate with Newton's method results in a smaller total relative error $\left(\theta_{\mathrm{ref}} - \theta^{(2)}\right)/\theta_{\mathrm{ref}}$ relative to the ultimate reference potential temperature (indicated by a smaller distance to the dashed zero-line above $45\,\mathrm{km}$ altitude). Nevertheless, the relative

approximation error, $\left(\theta_{\mathrm{ref}}^{\mathrm{approx}} - \theta^{(2)}\right)/\theta_{\mathrm{ref}}$, is larger compared to the second iterate with Householder's method. So, luckily, the second iterate with Newton's method provides a better approach to the reference potential temperature than that with Householder's method.

As for the discussion of the basic error in Section 5.2, the analysis of the total error should include all possible combinations of pressure and temperature in order to take into account fluctuations in the real atmosphere that deviate from the profile of the US Standard Atmosphere. Therefore, the extended analysis of the approximation error is summarised in Figure D2. The upper panels illustrate the total relative error of the second iterate for Newton's (Figure D2a) and Householder's method (Figure D2b). As previously shown, any further iteration with either method does not improve the approximation quality. The contour patterns in these panels show a remarkable similarity to the contours for the relative error of the basic approximation in Figure 5c. Also here (upper panels of Figure D2), two regions are highlighted by the contours, i.e., at $\sim 100\,\mathrm{hPa}$ and in a pressure range from $\sim 5\,\mathrm{hPa}$ to $1\,\mathrm{hPa}$, featuring the same impact on $\Delta\theta/\theta_{\mathrm{ref}}$ of identical strength as the basic error. This result may not be surprising, since the second iteration step with both methods, Newton's and Householder's, was already proven to approach the approximation comparatively well, without worsening the total error level (cf. Figure D1b).

Consequently, concerning the required number of iterations and the method to use, the second iteration of Newton's method can be recommended to deliver appropriate results, with a relative error of less than $0.3\,\%$, up to the stratopause level ($\sim 50\,\mathrm{km}$). Householder's method features an accelerated convergence rate, and its use up to its first iterate $\theta^{(1)}$ may be already appropriate for certain applications. According to the total error of Householder's method up to its first iterate $\theta^{(1)}$ (Figure D2c), the resulting relative error remains below $7\,\%$ to a pressure level of $\sim 50\,\mathrm{hPa}$ and $\Delta\theta$ stays below $0.3\,\%$ to pressures of $\sim 2\,\mathrm{hPa}$. Thus, Figure D2 may serve as guidance to decide how many iterations with one or the other method best meets the individual accuracy requirements.

Appendix E: The derivative of the reference potential temperature

As discussed in Section 5.1, the new reference potential temperature is defined as the zero of the function

$$F(x, p, T) = \int_x^T \frac{c_p(T')}{T'}\,\mathrm{d}T' - R_a \ln\left(\frac{p}{p_0}\right) \tag{E1}$$

for given values of pressure p and temperature T, see Equation (23). More precisely, for varying p, T, a function $(p, T) \mapsto \theta_{\mathrm{ref}}(p, T)$ is implicitly defined by the equation

$$F(\theta_{\mathrm{ref}}(p, T), p, T) = 0. \tag{E2}$$

According to the implicit function theorem (e.g., Protter and Morrey, 1985, chapter 7), equation (E2) is uniquely solvable for $\theta_{\mathrm{ref}}(p, T)$, i.e., the function $(p, T) \mapsto \theta_{\mathrm{ref}}(p, T)$ actually exists as a differentiable function of (p, T), if the condition $\frac{\partial F}{\partial \theta} \neq 0$ holds. According to (E1), this partial derivative equals

$$\frac{\partial F}{\partial \theta}(\theta_{\mathrm{ref}}, p, T) = -\frac{c_p(\theta_{\mathrm{ref}})}{\theta_{\mathrm{ref}}}, \tag{E3}$$

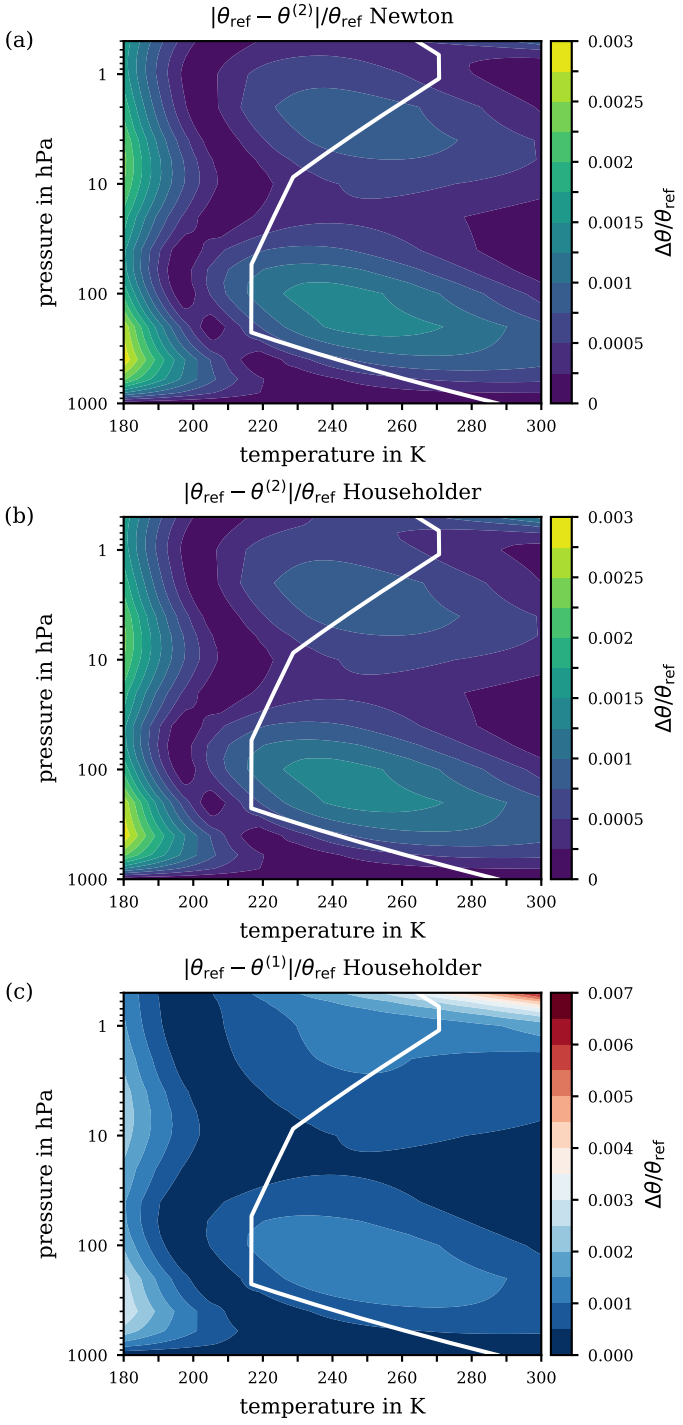

Figure D2. Relative error of the second iterates $\theta^{(2)}$ with (a) Newton's method and (b) Householder's method for the the ranges of pressure and temperature from $1000\,\mathrm{hPa}$ to $0.5\,\mathrm{hPa}$ and from $180\,\mathrm{K}$ to $300\,\mathrm{K}$, respectively. (c) The absolute error arising from the first iterate $\theta^{(1)}$ with Householder's method. The white solid line indicates the p-T-profile from the US Standard Atmosphere. Note the different ranges of the $\Delta\theta$ scales.

being strictly negative, since the specific heat capacity only attains positive values. Moreover, the implicit function theorem states that the derivatives of the implicit function $\theta_{\mathrm{ref}}(p,T)$ are given by

$$\begin{aligned}
&\left[\frac{\partial\theta_{\mathrm{ref}}}{\partial p}(p,T),\,\frac{\partial\theta_{\mathrm{ref}}}{\partial T}(p,T)\right]\\
&=-\left(\frac{\partial F}{\partial\theta}(\theta_{\mathrm{ref}},p,T)\right)^{-1}\left[\frac{\partial F}{\partial p}(\theta_{\mathrm{ref}},p,T),\,\frac{\partial F}{\partial T}(\theta_{\mathrm{ref}},p,T)\right]\\
&=\frac{\theta_{\mathrm{ref}}}{c_p(\theta_{\mathrm{ref}})}\left[-\frac{R_a}{p},\,\frac{c_p(T)}{T}\right]\\
&=\left[-\frac{R_a}{c_p(\theta_{\mathrm{ref}})}\frac{\theta_{\mathrm{ref}}}{p},\,\frac{\theta_{\mathrm{ref}}}{T}\frac{c_p(T)}{c_p(\theta_{\mathrm{ref}})}\right].
\end{aligned}\tag{E4}$$

Note, these partial derivatives coincide with the partial derivatives of θ_{c_p} in case of a constant specific heat capacity. Using the partial derivatives (E4), the total differential of θ_{ref} may be written as

$$\begin{aligned}
\mathrm{d}\theta_{\mathrm{ref}}&=\frac{\partial\theta_{\mathrm{ref}}}{\partial p}\,\mathrm{d}p+\frac{\partial\theta_{\mathrm{ref}}}{\partial T}\,\mathrm{d}T\\
&=-\frac{R_a}{c_p(\theta_{\mathrm{ref}})}\frac{\theta_{\mathrm{ref}}}{p}\,\mathrm{d}p+\frac{\theta_{\mathrm{ref}}}{T}\frac{c_p(T)}{c_p(\theta_{\mathrm{ref}})}\,\mathrm{d}T
\end{aligned}\tag{E5}$$

or

$$c_p(\theta_{\mathrm{ref}})\frac{\mathrm{d}\theta_{\mathrm{ref}}}{\theta_{\mathrm{ref}}}=c_p(T)\frac{\mathrm{d}T}{T}-R_a\frac{\mathrm{d}p}{p}.\tag{E6}$$

Author contributions. MB, RW, and PS conceived, designed, and carried out the main part of the research. UA contributed the URAP data and implications on breaking heights of gravity waves. AH gave advice about the heat capacity and performed the calculations of real-gas potential temperatures. FP contributed the implications on the diabatic heating. MB and RW wrote the manuscript with contributions and reviews from all authors.

Competing interests. The authors declare that they have no conflict of interest.

Acknowledgements. We thank Eric W. Lemmon for his advice on the equation of state of dry air, Vera Bense for fruitful discussions on gravity wave breaking, Gergely Bölöni for providing us the URAP vertical profiles in Section 7, and Miklós Szakáll for the hint concerning Titan's atmosphere, and Heini Wernli for his interest in an early version of the draft. We thank Pascal Marquet and an anonymous reviewer for their very valuable comments and hints which led to a significantly improved manuscript. Manuel Baumgartner and Peter Spichtinger acknowledge support by the Deutsche Forschungsgemeinschaft (DFG) within the Transregional Collaborative Research Centre TRR165 Waves to Weather, (www.wavestoweather.de), projects B7 and Z2. Ralf Weigel received financial support by the *Bundesministerium für Bildung und Forschung*

(BMBF) under the joint ROMIC-project *SPITFIRE* (01LG1205A). Ulrich Achatz and Peter Spichtinger acknowledge partial support by the DFG through the research unit Multiscale Dynamics of Gravity Waves (MS-GWaves) and through grants AC 71/12-2 and SP 1163/5-2.

References

Ambaum, M. H. P.: Thermal Physics of the Atmosphere, John Wiley & Sons, Ltd, https://doi.org/10.1002/9780470710364, 2010.

Awano, S.: JS-Diagrams for Air, Report of Aeronautical Research Institute, Tokyo Imperial University, 11, https://doi.org/10.1175/1520-0469(1970)027<0919:TDOICI>2.0.CO;2, 1936.

Bauer, L. A.: The relation between "potential temperature" and "entropy", Phys. Rev., 26, 177–183, 1908.

Bohren, C., Albrecht, B., and Albrecht, P.: Atmospheric Thermodynamics, Oxford University Press, 1998.

Bölöni, G., Ribstein, B., Muraschko, J., Sgoff, C., Wei, J., and Achatz, U.: The Interaction between Atmospheric Gravity Waves and Large-Scale Flows: An Efficient Description beyond the Nonacceleration Paradigm, Journal of the Atmospheric Sciences, 73, 4833–4852, https://doi.org/10.1175/JAS-D-16-0069.1, 2016.

Bolton, D.: The Computation of Equivalent Potential Temperature, Monthly Weather Review, 108, 1046–1053, https://doi.org/10.1175/1520-0493(1980)108<1046:TCOEPT>2.0.CO;2, 1980.

Borchert, S., Zhou, G., Baldauf, M., Schmidt, H., Zängl, G., and Reinert, D.: The upper-atmosphere extension of the ICON general circulation model (version: ua-icon-1.0), Geoscientific Model Development, 12, 3541–3569, https://doi.org/10.5194/gmd-12-3541-2019, 2019.

Borrmann, S., Kunkel, D., Weigel, R., Minikin, A., Deshler, T., Wilson, J. C., Curtius, J., Volk, C. M., Homan, C. D., Ulanovsky, A., Ravegnani, F., Viciani, S., Shur, G. N., Belyaev, G. V., Law, K. S., and Cairo, F.: Aerosols in the tropical and subtropical UT/LS: in-situ measurements of submicron particle abundance and volatility, Atmospheric Chemistry and Physics, 10, 5573–5592, https://doi.org/10.5194/acp-10-5573-2010, 2010.

Brasseur, G. P. and Solomon, S.: Aeronomy of the Middle Atmosphere, Springer, https://doi.org/10.1007/1-4020-3824-0, 2005.

Brusseau, M., Pepper, I. L., and Gerba, C. P.: Environmental and Pollution Science, Elsevier, third edn., https://doi.org/10.1016/C2017-0-00480-9, 2019.

Bücker, D., Span, R., and Wagner, W.: Thermodynamic Property Models for Moist Air and Combustion Gases, Journal of Engineering for Gas Turbines and Power, 125, 374–384, https://doi.org/10.1115/1.1520154, 2002.

Catling, D. C.: 10.13 - Planetary Atmospheres, in: Treatise on Geophysics, edited by Schubert, G., pp. 429 – 472, Elsevier, Oxford, second edn., https://doi.org/10.1016/B978-0-444-53802-4.00185-8, 2015.

Chang, X., Zhao, W., Zhang, Z., and Su, Y.: Sap flow and tree conductance of shelter-belt in arid region of China, Agricultural and Forest Meteorology, 138, 132 – 141, https://doi.org/10.1016/j.agrformet.2006.04.003, 2006.

Chipperfield, M. P.: New version of the TOMCAT/SLIMCAT off-line chemical transport model: Intercomparison of stratospheric tracer experiments, Quarterly Journal of the Royal Meteorological Society, 132, 1179–1203, https://doi.org/10.1256/qj.05.51, 2006.

Choi, H.-J. and Chun, H.-Y.: Momentum Flux Spectrum of Convective Gravity Waves. Part I: An Update of a Parameterization Using Mesoscale Simulations, J. Atmos. Sci., 68, 739–759, https://doi.org/10.1175/2010JAS3552.1, 2011.

Cotton, W. R., Bryan, G. H., and van den Heever, S. C.: Storm and Cloud Dynamics, Academic Press, second edn., 2011.

Curry, J. and Webster, P.: Thermodynamics of Atmospheres and Oceans, vol. 65 of *International Geophysics*, Elsevier, 1998.

Curtius, J., Weigel, R., Vössing, H.-J., Wernli, H., Werner, A., Volk, C.-M., Konopka, P., Krebsbach, M., Schiller, C., Roiger, A., Schlager, H., Dreiling, V., and Borrmann, S.: Observations of meteoric material and implications for aerosol nucleation in the winter Arctic lower stratosphere derived from in situ particle measurements, Atmospheric Chemistry and Physics, 5, 3053–3069, https://doi.org/10.5194/acp-5-3053-2005, 2005.

Davies, S., Mann, G. W., Carslaw, K. S., Chipperfield, M. P., Remedios, J. J., Allen, G., Waterfall, A. M., Spang, R., and Toon, G. C.: Testing our understanding of Arctic denitrification using MIPAS-E satellite measurements in winter 2002/2003, Atmospheric Chemistry and Physics, 6, 3149–3161, https://doi.org/10.5194/acp-6-3149-2006, 2006.

Dee, D. P., Uppala, S. M., Simmons, A. J., Berrisford, P., Poli, P., Kobayashi, S., Andrae, U., Balmaseda, M. A., Balsamo, G., Bauer, P., Bechtold, P., Beljaars, A. C. M., van de Berg, L., Bidlot, J., Bormann, N., Delsol, C., Dragani, R., Fuentes, M., Geer, A. J., Haimberger, L., Healy, S. B., Hersbach, H., Hólm, E. V., Isaksen, L., Kållberg, P., Köhler, M., Matricardi, M., McNally, A. P., Monge-Sanz, B. M., Morcrette, J.-J., Park, B.-K., Peubey, C., de Rosnay, P., Tavolato, C., Thépaut, J.-N., and Vitart, F.: The ERA-Interim reanalysis: configuration and performance of the data assimilation system, Quarterly Journal of the Royal Meteorological Society, 137, 553–597, https://doi.org/10.1002/qj.828, 2011.

Dessler, A. E.: The effect of deep, tropical convection on the tropical tropopause layer, Journal of Geophysical Research: Atmospheres, 107, ACH 6–1–ACH 6–5, https://doi.org/10.1029/2001JD000511, 2002.

Deuflhard, P.: Newton Methods for Nonlinear Problems, vol. 35 of *Springer Series in Computational Mathematics*, Springer-Verlag, Berlin Heidelberg, https://doi.org/10.1007/978-3-642-23899-4, 2011.

Dixon, J. C.: The Shock Absorber Handbook, John Wiley & Sons Ltd, Chichester, second edn., 2007.

Durran, D. R. and Klemp, J. B.: On the Effects of Moisture on the Brunt-Väisälä Frequency, Journal of the Atmospheric Sciences, 39, 2152–2158, https://doi.org/10.1175/1520-0469(1982)039<2152:OTEOMO>2.0.CO;2, 1982.

Emanuel, K. A.: Atmospheric Convection, Oxford University Press, 1994.

Ertel, H.: Ein neuer hydrodynamischer Wirbelsatz, Meteorolog. Zeitschr., 59, 277–281, 1942.

Fay, J. A.: Molecular Thermodynamics, Engineering Sciences, Addison-Wesley, Reading, Massachusetts, 1965.

Feistel, R.: A Gibbs function for seawater thermodynamics for -6 to $80\,^{\circ}\mathrm{C}$ and salinity up to $120\,\mathrm{g\,kg^{-1}}$, Deep Sea Research Part I: Oceanographic Research Papers, 55, 1639 – 1671, https://doi.org/10.1016/j.dsr.2008.07.004, 2008.

Frey, W.: Airborne in situ measurements of ice particles in the tropical tropopause layer, Ph.D. thesis, Universität Mainz, Mainz, 2011.

Gettelman, A., Hoor, P., Pan, L. L., Randel, W. J., Hegglin, M. I., and Birner, T.: The Extratropical Upper Troposphere and Lower Stratosphere, Reviews of Geophysics, 49, https://doi.org/10.1029/2011RG000355, 2011.

Hallam, A.: Alfred Wegener and the Hypothesis of Continental Drift, Scientific American, 232, 88–97, http://www.jstor.org/stable/24949733, 1975.

Hauf, T. and Höller, H.: Entropy and Potential Temperature, Journal of the Atmospheric Sciences, 44, 2887–2901, https://doi.org/10.1175/1520-0469(1987)044<2887:EAPT>2.0.CO;2, 1987.

Holton, J. R.: An Introduction to Dynamic Meteorology, vol. 88 of *International Geophysics Series*, Elsevier Academic Press, fourth edn., 2004.

Holton, J. R., Haynes, P. H., McIntyre, M. E., Douglass, A. R., Rood, R. B., and Pfister, L.: Stratosphere-troposphere exchange, Reviews of Geophysics, 33, 403–439, https://doi.org/10.1029/95RG02097, 1995.

Höpfner, M., Ungermann, J., Borrmann, S., Wagner, R., Spang, R., Riese, M., Stiller, G., Appel, O., Batenburg, A. M., Bucci, S., Cairo, F., Dragoneas, A., Friedl-Vallon, F., Hünig, A., Johansson, S., Krasauskas, L., Legras, B., Leisner, T., Mahnke, C., Möhler, O., Molleker, S., Müller, R., Neubert, T., Orphal, J., Preusse, P., Rex, M., Saathoff, H., Stroh, F., Weigel, R., and Wohltmann, I.: Ammonium nitrate particles formed in upper troposphere from ground ammonia sources during Asian monsoons, Nat Geosci, 12, 608–612, https://doi.org/10.1038/s41561-019-0385-8, 2019.

Hoskins, B. J., McIntyre, M. E., and Robertson, A. W.: On the use and significance of isentropic potential vorticity maps, Quart. J. R. Met. Soc., 111, 877–946, 1985.

Houghton, J.: The Physics of Atmospheres, Cambridge University Press, 2002.

Huang, K.: Statistical Mechanics, John Wiley & Sons, New York, second edn., 1987.

Jakob, M.: Die spezifische Wärme der Luft im Bereich von 0 bis 200 at und von -80 bis 250°, Mitteilungen aus der Physikalisch-Technischen Reichsanstalt, Zeitschr. f. techn. Physik, pp. 460–468, 1923.

Kondepudi, D. and Prigogine, I.: Modern Thermodynamics, John Wiley & Son, Chichester, 1998.

Köppen, W. P.: Über Luftmischung und potentielle Temperatur, in Anlehnung an die neueste Abhandlung von Herrn v. Helmholtz, 1888.

Kunz, O. and Wagner, W.: The GERG-2008 Wide-Range Equation of State for Natural Gases and Other Mixtures: An Expansion of GERG-2004, J. Chem. Eng. Data, 57, 3032 – 3091, https://doi.org/10.1021/je300655b, 2012.

Kutzbach, G.: The Thermal Theory of Cyclones: A History of Meteorological Thought in the Nineteenth Century, Meteorological Monographs, American Meteorological Society, 2016.

Lary, D. J., Chipperfield, M. P., Pyle, J. A., Norton, W. A., and Riishøjgaard, L. P.: Three-dimensional tracer initialization and general diagnostics using equivalent PV latitude–potential-temperature coordinates, Quarterly Journal of the Royal Meteorological Society, 121, 187–210, https://doi.org/10.1002/qj.49712152109, 1995.

Lemmon, E. W., Jacobsen, R. T., Penoncello, S. G., and Friend, D. G.: Thermodynamic Properties of Air and Mixtures of Nitrogen, Argon, and Oxygen From 60 to 2000 K at Pressures to 2000 MPa, Journal of Physical and Chemical Reference Data, 29, 331–385, https://doi.org/10.1063/1.1285884, 2000.

Lemmon, E. W., Bell, I. H., Huber, M. L., and McLinden, M. O.: NIST Standard Reference Database 23: Reference Fluid Thermodynamic and Transport Properties-REFPROP, Version 10.0, National Institute of Standards and Technology, https://doi.org/10.18434/T4/1502528, 2018.

Li, C. and Chen, X.: Simulating Nonhydrostatic Atmospheres on Planets (SNAP): Formulation, Validation, and Application to the Jovian Atmosphere, The Astrophysical Journal Supplement Series, 240, 37, https://doi.org/10.3847/1538-4365/aafdaa, 2019.

Li, C., Ingersoll, A. P., and Oyafuso, F.: Moist Adiabats with Multiple Condensing Species: A New Theory with Application to Giant-Planet Atmospheres, Journal of the Atmospheric Sciences, 75, 1063–1072, https://doi.org/10.1175/JAS-D-17-0257.1, 2018.

Lindzen, R. S.: Turbulence and stress owing to gravity wave and tidal breakdown, J. Geophys. Res., 86, 9707–9714, 1981.

Liou, K. N.: An Introduction to Atmospheric Radiation, vol. 84 of *International Geophysics*, Elsevier, second edn., 2002.

Marquet, P.: Definition of a moist entropy potential temperature: application to FIRE-I data flights, Quarterly Journal of the Royal Meteorological Society, 137, 768–791, https://doi.org/10.1002/qj.787, 2011.

Marquet, P.: On the definition of a moist-air potential vorticity, Quarterly Journal of the Royal Meteorological Society, 140, 917–929, https://doi.org/10.1002/qj.2182, 2014.

Marquet, P.: Le troisième principe de la thermodynamique ou une définition absolue de l'entropie - Partie 2 : Définitions et applications en météorologie et en climat, https://doi.org/10.4267/2042/70559, an english translation is available at arXiv: https://arxiv.org/abs/1904.11699, 2019.

Marquet, P. and Geleyn, J.-F.: On a general definition of the squared Brunt-Väisälä frequency associated with the specific moist entropy potential temperature, Quarterly Journal of the Royal Meteorological Society, 139, 85–100, https://doi.org/10.1002/qj.1957, 2013.

Marquet, P. and Geleyn, J.-F.: Formulations of moist thermodynamics for atmospheric modelling, chap. Chapter 22, pp. 221–274, https://doi.org/10.1142/9781783266913_0026, 2015.

McDougall, T. J., Jackett, D. R., Wright, D. G., and Feistel, R.: Accurate and Computationally Efficient Algorithms for Potential Temperature and Density of Seawater, Journal of Atmospheric and Oceanic Technology, 20, 730–741, https://doi.org/10.1175/1520-0426(2003)20<730:AACEAF>2.0.CO;2, 2003.

Mote, P. W., Rosenlof, K. H., McIntyre, M. E., Carr, E. S., Gille, J. G., Holton, J. R., Kinnersley, J. S., Pumphrey, H. C., Russell III, J. M., and Waters, J. W.: An atmospheric tape recorder: The imprint of tropical tropopause temperatures on stratospheric water vapor, jgr, 101, 3989 – 4006, 1996.

Müller-Wodarg, I., Griffith, C. A., Lellouch, E., and Cravens, T. E.: Titan: Interior, Surface, Atmosphere, and Space Environment, vol. 14 of *Cambridge Planetary Science*, Cambridge University Press, 2014.

Murphy, D. M., Cziczo, D. J., Hudson, P. K., and Thomson, D. S.: Carbonaceous material in aerosol particles in the lower stratosphere and tropopause region, Journal of Geophysical Research: Atmospheres, 112, https://doi.org/10.1029/2006JD007297, 2007.

Newell, D. B., Cabiati, F., Fischer, J., Fujii, K., Karshenboim, S. G., Margolis, H. S., de Mirandés, E., Mohr, P. J., Nez, F., Pachucki, K., Quinn, T. J., Taylor, B. N., Wang, M., Wood, B. M., and Zhang, Z.: The CODATA 2017 values of h, e, k, and N_{A} for the revision of the SI, Metrologia, 55, L13–L16, https://doi.org/10.1088/1681-7575/aa950a, 2018.

Ooyama, K. V.: A Thermodynamic Foundation for Modeling the Moist Atmosphere, Journal of the Atmospheric Sciences, 47, 2580–2593, https://doi.org/10.1175/1520-0469(1990)047<2580:ATFFMT>2.0.CO;2, 1990.

Ooyama, K. V.: A Dynamic and Thermodynamic Foundation for Modeling the Moist Atmosphere with Parameterized Microphysics, Journal of the Atmospheric Sciences, 58, 2073–2102, https://doi.org/10.1175/1520-0469(2001)058<2073:ADATFF>2.0.CO;2, 2001.

Palmer, T. N., Shutts, G. J., and Swinbank, R.: Alleviation of a systematic westerly bias in general circulation and numerical weather-prediction models through an orographic gravity wave drag parametrization, Q. J. R. Meteorol. Soc., 112, 1001–1039, 1986.

Plougonven, R. and Zhang, F.: Internal gravity waves from atmospheric jets and fronts, Rev. Geophys., 52, 33–76, https://doi.org/10.1002/2012RG000419, 2014.

Poisson, S. D.: Traité de mécanique, Bachelier, Paris, seconde edn., https://gallica.bnf.fr/ark:/12148/bpt6k9605452x.texteImage, 1833.

Pommrich, R., Müller, R., Grooß, J.-U., Konopka, P., Ploeger, F., Vogel, B., Tao, M., Hoppe, C. M., Günther, G., Spelten, N., Hoffmann, L., Pumphrey, H.-C., Viciani, S., D'Amato, F., Volk, C. M., Hoor, P., Schlager, H., and Riese, M.: Tropical troposphere to stratosphere transport of carbon monoxide and long-lived trace species in the Chemical Lagrangian Model of the Stratosphere (CLaMS), Geoscientific Model Development, 7, 2895–2916, https://doi.org/10.5194/gmd-7-2895-2014, 2014.

Protter, M. H. and Morrey, C. B.: Intermediate Calculus, Undergraduate Texts in Mathematics, second edn., https://doi.org/10.1007/978-1-4612-1086-3, 1985.

Pruppacher, H. R. and Klett, J. D.: Microphysics of Clouds and Precipitation, vol. 18 of *Atmospheric and Oceanographic Sciences Library*, Kluwer Academic Publishers, Dordrecht, 2010.

Reinke-Kunze, C.: Alfred Wegener: Polarforscher und Entdecker der Kontinentaldrift, Lebensgeschichten aus der Wissenschaft, Birkhäuser Basel, 2013.

Richardson, M. I., Toigo, A. D., and Newman, C. E.: PlanetWRF: A general purpose, local to global numerical model for planetary atmospheric and climate dynamics, Journal of Geophysical Research: Planets, 112, https://doi.org/10.1029/2006JE002825, 2007.

Roebuck, J. R.: The Joule-Thomson Effect in Air, Proceedings of the American Academy of Arts and Sciences, 60, 537–596, http://www.jstor.org/stable/25130079, 1925.

Roebuck, J. R.: The Joule-Thomson Effect in Air. Second Paper, Proceedings of the American Academy of Arts and Sciences, 64, 287–334, http://www.jstor.org/stable/20026275, 1930.

Roedel, W. and Wagner, T.: Physik unserer Umwelt: Die Atmosphäre, Springer Berlin Heidelberg, https://doi.org/10.1007/978-3-642-15729-5, 2011.

Scheel, K. and Heuse, W.: Die spezifische Wärme der Luft bei Zimmertemperatur und bei tiefen Temperaturen, Annalen der Physik, 342, 79–95, https://doi.org/10.1002/andp.19113420106, 1912.

Schmidt, R. and Wagner, W.: A new form of the equation of state for pure substances and its application to oxygen, Fluid Phase Equilibria, 19, 175 – 200, https://doi.org/10.1016/0378-3812(85)87016-3, 1985.

Schubert, W., Ruprecht, E., Hertenstein, R., Ferreira, R. N., Taft, R., Rozoff, C., Ciesielski, P., and Kuo, H.-C.: English translations of twenty-one of Ertel's papers on geophysical fluid dynamics, Meteorologische Zeitschrift, 13, 527–576, https://doi.org/10.1127/0941-2948/2004/0013-0527, 2004.

Schumann, U.: Atmospheric Physics; Background – Methods – Trends, Research Topics in Aerospace, Springer-Verlag, Berlin Heidelberg, https://doi.org/10.1007/978-3-642-30183-4, 2012.

Seinfeld, J. H. and Pandis, S. N.: Atmospheric Chemistry and Physics: From Air Pollution to Climate Change, Wiley, 2006.

Skamarock, W. C. and Klemp, J. B.: A time-split nonhydrostatic atmospheric model for weather research and forecasting applications, Journal of Computational Physics, 227, 3465 – 3485, https://doi.org/10.1016/j.jcp.2007.01.037, 2008.

Skamarock, W. C., Klemp, J. B., Dudhia, J., Gill, D. O., Barker, D. M., Wang, W., and Powers, J. G.: A Description of the Advanced Research WRF Version 2, https://doi.org/10.5065/D6DZ069T, (No. NCAR/TN-468+STR), 2005.

Span, R., Lemmon, E. W., Jacobsen, R. T., Wagner, W., and Yokozeki, A.: A Reference Equation of State for the Thermodynamic Properties of Nitrogen for Temperatures from 63.151 to 1000 K and Pressures to 2200 MPa, Journal of Physical and Chemical Reference Data, 29, 1361–1433, https://doi.org/10.1063/1.1349047, 2000.

Spang, R., Remedios, J. J., Kramer, L. J., Poole, L. R., Fromm, M. D., Müller, M., Baumgarten, G., and Konopka, P.: Polar stratospheric cloud observations by MIPAS on ENVISAT: detection method, validation and analysis of the northern hemisphere winter 2002/2003, Atmospheric Chemistry and Physics, 5, 679–692, https://doi.org/10.5194/acp-5-679-2005, 2005.

Spichtinger, P.: Shallow cirrus convection - a source for ice supersaturation, Tellus A, 66, http://www.tellusa.net/index.php/tellusa/article/view/19937, 2014.

Stamnes, K., Thomas, G. E., and Stamnes, J. J.: Radiative Transfer in the Atmosphere and Ocean, Cambridge University Press, https://doi.org/10.1017/9781316148549, 2017.

Stohl, A., Bonasoni, P., Cristofanelli, P., Collins, W., Feichter, J., Frank, A., Forster, C., Gerasopoulos, E., Gäggeler, H., James, P., Kentarchos, T., Kromp-Kolb, H., Krüger, B., Land, C., Meloen, J., Papayannis, A., Priller, A., Seibert, P., Sprenger, M., Roelofs, G. J., Scheel, H. E., Schnabel, C., Siegmund, P., Tobler, L., Trickl, T., Wernli, H., Wirth, V., Zanis, P., and Zerefos, C.: Stratosphere-troposphere exchange: A review, and what we have learned from STACCATO, Journal of Geophysical Research: Atmospheres, 108, https://doi.org/10.1029/2002JD002490, 2003.

Swann, W. F. G. and Callendar, H. L.: VI. On the specific heats of air and carbon dioxide at atmospheric pressure by the continuous electric method at $20\,^{\circ}\mathrm{C}$ and $100\,^{\circ}\mathrm{C}$, Philosophical Transactions of the Royal Society of London. Series A, 210, 199–238, https://doi.org/10.1098/rsta.1911.0006, 1911.

Swinbank, R. and Ortland, D. A.: Compilation of wind data for the (UARS) Reference Atmosphere Project, J. Geophys. Res., 108, D19, 4615, https://doi.org/10.1029/2002JD003135, 2003.

Tao, M., Konopka, P., Ploeger, F., Yan, X., Wright, J. S., Diallo, M., Fueglistaler, S., and Riese, M.: Multitimescale variations in modeled stratospheric water vapor derived from three modern reanalysis products, Atmospheric Chemistry and Physics, 19, 6509–6534, https://doi.org/10.5194/acp-19-6509-2019, 2019.

Tegeler, C., Span, R., and Wagner, W.: A New Equation of State for Argon Covering the Fluid Region for Temperatures from the Melting Line to 700 K at Pressures up to 1000 MPa, J. Phys. Chem. Ref. Data, 28, 779 – 850, https://doi.org/10.1063/1.556037, 1999.

Thomson, W.: On the convective equilibrium of temperature in the atmosphere, Manch. Lit. Philos. Soc., 2, 170–176, https://ia800500.us.archive.org/3/items/memoirsoflite32186522man/memoirsoflite32186522man.pdf, 1862.

Tiesinga, E., Mohr, P. J., Newell, D. B., and Taylor, B. N.: The 2018 CODATA Recommended Values of the Fundamental Physical Constants, Web Version 8.1, Database developed by J. Baker, M. Douma, and S. Kotochigova. Available at http://physics.nist.gov/constants, 2020.

Tiwary, A. and Williams, I.: Air Pollution: Measurement, Modelling and Mitigation, CRC Press, fourth edn., 2019.

Tripoli, G. J. and Cotton, W. R.: The Use of lce-Liquid Water Potential Temperature as a Thermodynamic Variable In Deep Atmospheric Models, Monthly Weather Review, 109, 1094–1102, https://doi.org/10.1175/1520-0493(1981)109<1094:TUOLLW>2.0.CO;2, 1981.

Tsilingiris, P. T.: Thermophysical and transport properties of humid air at temperature range between 0 and 100 °C, Energy Conversion and Management, 49, 1098 – 1110, https://doi.org/10.1016/j.enconman.2007.09.015, 2008.

United States Committee on Extension to the Standard Atmosphere: U.S. standard atmosphere, 1976, National Oceanic and Atmospheric Administration, U.S. Government Printing Office, Washington D. C., https://ntrs.nasa.gov/archive/nasa/casi.ntrs.nasa.gov/19770009539.pdf, 1976.

Vallis, G. K.: Atmospheric and Oceanic Fluid Dynamics, Cambridge University Press, Cambridge, U.K., 2006.

Vasserman, A. A., Kazavchinskii, Y. Z., and Rabinovich, V. A.: Thermophysical Properties of Air and Air Components, Academy of Sciences of the USSR, Israel Program for Scientific Translation Ltd., Jerusalem 1971, 1966.

Vernier, J.-P., Fairlie, T. D., Deshler, T., Ratnam, M. V., Gadhavi, H., Kumar, B. S., Natarajan, M., Pandit, A. K., Raj, S. T. A., Kumar, A. H., Jayaraman, A., Singh, A. K., Rastogi, N., Sinha, P. R., Kumar, S., Tiwari, S., Wegner, T., Baker, N., Vignelles, D., Stenchikov, G., Shevchenko, I., Smith, J., Bedka, K., Kesarkar, A., Singh, V., Bhate, J., Ravikiran, V., Rao, M. D., Ravindrababu, S., Patel, A., Vernier, H., Wienhold, F. G., Liu, H., Knepp, T. N., Thomason, L., Crawford, J., Ziemba, L., Moore, J., Crumeyrolle, S., Williamson, M., Berthet, G., Jégou, F., and Renard, J.-B.: BATAL: The Balloon Measurement Campaigns of the Asian Tropopause Aerosol Layer, B Am Meteorol Soc, 99, 955–973, https://doi.org/10.1175/bams-d-17-0014.1, 2018.

Voigt, C., Schumann, U., Minikin, A., Abdelmonem, A., Afchine, A., Borrmann, S., Boettcher, M., Bucuchholz, B., Bugliaro, L., Costa, A., Curtius, J., Dollner, M., Dörnbrack, A., Dreiling, V., Ebert, V., Ehrlich, A., Fix, A., Forster, L., Frank, F., Futterer, D., Giez, A., Graf, K., Grooss, J. U., Gross, S., Heimerl, K., Heinold, B., Huneke, T., Järvinen, E., Jurkat, T., Kaufmann, S., Kenntner, M., Klingebiel, M., Klimach, T., Kohl, R., Krämer, M., Krisna, T. C., Luebke, A., Mayer, B., Mertes, S., Molleker, S., Petzold, A., Pfeilsticker, K., Port, M., Rapp, M., Reutter, P., Rolf, C., Rose, D., Sauer, D., Schafer, A., Schlage, R., Schnaiter, M., Schneider, J., Spelten, N., Spichtinger, P., Stock, P., Walser, A., Weigel, R., Weinzierl, B., Wendisch, M., Werner, F., Wernli, H., Wirth, M., Zahn, A., Ziereis, H., , and Zoger, M.: Ml-Cirrus the Airborne Experiment on Natural Cirrus and Contrail Cirrus with the High-Altitude Long-Range Research Aircraft Halo, B Am Meteorol Soc, 98, 271–288, https://doi.org/10.1175/Bams-D-15-00213.1, 2017.

von Bezold, W.: Zur Thermodynamik der Atmosphaere, pp. 1189 – 1206, Verlag der königlichen Akademie der Wissnschaften, Berlin, 1888.

von Helmholtz, H.: Über atmosphaerische Bewegungen, pp. 647 – 663, Verlag der königlichen Akademie der Wissnschaften, Berlin, 1888.

Wagner, W. and de Reuck, K. M.: Oxygen, International Thermodynamic Tables of the Fluid State, vol. 9 of *IUPAC Thermodynamic Tables Project*, Blackwell Science, Oxford, UK, 1987.

Wallace, J. M. and Hobbs, P. V.: Atmospheric Science, vol. 92 of *International Geophysics Series*, Academic Press, second edn., 2006.

Wegener, A.: Thermodynamik der Atmosphäre, J. A. Barth, Leipzig, 1911.

Wegener, A. and Wegener, K.: Vorlesung über Physik der Atmosphäre, J. A. Barth, Leipzig, 1935.

Weigel, R., Volk, C. M., Kandler, K., Hösen, E., Günther, G., Vogel, B., Grooß, J.-U., Khaykin, S., Belyaev, G. V., and Borrmann, S.: Enhancements of the refractory submicron aerosol fraction in the Arctic polar vortex: feature or exception?, Atmospheric Chemistry and Physics, 14, 12 319–12 342, https://doi.org/10.5194/acp-14-12319-2014, 2014.

Weigel, R., Spichtinger, P., Mahnke, C., Klingebiel, M., Afchine, A., Petzold, A., Krämer, M., Costa, A., Molleker, S., Reutter, P., Szakáll, M., Port, M., Grulich, L., Jurkat, T., Minikin, A., and Borrmann, S.: Thermodynamic correction of particle concentrations measured by underwing probes on fast-flying aircraft, Atmospheric Measurement Techniques, 9, 5135–5162, https://doi.org/10.5194/amt-9-5135-2016, 2016.

Wendisch, M. and Brenguier, J.-L.: Airborne Measurements for Environmental Research: Methods and Instruments, Wiley-VCH, Weinheim, https://doi.org/10.1002/9783527653218, 2013.

Wendisch, M., Pöschl, U., Andreae, M. O., Machado, L. A. T., Albrecht, R., Schlager, H., Rosenfeld, D., Martin, S. T., Abdelmonem, A., Afchine, A., Araùjo, A., Artaxo, P., Aufmhoff, H., Barbosa, H. M. J., Borrmann, S., Braga, R., Buchholz, B., Cecchini, M. A., Costa, A., Curtius, J., Dollner, M., Dorf, M., Dreiling, V., Ebert, V., Ehrlich, A., Ewald, F., Fisch, G., Fix, A., Frank, F., Fütterer, D., Heckl, C., Heidelberg, F., Hüneke, T., Jäkel, E., Järvinen, E., Jurkat, T., Kanter, S., Kästner, U., Kenntner, M., Kesselmeier, J., Klimach, T., Knecht, M., Kohl, R., Kölling, T., Krämer, M., Krüger, M., Krisna, T. C., Lavric, J. V., Longo, K., Mahnke, C., Manzi, A. O., Mayer, B., Mertes, S., Minikin, A., Molleker, S., Münch, S., Nillius, B., Pfeilsticker, K., Pöhlker, C., Roiger, A., Rose, D., Rosenow, D., Sauer, D., Schnaiter, M., Schneider, J., Schulz, C., Souza, R. A. F. d., Spanu, A., Stock, P., Vila, D., Voigt, C., Walser, A., Walter, D., Weigel, R., Weinzierl, B., Werner, F., Yamasoe, M. A., Ziereis, H., Zinner, T., , and Zöger, M.: The ACRIDICON-CHUVA campaign: Studying tropical deep convective clouds and precipitation over Amazonia using the new German research aircraft HALO, B Am Meteorol Soc, https://doi.org/10.1175/BAMS-D-14-00255.1, 2016.

Wilson, J. C., Loewenstein, M., Fahey, D. W., Gary, B., Smith, S. D., Kelly, K. K., Ferry, G. V., and Chan, K. R.: Observations of condensation nuclei in the Airborne Antarctic Ozone Experiment: Implications for new particle formation and polar stratospheric cloud formation, Journal of Geophysical Research: Atmospheres, 94, 16 437–16 448, https://doi.org/10.1029/JD094iD14p16437, 1989.

Witkowski, A. W.: I. Thermodynamic properties of air, The London, Edinburgh, and Dublin Philosophical Magazine and Journal of Science, 42, 1–37, https://doi.org/10.1080/14786449608620887, 1896.

WMO: Meteorology—A three-dimensional science, WMO Bull., 6, 134–138, 1957.

WMO: International Meteorological Tables, WMO-No.188.TP97, Secretariat of the World Meteorological Organization, Geneva, Switzerland, https://library.wmo.int/pmb_ged/wmo_188e.pdf, 1966.

Zängl, G., Reinert, D., Rípodas, P., and Baldauf, M.: The ICON (ICOsahedral Non-hydrostatic) modelling framework of DWD and MPI-M: Description of the non-hydrostatic dynamical core, Quarterly Journal of the Royal Meteorological Society, 141, 563–579, https://doi.org/10.1002/qj.2378, 2015.

Zdunkowski, W. and Bott, A.: Dynamics of the Atmosphere: A Course in Theoretical Meteorology, Cambridge University Press, 2003.